JAERI-Data/Code
98-021

DATA COLLECTION OF FUSION NEUTRONICS BENCHMARK EXPERIMENT CONDUCTED AT FNS/JAERI

August 1998

Fujio MAEKAWA, Chikara KONNO, Yoshimi KASUGAI,
Yukio OYAMA and Yujiro IKEDA

日本原子力研究所
Japan Atomic Energy Research Institute

本レポートは，日本原子力研究所が不定期に公刊している研究報告書です。
入手の問合わせは，日本原子力研究所研究情報部研究情報課（〒319-1195　茨城県那珂郡東海村）あて，お申し越しください。なお，このほかに財団法人原子力弘済会資料センター（〒319-1195　茨城県那珂郡東海村日本原子力研究所内）で複写による実費頒布をおこなっております。

This report is issued irregularly.
Inquiries about availability of the reports should be addressed to Research Information Division, Department of Intellectual Resources, Japan Atomic Energy Research Institute, Tokai-mura, Naka-gun, Ibaraki-ken, 319-1195, Japan.

編集兼発行　　日本原子力研究所

JAERI-Data/Code 98-021

Data Collection of Fusion Neutronics Benchmark Experiment Conducted at FNS/JAERI

Fujio MAEKAWA, Chikara KONNO, Yoshimi KASUGAI,
Yukio OYAMA and Yujiro IKEDA

Department of Materials Science
Tokai Research Establishment
Japan Atomic Energy Research Institute
Tokai-mura, Naka-gun, Ibaraki-ken

(Received July 1, 1998)

Fusion neutronics benchmark experimental data have been continued at the Fusion Neutronics Source (FNS) facility in JAERI. This report compiles unpublished results of the in-situ measurement experiments conducted by the end of 1996. Experimental data of neutron spectra in entire energy range, dosimetry reaction rates, gamma-ray spectrum and gamma-ray heating rates are acquired for five materials of beryllium, vanadium, iron, copper and tungsten. These experimental data along with data previously reported are effective for validating cross section data stored in evaluated nuclear data files such as JENDL.

Keywords : Fusion Neutronics, Benchmark Experiment, Data Collection, FNS, Beryllium, Vanadium, Iron, Copper, Tungsten

JAERI-Data/Code 98-021

原研 FNS で行われた核融合中性子工学ベンチマーク実験のデータ集

日本原子力研究所東海研究所物質科学研究部
前川　藤夫・今野　力・春日井好巳
大山　幸夫・池田裕二郎

（1998年 7月 1日受理）

原研・核融合中性子工学研究用中性子源（FNS）施設において、核融合中性子工学ベンチマーク実験を行っている。本レポートは、1996 年末までに行われた体系内測定実験のうち未公開のものを収録している。測定対象となったのはベリリウム、バナジウム、鉄、銅、タングステンの5物質であり、全エネルギーにわたる中性子スペクトル、ドシメトリ反応率、γ線スペクトル、γ線核発熱率の実験データが取得されている。これらの実験データは既に公開している一連のデータとともに、JENDL等の評価済み核データファイルに収められた断面積データの精度検証に対して有効である。

東海研究所：〒319-1195 茨城県那珂郡東海村白方白根 2-4

Contents

目　　次

1. Introduction

Since the first operation of the Fusion Neutronics Source (FNS) facility [1] in 1981, a number of fusion neutronics benchmark experiments for various materials have been conducted by using D-T neutrons at FNS. These experimental data have contributed to improvement and validation of evaluated nuclear data files, such as the Japanese Evaluated Nuclear Data Library [2] (JENDL) and the Fusion Evaluated Nuclear Data Library [3] (FENDL), which are used for nuclear designs of fusion reactors and many other applications.

The benchmark experiments at FNS are classified into two categories: (1) the Time-Of-Flight (TOF) neutron spectrum measurement and (2) the in-situ neutron and gamma-ray measurement; the latter is so-called the clean benchmark experiment. Experimental data obtained by the end of 1992 have been already summarized in several JAERI reports [4-8]. Since then, experimental efforts have still been continued mainly in the clean benchmark experiment for fusion relevant important materials including V and W. Also, there have been development of new measurement techniques.

There are several distinctive features in the comprehensive clean benchmark experiment;

(i) whole energy neutron spectrum with a combination of three techniques, i.e., an NE213 spectrometer, proton recoil gas proportional counters and the slowing down time method for the energy regions of MeV, keV and eV, respectively,
(ii) many dosimetry reaction rates by the foil activation method to provide spectrum indices,
(iii) secondary gamma-ray spectrum and heating rate,
(iv) secondary gamma-ray data associated with both the threshold and the (n,γ) reactions,
(v) thick experimental assemblies suitable to investigate transport effects for deeply penetrated 14-MeV neutrons as well as multiply scattered low energy neutrons, and
(vi) negligibly small background neutrons from outside of the assembly because the experimental assemblies function as a shield materials against the background neutrons by themselves.

Table 1 summarizes materials and measured quantities in the clean benchmark experiments by the end of 1996. This report compiles numerical experimental data and figures for beryllium, vanadium, iron, copper and tungsten, which have not been reported so far. Experimental data contained in this report are indicated by black circles in Table 1.

2. Clean Benchmark Experiment

2.1 Experimental Configuration

The experimental configuration was basically the same as the previous one [4-7]. Table 2.1.1 summarizes dimensions of the experimental assemblies. The experimental assemblies of beryllium, copper and tungsten were made by stacking bricks of (50.7 ~ 50.8 mm)^3 with thin aluminum support frames in quasi-cylindrical shapes. Figure 2.1.1 shows an example view of the copper assembly. The vanadium assembly was a cube of (254 mm)^3. Four side surfaces and a rear surface of the vanadium assembly was covered with a graphite reflector of 51 mm in thickness, as shown in Fig. 2.1.2, to reduce leakage neutrons from the rather small assembly and incoming background neutrons from the outside. The iron assembly had a real cylindrical shape as shown in Fig. 2.1.3. Several experimental channels for insertion of detectors were set on the lateral surface of the assembly, and detectors were placed on the central axis of the assembly. The experimental assemblies were apart from the experimental room walls and floor at least 4 m, and the diameters and thicknesses of the assemblies were large. Hence, contribution of the background neutrons and gamma-rays coming from the room walls and floor on the measured quantities was negligibly small.

The experimental assembly was located in front of the neutron source at a distance of 200 mm from the target. The tritium target of ~ 3.7 x 10^{11} Bq was bombarded by a deuteron beam of 350 keV energy to produce D-T neutrons. A number of source D-T neutrons produced during a measurement was determined by the associated alpha-particle detector [9] with accuracy of 2~3 %. For on-line measurements such as spectrum measurements, a counter was inserted into one of the experimental channels and a measurement was performed during neutron generation. The similar measurement was repeated changing the detector position one by one. For off-line measurements such as irradiation of dosimetry foils and TLD, samples were located in the plural detector channels at the same time, and irradiated simultaneously for necessary period of time (5 minutes ~ 10 hours).

2.2 Source Condition

The D-T neutron source can be roughly described as an isotropic point 14-MeV neutron source. The source neutron spectrum and intensity, however, depend slightly on the emission angle with respect to the deuteron beam direction. The angle-dependent source characteristics were investigated experimentally and theoretically in detail, and a source subroutine of the Monte Carlo transport calculation code MCNP-4 [10] has been established to simulate the source condition precisely. [11] Although use of the source subroutine is recommended to give the best results, the source spectrum of neutrons emitted toward the 0 degree direction can be used as the incident neutron spectrum on the whole front surface of the assembly. It has revealed that there is no serious degradation in the calculated results. The source neutron spectrum toward the 0 degree is shown in Fig. 2.2.1, and input cards of MCNP for description of the source spectrum are shown in Fig. 2.2.2. The `si1` and `sp1` cards indicate upper neutron energies of the energy bins in MeV and probabilities in the bins, respectively. The `dir` and `vec` parameters with the `sb2` card are used for variance reduction with the source biassing method. The weight of a source neutron specified by the `wgt` parameter, 1.1261, is larger than 1.0 because generated D-T neutrons are emitted to the forward direction more than the backward direction with respect to the deuteron beam direction.

The tritium target region is also a source of gamma-rays, namely, target gamma-rays, by interaction of the source neutrons with structural materials of the target. Consideration of the target gamma-rays, however, is not needed in calculations of gamma-ray heating rates because contribution of the target gamma-ray to the measured heating rates has been already subtracted in the experimental data. On the other hand, the target gamma-ray contribution is involved in the measured gamma-ray spectra. The contribution at the detector positions deep inside the experimental assemblies is negligible, at most a few percentage, because the experimental assembly largely attenuate the target gamma-rays. Accordingly, it is not necessary to consider the target gamma-rays in transport calculations for the clean benchmark experiments.

2.3 Measurement Techniques

2.3.1 Neutron Spectrum in MeV Energy Region by NE213

NE213 Spectrometer

A 14 mm-diameter spherical NE213 liquid organic scintillator [12] is used as the fast neutron spectrometer. An NE213 liquid of 1.38 x 10^3 mm^3 is contained in a spherical cell of Pyrex glass of 1 mm in thickness. A sectional view of the detector is shown in Fig. 2.3.1. The scintillator is mounted on a photomultiplier tube (Hamamatsu Photonics, R647-02) with a quartz light guide of 11 mm diameter and 5 mm length. One side of the light glass is shaped in sphere so as to fit the light guide to the surface of the glass cell. The glass cell and the light guide are coated with the NE560 reflector paint made of MgO.

Measurement

Measurements were carried out by inserting the detector into the experimental channel hole of 22 mm ϕ. Figure 2.3.2 shows the electronic circuit used for the measurements. Output signals from the anode were terminated by a 100 kΩ register at the input of the pre-amplifier. The output signals from the pre-amplifier were then fed to a delay-line amplifier. For the neutron-gamma-separation, the rise time discrimination techniques was used. The rise time and pulse height data were taken in a two-dimensional array. Typical measuring time for each experimental run was 2000 sec. The neutron intensity was adjusted so that counting rates do not exceed 2000 cps.

Data Processing

The two dimensional data were separated into neutron and gamma-ray events, and a pulse height spectrum due to only neutrons was obtained. The pulse height spectrum was then unfolded to obtain neutron energy spectrum by the FORIST code [13] using the neutron response matrix previously determined. [14] The response matrix is calculated by a Monte Carlo method, while the responses in specially important energy regions, i.e., 13.6 to 14.8 MeV, are directly measured and replaced with the calculated response. The FORIST code provides the appropriate energy resolution function by internal iteration. The resolution function, defined as the window function W(E) in the code, is given together with the unfolded results for each run. The spectrum observed, $\Phi_{obs}(E)$, is expressed as follows:

$$\Phi_{obs}(E) = \int_0^\infty \frac{1}{\sqrt{2\pi}\sigma(E)} exp\left[-\frac{(E-E')^2}{2\sigma^2(E)} \right] \Phi_{true}(E')dE' , \qquad (2\text{-}1)$$

where $\Phi_{true}(E)$ is the true neutron spectrum without any deformation, and

$$\sigma(E) = \frac{W(E)\cdot E}{235.5} . \qquad (2\text{-}2)$$

The obtained spectrum at the front surface of the experimental assembly has an oscillatory structure caused by the unfolding procedure due to mismatching between the real detector response function and the used one. At the position, since the 14-MeV peak flux is usually by more than two orders of magnitude larger than the flux around 5-10 MeV region, the flux error in the 5-10 MeV region is by two orders of magnitude more sensitive to the error of the peak flux through the response function. In the deep position, some small and broad oscillation below 8 MeV is sometimes seen. This is partly due to the incompleteness of neutron and gamma-ray separation. A fraction of gamma-rays increase with the depth and then some of γ-ray contribution are counted as the neutron events.

Error Assessment

The accuracy of the neutron response in the neutron energy range of 13.6 to 14.8 MeV is about 2 % which was experimentally confirmed. However, the calculated light output response corresponding to the proton energy below ~ 2 MeV gives a relatively poor representation. Hence, the errors increase in the lower energy range by accumulation of errors in the higher energy range, especially for the case where 14 MeV neutrons are dominant. Table 2.3.1 summarizes the systematic errors which are estimated from the unfolded results for measurement of mono-energetic neutrons of 14.8 MeV. The error in the range below the peak energy is generated by the mismatch of the response for 14.8 MeV neutrons. The fraction in the table denotes the ratio of the error in the interested energy range due to the response error to that of the peak flux around 14 MeV. Here the energy dependent error is represented as:

$$Error(\%)\ for\ \Phi(E_n) = (fraction) \times \frac{\Phi_{peak}}{\Phi(E_n)} \times 100. \qquad (2\text{-}3)$$

If the peak flux around 14 MeV is, for example, ten times larger than the flux below 10 MeV, the proton spectra in the range of 6 to 10 MeV might be distorted by -10 to -20 % , at maximum.

The energy calibration error also affects the unfolded results. The effects of variation in the energy axis are about 3 % above 10 MeV and less than 2 % for 1 to 10 MeV range, respectively. Lastly, there is the common error of 2 % for the neutron source intensity. The overall error range was 4 % for the flux above 10 MeV and 10 - 20 % below 10 MeV depending on the spectrum shape.

2.3.2 Neutron Spectrum in keV Energy Region by Proton Recoil Gas Proportional Counters

Proton Recoil Gas Proportional Counters

A small counter head, a new data acquisition technique and the related electronics for proton-recoil gas proportional counter (PRC) were developed[15, 16] by E. F. Bennett at Argonne National Laboratory to measure the neutron spectrum inside the experimental assembly in the frame of the JAERI/USDOE collaboration program on fusion blanket neutronics. Experimental details for the iron assembly is described in the reference[17].

The counter has a cylindrical shape as shown in Fig. 2.3.3. It is made of type 304 stainless steel of 0.41 mm in thickness. The outer diameter of the counter is 19 mm to attain better spatial resolution with respect the depth in the experimental assembly while the effective length of the counter is 127 mm. The thickness of the anode wire is 20 μm. Field tubes are also added to define the active counter volume. The counter is inserted into an experimental hole of 21 mm in diameter with its pre-amplifier.

There are two types of counter to measure neutron spectrum in a wide energy range. Both counters are identical in their dimensions, but different gases are filled in. Hydrogen gas at 0.5677 MPa (5.789 kgf/cm^2) with 1 percent of CH_4 is filled in one counter for low-energy neutrons from 3 keV to 150 keV while 50-50 mixture of hydrogen and argon gases with 1.8 percent of nitrogen at 0.6102 MPa (6.222 kgf/cm^2) are filled in another counter for high-energy neutrons from 150 keV to 1 MeV. Argon atoms reduce ranges of recoiled proton since they have large stopping power. Energy scale is calibrated by using the peak at 27 keV corresponding to the resonance valley of iron cross section and the thermal peak at 626 keV of the $^{14}N(n,p)^{14}C$ reaction.

Electronics and Measurement

A new data acquisition technique[15] was developed to reduce overall time for measurement and data process. In the conventional technique, several runs changing high voltages many times are needed to obtain a spectrum, while in the new technique, data are taken by a single measurement run using high voltage sweep in a ramp shape.

The block diagram of the data acquisition system is shown in Fig. 2.3.4. A specially designed small preamplifier of 20 mm x 20 mm x 200 mm, which could be inserted in the experimental assembly, was attached to the counter head. Time-dependent saw-tooth shape voltage was generated by an analog function generator. The voltage was supplied to a programmable high-voltage DC/DC converter, and then, output high voltage, which changed slowly with a period of 165 seconds in the saw-tooth shape, was supplied to the counter. The high voltage ranged from 3000 to 4200 V and from 2400 to 3000 V for hydrogen and hydrogen/argon counters, respectively. The generated high voltage was monitored using a dividing resistance, which scaled down the high voltage by ~ 1/500. Test pulses of which rise time was larger than that of pulses caused by ionizing events were fed to the preamplifier.

One of the counters was inserted in the experimental assembly or attached on the front surface of the assembly. Measurement was performed with generating D-T

neutrons at the target. Measurement with the other counter was also performed.

Two analog pulse amplifiers were used for pulse shape discrimination against gamma ray events. One was an simple integration amplifier (Y-amplifier) to produced output signals proportional to input pulse heights, i. e., recoiled proton energies. The other amplifier (X-amplifier) had a much shorter shaping time constant compared with the Y-amplifier. The output signal was proportional to the pulse height of input signal as well as the reciprocal of rise time of the input signal. The output signals of X-amplifier, Y-amplifier and the dividing resistor were digitized into 4096 channels by an analog-digital converter using a multiplexer and logical circuits. The digitized data are taken to a personal computer through an interface board of LSI 8255A. The data acquisition program calculated 1) ratios of pulse heights for the X-amplifier to those of the Y-amplifier, which was proportional to the reciprocal of the rise times, 2) gas multiplication factors corresponding to the applied high voltage and 3) the recoiled proton energies in logarithmic scale by using the output signals from the Y-amplifier and the gas multiplication factors, event by event. The ratios of X/Y and the recoiled proton energies were stored in a two dimensional array (32 channels x 512 channels).

Data Processing

In the off-line data processing, recoil proton events and test pulse events were separated by using the rise time information for each recoiled proton energy. The test pulse events were used to estimate dead time loss and to normalize recoil proton events. Neutron spectra $\Phi(E)$ was derived using the following equation,

$$\Phi(E) = \frac{1}{N \cdot S \cdot \sigma(E)} \cdot \frac{E}{\sigma(E)} \cdot \frac{dD(E)}{dE}, \qquad (2\text{-}4)$$

where N: hydrogen atom number,
S: source neutron strength,
$\sigma(E)$: n-p scattering cross-section, and
$D(E)$: recoil proton spectrum.

Error Assessment

Possible error sources of this technique are gas pressure (hydrogen atom number), n-p scattering cross section, fitting error for differentiation of recoil proton spectrum due to count statistics and calibration of recoil proton energy. The fitting error is the largest, ~ 3-10 % above 10 keV, while the other errors are expected to be less than 1%. Neutron spectra below 10 keV tend to become smaller due to the uncertainty of the W-value, which is the average energy loss per ion pair. The error due to W-value is not included in the experimental errors.

2.3.3 Neutron Spectrum in eV Energy Region by the Slowing Down Time Method

Measurement

Neutron spectra in the energy region below 10 keV were measured by the Slowing Down Time (SDT) method[18-20] in the beryllium, vanadium, iron and copper assemblies. The technique utilizes characteristics of neutron slowing down in a medium incorporating with a pulsed neutron source. A measurement for the tungsten assembly was also attempted, but it was not in successful due to practically too small number of neutrons in the energy region of interest.

A BF_3 gas proportional counter of 14 mm in outer diameter and 99 mm in effective length containing 96 % boron-10 enriched BF_3 gas of 71.5 kPa was used for neutron detection. The effective number of boron-10 atoms in the counter was determined as 2.18×10^{20} with accuracy of 3 % by utilizing a standard thermal neutron field. The counter was inserted into one of the experimental holes of the experimental assembly.

Pulsed neutrons, typically 1 μs in pulse width and 200 μs in pulse interval, were injected into the experimental assembly. The pulse interval of 200 μs was determined in the manner that all neutrons disappear in the experimental assembly in the time range. A block diagram of the electronic circuit employed is shown in Fig. 2.3.5. Timing signals of the BF_3 counter prepared by a constant fraction timing circuit triggered to start the time-to-pulse-height convertor (TPHC). Timing signals from a master pulse generator were delayed for about 160 μs, and fed into TPHC as stop signals. Electronic noise signals and gamma-ray events were rejected by pulse height discrimination. Time-spectra of the $^{10}B(n,\alpha)$ reaction rate was recorded by a multi-channel analyzer. Typical counting time and total number of generated neutrons were 20 - 60 minutes and $0.1\text{-}1 \times 10^{12}$ neutrons, respectively.

To calibrate the energy scale of the measured time-spectra, the resonance filter method and the capture-gamma method were adopted with various resonance filters such as Mn (1.1 mm thickness), Co (0.2 mm), Cu (2 mm), In (0.1 mm), W (0.2 mm) and Au (0.04 mm). The energies of the resonance peaks were in a range from 1.46 eV of In to 579 eV of Cu. In the resonance filter method, the BF_3 counter was covered with one of the filters, and time-spectra of the $^{10}B(n,\alpha)$ reaction rate were measured in just the same way as without the filters. For the capture-gamma method, an argon gas proportional counter was used. Time-spectra of detected gamma-ray events were measured with and without the resonance filters.

Rejection of Thermal Neutron Events in the Beryllium Experiment[19]

Since the neutron capture cross section of beryllium was extremely small, there were a great number of thermal neutrons in the assembly. Most of detection events by the BF_3 counter, more than 99 %, were caused by the thermal neutrons. Hence counting rates for object neutrons between 0.3 eV and 10 keV had to be suppressed in a very low level to keep total counting rates constant. In addition, it took a long time to decay out thermal neutron fluxes in the assembly, the neutron pulse interval of 15 ms was required

to confirm disappearance of thermal neutrons from the assembly. Measurement with the long pulse interval was inefficient due to very low counting rate, which must be much less than neutron pulse generation rate for the electronic circuit employed in the measurement. In this case, the counting rate had to be less than 10 cps.

To reduce the thermal neutron detection, the BF_3 counter was covered with a cadmium sleeve of 1 mm in thickness. The thermal neutron detection was almost completely eliminated by the Cd sleeve, and time-spectra could be measured with the pulse intervals of 200 μs. Accordingly, neutron spectra between 1 eV and 10 keV were obtained with the necessary correction of neutron absorption by the cadmium sleeve.

Data Processing

The used filter materials have prominent resonance peaks in their neutron cross sections. When two time-spectra, with and without a resonance filter, were compared, a small dip and peak were observed in the time-spectrum with the resonance filter for the resonance filter method and the capture-gamma method, respectively. Since the dip and peak were produced by the prominent resonance peak of the filter materials, the time difference between the neutron generation and the dip and peak just corresponded to the neutron slowing down time from the source energy to the resonance peak energy. By adopting this principle,neutron slowing down times could be determined experimentally for all the time-spectra with the filters.

The energy calibration curve, $\overline{E}(t)$, was calculated from time-dependent neutron energy spectra, $\phi(t,E)$, given by transport calculations. The $\overline{E}(t)$ is given as,

$$\overline{E}(t)=\frac{\int \phi(t,E)\cdot E\cdot dE}{\int \phi(t,E)\cdot dE} \qquad (2\text{-}5)$$

The measured slowing down times did not always agree with the calculated curve. To attain good agreement between both, the time origin of the calculation was adjusted. Figure 2.3.6 shows examples of the calibration curves for the beryllium and copper assemblies.

The time-scale of the measured time-spectrum of the $^{10}B(n,\alpha)$ reaction rate was converted into an energy-scale by using the adjusted calibration curve to obtain an energy-spectrum of the reaction, $C(E)$. Finally, neutron energy-spectra $\phi(E)$ were derived in the energy range between 0.3 eV and 10 keV by taking account of the cross section of $^{10}B(n,\alpha)$ reaction $\sigma(E)$, the number of effective ^{10}B atoms in the counter N, the number of neutrons generated during the measurement Y_n, a self-shielding correction factor of the counter $f_{ss}(E)$ and a correction factor for the effective ^{10}B cross section weighted by broadened neutron spectrum at a moment centered at E $f_\sigma(E)$. The $\phi(E)$ is given as,

$$\phi(E)=\frac{C(E)}{\sigma(E)\cdot N\cdot Y_n\cdot f_{ss}(E)\cdot f_\sigma(E)} \ . \qquad (2\text{-}6)$$

Experimental Uncertainty

Experimental uncertainties associated with the measured spectra are summarized in Table 2.3.2. The overall experimental uncertainties are dominated mostly by the uncertainties of the energy calibration curves. The lowest and highest energies calibrated are 1.4 eV and 579 eV. In the energy ranges outside the calibration energies, roughly below 1 eV and above 1 keV, the adjusted calibration curves are used. Especially in the higher energy region above 1 keV where the slowing down time is short, larger uncertainties in the calibration curves are involved due to, in particular, the extrapolation process. Thus the experimental uncertainties for the energy region between 1 and 10 keV are larger than those below 1 keV, as indicated in Table 2.3.2. In the energy range below 1 keV, experimental uncertainties are around 10 %.

Energy Resolution and Correction Factor

The energy resolution and the correction factor are estimated by time-dependent Monte Carlo transport calculations by the manner explained elsewhere [18]. Table 2.3.2 also summarizes typical energy resolution.

The best energy resolution of about 50~60 % for vanadium, iron and copper, and that of 130 % for beryllium are consistent with the theoretically expected values [18]. The energy resolution for vanadium, iron and copper in energy regions where large resonance peaks exist on their cross section, roughly above 300 eV, is worse than the theoretical resolution. Energy resolution of a measured neutron spectrum at energy E comes from a divergence of neutron energy at a moment when mean neutron energy is E. If a resonance peak exists near the mean neutron energy E, it increases the divergence of neutron energy, and also, energy resolution of the measured neutron spectrum near the peak.

The correction factor for the effective $^{10}B(n,\alpha)^{7}Li$ cross section $f_{\sigma}(E)$, appeared in Eq. (2-6), is defined as a ratio of the cross section at a discrete energy E to the cross section averaged with a neutron spectrum at the moment when a mean neutron energy is E. Hence, better energy resolution gives a smaller correction factor. For vanadium, iron and copper, the correction factors for the energy range below 1 keV are less than 3 %, and they increase up to 20 % with increase of energy. For these three materials and beryllium, the correction factors were not so large as at most 20 %.

2.3.4 Foil Activation Method

Dosimetry Reactions

The reaction rates were measured by the foil activation technique. To give spectral indices for wide energy range, plural reactions with different threshold energies were applied. Also some (n,γ) reactions were added in the reaction rate measurement. In Table 2.3.3, reactions used are listed with their effective threshold energies. Four dosimetry reactions, i.e., the $^{27}Al(n,\alpha)^{24}Na$, $^{93}Nb(n,2n)^{92m}Nb$, $^{115}In(n,n')^{115m}In$ and $^{197}Au(n,\gamma)^{198}Au$ reactions, were commonly used for all the experiments because of facilitating the comparative study of neutronics products on different material configurations. Cross sections of the dosimetry reactions taken from JENDL Dosimetry File[21] are shown in Figs. 2.3.7 and 2.3.8.

Activation Foils and Irradiation

Typical sample size was 10 mm in diameter and 1 mm in thickness for activation foils except indium and gold. Indium foils had a dimension of 10 x 10 x 1 mm^3. In order to minimize the self-shielding effect for the $^{197}Au(n,\gamma)^{198}Au$ reaction, gold foils with a size of 10 x 10 x 0.001 mm^3 were adopted. The other ordinary threshold foils were set in the experimental drawer channels for the axial distribution measurement.

The foils were irradiated for 4 ~ 10 hours with D-T neutrons and total neutron yields at the target required were 2 to 5 x 10^{15} n. Neutron yield was monitored by the associated α-particle counting method. The irradiation history was recorded by using the multi-channel scaling (MCS) for the decay correction during irradiation.

Reaction Rate Determination

After the irradiation, gamma-rays were measured with high-pure Ge detectors. The detector efficiencies were calibrated by using the standard calibration gamma-ray sources.

Reaction rate, *RR*, were derived from the corresponding gamma-ray peak counts with necessary corrections. The *RR* is given as,

$$RR = \frac{\lambda \cdot C \cdot A}{\varepsilon \cdot W \cdot N_a \cdot a \cdot b \cdot Y \cdot S_a \cdot \mu \cdot \left(1 - exp(-\lambda \cdot t_i)\right) \cdot exp(-\lambda \cdot t_c) \cdot \left(1 - exp(-\lambda \cdot t_m)\right)}, \quad (2\text{-}7)$$

where,

- λ: decay constant (/sec),
- C: gamma-ray peak counts,
- A: atomic mass,
- ε: detector efficiency,
- W: sample weight,
- N_a: Avogadro's number,
- a: natural abundance of the target element,
- b: gamma-ray branching ratio,

Y: neutron source strength (/sec)
S_a: correction factor for the decay during irradiation,
m: gamma-ray self absorption correction factor,
t_i: irradiation time,
t_c: cooling time, and
t_m: collection time.

The neutron yield fluctuation monitored with the MCS was used for the correction of S_a. Counting loss due to coincidental sum-peak in the cascade gamma-rays was corrected.

Experimental Error and Uncertainty

Major sources of the error for the reaction rate were the gamma-ray counting statistics (0.1 ~ several %) and the detector efficiency (2 ~ 3 %). The error for sum-peak correction was estimated less than 2 % depending on the decay mode and fraction of multiple gamma-ray cascade. The error for the decay correction was reflected from the error of half-life of the activity. If the half-life was accurate, the error for the saturation factor should be less than 1 % even for the short half-life activities.

The other errors associated with foil weight, gamma-ray self-absorption, irradiation time, cooling time and counting time were negligibly small. The error for neutron yield was estimated to be 2 %. The overall error for the major part of reaction rate ranged 3 ~ 6 %. Some data for high threshold reaction in the deep positions suffered from poor counting statistics due to low activation rate.

2.3.5 Tritium Production Rate with Li-Containing Pellet

Tritium production rates for lithium-6 and -7 in the beryllium assembly were measured with lithium-containing pellets. The tritium production cross sections taken from the JENDL Dosimetry File are shown in Figs. 2.3.9 and 2.3.10. The conventional experimental technique was adopted for the preparation of the Li-containing pellets and the irradiations while a newly developed technique was employed for the preparation of samples for liquid scintillation counting. The new technique is described in detail in Refs. 22) and 23).

Preparation of Li-Containing Pellet and Irradiation

Detector pellets of 12.8 mm in diameter and 2 mm in thickness were produced by cold-pressing lithium carbonate (Li_2CO_3) powder at ~ 6 ton/cm^2 for 10 seconds. Weight of the pellets was ~ 0.45 g. Two types of lithium carbonate powder, lithium-6 enriched at 95.616 ± 0.005 atom % and lithium-7 enriched at 99.934 ± 0.005 atom %, were used to measure the ^{6}Li(n,α)T and ^{7}Li(n,n'α)T reaction rates, respectively. The pellets were embeded in the beryllium experimental assembly, and irradiated by D-T neutrons for ~ 10 hours. Total nomber of neutrons generated during the irradiation was 1.00 x 10^{16}.

Chemical Processing and Measurement

An irradiated pellet was put into a Teflon vial of 20 ml. A binary-acid solvent which contained 0.81 ml of HNO_3 (61%) and 0.17 ml of CH_3COOH (100 %) was poured into the vial to solve the pellet. At the beginning of the solution for 5 minutes, the vial was cooled in cold water to remove heat of disolution. After 12 hours, 17 ml of liquid scintillation cocktail (Clear-Sol) was added in the vial, and the vial was shaked to obtain a complete mixture. Tritium activity in the sample was measured by a low background liquid scintillation counting system (OKEN LSC-7100). The external standard ratio method was adopted for determination of counting efficiency for each sample. The typical counting efficiencies were ~ 22 %. The tritium activity was normalized by the standard tritium water provided by National Institute of Standard and Technology of U.S. Tritium production rates for the ^{6}Li(n,α)T and ^{7}Li(n,n'α)T reactions were deduced by considering the isotopic enrichments of lithium-6 and -7. The typical experimental error was 4.5 %.

2.3.6 Cherencov Radiation Counting Method for ^{32}P Activities

Outline of the Cherenkov Radiation Counting Method

Since a large number of radioactive nuclides exhibit β-ray emission above 263 keV, the threshold energy for the excitation of Cherenkov radiation in water, Cherenkov response can be used for measurements of β-activity. There are remarkable advantages of this technique in terms of extreme simplicity of sample preparation and the ability to count in aqueous systems without use of organic fluors. The main disadvantage is low detection efficiency compared with liquid scintillation counting. All the decay events cannot be detected because there is a finite number of β-rays that fall below the Cherenkov threshold. The theoretical efficiency is ~ 86% when all the β-rays above the Cherenkov threshold are detected, however, the experimental detection efficiency is about two times less than the theoretical result when the ordinary liquid scintillation counting equipment is used.

Reaction rates of the $^{31}P(n,\gamma)^{32}P$, $^{32}S(n,p)^{32}P$ and $^{35}Cl(n,\alpha)^{32}P$ reactions were measured by the Cherenkov radiation counting method. As all of the reactions produce the ^{32}P activity which emits high energy (maximum energy = 1.711 MeV) β-rays, they are suitable for the method. Cross section of the reactions are shown in Figs. 2.3.9 and 2.3.10. The cross section for the $^{32}S(n,p)^{32}P$ reaction is taken from the JENDL Dosimetry File while the other two cross sections are taken from FENDL/A-2.0 [24]. Especially, cross section of the $^{32}S(n,p)^{32}P$ and $^{35}Cl(n,\alpha)^{32}P$ reactions are investigated in detail elsewhere [25].

Pellet Preparation

The selected compounds for the pellets are listed in Table 2.3.4. Natural phosphor-, sulfur- and chlorine-containing compounds in powder form were chosen because of the availability of these compounds in high purity (analytical grade), the ease of forming the powder into pellets and their good water solubility. It was investigated that impurities which may present in the powder have low activation cross sections. Special care was paid to the phosphorus content in the sulfur- and chlorine-containing powder because the $^{31}P(n,\gamma)^{32}P$ reactions produce the same nuclide of interest, mainly with low-energy neutrons. In order to estimate activities from ^{31}P impurities, measurements of ^{32}P activity in pellets with and without Cd covers was made. No difference between the two pellets was observed. Thus it was concluded that there was no interference due to phosphorus contamination in the $^{32}S(n,p)^{32}P$ and $^{35}Cl(n,\alpha)^{32}P$ reaction rate measurements.

The powder was pressed into pellets of known and reproducible area with a diameter of 12 mm and 1 mm thickness under a pressure of about 7 ton/cm^2. Although pellets were pressed without extraneous binding agent, they did not powder or crack under normal handling and irradiation conditions. The pellets were contained in thin aluminum foil to protect them from contamination during irradiations.

Experimental Assembly and Irradiation

Beryllium blocks of typical 50.8 x 50.8 x 101.6 mm^3 were stacked to make the assembly in the form of quasi-cylindrical slab of 630 mm in equivalent diameter and 456 mm in thickness. The central part of this assembly with dimensions of 50.8 x 50.8 mm^2 served as an experimental channel. During the construction of the assembly, irradiation pellet packets were sandwiched between two beryllium blocks in the experimental channel. Gap widths for the pellets between two adjacent beryllium blocks were about 3 mm. A pellet packet was also attached on the front surface of the experimental assembly. The sample positions were -1, 52, 157, 261 and 366 mm, measured from the front surface of the assembly. After construction, the slab assembly was positioned at 200 mm distance from the 14-MeV neutron source.

The pellets were irradiated for ten hours with D-T neutrons. Total neutron yield was 1.01 X 10^{16} n. The irradiation history was recorded by using multi-channel scaling (MCS) to allow for the decay correction during irradiation.

Measurement of Induced β-activity

After neutron irradiation the ^{32}P activity produced in the pellets was measured with the Cherenkov radiation counting method. As no scintillator is required and chemical quenching is absent, sample preparation is extremely simple and the technique is ideal for the assay of ^{32}P in an aqueous solution. Also this technique allows for a reduction of experimental error because self-absorption and self-scattering corrections are not necessary for determination of absolute β-activity. Since Cherenkov radiation formed only small proportion of the total energy losses, a liquid scintillation counting system (Oken LSC-7100) capable of detecting very weak light pulses was used for this measurement.

In order to eliminate the effect of absorption of phosphorous-32 onto vial walls, 60 μg of inactive $NH_4PH_2O_2$ carrier was dissolved in 15 ml of water before dissolution of the pellet. Aqueous solutions were assayed in 20 ml opaque teflon vials which were found to yield a higher counting efficiency than low background glass vials presumably owing to diffusion of the directional Cherenkov emissions.

Impurities in the irradiated pellets were analyzed by their radioactive decays. Counting immediately after the irradiation showed existance of some short-lived radioactive nuclides in the pellets. The most important radio-nuclei was the ^{31}Si ($T_{1/2}$ = 2.62 hours) formed by the $^{34}S(n,\alpha)^{31}Si$ reaction. After one day cooling, these activities eliminated. It was considered that the ^{35}S ($T_{1/2}$ = 87 days) and ^{33}P ($T_{1/2}$ = 25.3 days) radionuclides which could be formed in the pellet gave no counts because their β-energies were below the Cherenkov threshold in water. With these precautions, the measured β-activity was found to decay with the exact half-life of ^{32}P. For a few selected irradiated pellets, the decay was followed for seven half-lives and no impurity activity was observed.

Although the $^{33}S(n,np)^{32}P$ reaction contributed to the production of ^{32}P activities, it was not considered in this measurement. The omission was justified because of considerably low isotopic abundance of ^{32}S and relatively low cross section of the

$^{33}S(n,np)^{32}P$ reaction around 14 MeV.

The counting efficiency was determined by adding 1 ml of a certified solution of ^{32}P activity (2.5% accuracy), obtained from Commissariat à l'Energie Atomique / France, to a vial containing the solution of interest. Variations of solution volume gave an insignificant effect on counting efficiency in the range from 12 to 17 ml. Efficiency (ε) was calculated by the following equation:

$$\varepsilon(\%) = \frac{N_1 - N_2}{Number\ of\ ^{32}P\ decays\ per\ minute} \times 100 \qquad (2\text{-}8)$$

where, N_1 - number of counts per minute after adding of standard solution, and

N_2 - number of counts per minute before adding of standard solution.

As a result, the counting efficiency of ^{32}P was found to be 52.2 %. Although this is lower than the efficiency of liquid scintillation counting, the minimum detectable level of ^{32}P activity was much lower than the liquid scintillation counting methd because the Cherenkov background activity was lower and the volume of the aqueous sample for counting was much lager.

The reaction rate, RR, was then derived from the β-ray counts following application of the necessary corrections. The RR is given as,

$$RR = \frac{\lambda \cdot C \cdot A}{\varepsilon \cdot W \cdot N_a \cdot a \cdot b \cdot Y \cdot S_a \cdot \left(1 - exp(-\lambda \cdot t_i)\right) \cdot exp(-\lambda \cdot t_c) \cdot \left(1 - exp(-\lambda \cdot t_m)\right)}, \qquad (2\text{-}9)$$

where,

λ : decay constant (1/sec),

C : Cherenkov counts,

A : atomic mass,

ε : counting efficiency,

N_a : Avogadro's number,

a : natural abundance of the target nuclei,

b : branching ratio,

Y : neutron source strength (n/sec),

S_a : correction factor for the decay during irradiation, and

$t_{i,c,m}$: irradiation, cooling, and collection times, respectivily.

The neutron yield fluctuation monitored with MCS was used for determining the correction factor S_a.

Experimental Error

Major sources of the error in the reaction rate were the counting efficiency of Cherenkov radiation (3.1 %), the neutron yield (2 %) and the counting statistics (1 %). The errors associated with weight, irradiation time, cooling time and counting time were estimated to be less than 0.2 %. A typical experimental error for the reaction rate was 3.8 %.

2.3.7 Gamma-Ray Spectrum by BC537

Gamma-Ray Spectrometer

Prompt gamma-ray spectra in the assembly were measured by an in-situ gamma-ray spectrometer. Because hydrogen and boron nuclei have large cross section for low energy neutrons and emit unnecessary gamma-rays following the $^{1}H(n,\gamma)^{2}H$ and $^{10}B(n,\alpha)^{7}Li^{*}$ reactions, the spectrometer is specially designed. Hydrogen-1 nuclei contained in usual organic scintillator and boron-10 nuclei in boric-silicic glass container are eliminated by using the deuterated liquid organic scintillator, BC537 (BICRON, USA), with a quartz glass container. Figur 2.3.11 illustrates the spectrometer. The scintillator is in spherical shape of 40 mm in diameter. Outer dimensions of the detector are 48 mm in diameter and 262 mm in length including a photomultiplier assembly.

Measurement

The spectrometer was inserted into the experimental channel of 50 mm in diameter or 51 mm x 51 mm square, and void space around cables connected to the spectrometer was filled with the same material as the assembly. Pulse height spectra from the spectrometer were measured during D-T neutron irradiation. The electronic circuit employed for the measurement is shown in Fig. 2.3.12. The pulse shape discrimination technique was adopted to reject neutron events from gamma-ray events. Two different gains were simultaneously adopted to obtain gamma-ray spectra in a wide energy range. Energy scales of the measured pulse-height spectra were calibrated with 1.275 MeV gamma-rays from a sodium-22 source. In a measurement of prompt gamma-rays, it is important to explicitly reject decay gamma-rays emitted by disintegrations of radioactive nuclei produced by activation reactions. To measure pulse height spectra due to decay gamma-rays accurately, the pulsed neutron method [26] was adopted. Figure 2.3.13 illustrates the pulsed neutron method.

Data Processing

The measured pulse-height spectra after subtraction of decay gamma-ray spectra were unfolded with the FORIST code [13] to obtain the energy spectra. The response matrix used in the unfolding procedure was calculated with the MARTHA code [27]. As the original MARTHA code was for NaI(Tl) scintillators, the cross section data in the code was replaced for the BC537 scintillator.

It was confirmed that a number of gamma-rays from several calibrated sources can be estimated with an accuracy of 3% by the same procedure. In general, however, the measured spectrum fluxes in these assemblies were observed larger than those with an ideal infinitesimal detector, because attenuation of gamma-ray fluxes in the detector was smaller than that in the materials of the assemblies. To correct the overestimation, the measured spectra were normalized to the measured gamma-ray heating rates by TLD because the detector size effect of the TLD measurement was negligibly small. The normalization factor, F, was determined by the following formula;

$$F = \frac{H_\gamma^{TLD}}{\int_{E_0}^{\infty} \phi_\gamma^{exp}(E)\cdot f(E)\cdot dE} \cdot \frac{\int_{E_0}^{\infty} \phi_\gamma^{cal}(E)\cdot f(E)\cdot dE}{\int_{0}^{\infty} \phi_\gamma^{cal}(E)\cdot f(E)\cdot dE} \qquad (2\text{-}10)$$

where

H_γ^{TLD}: measured gamma-ray heating rate with TLD,
$\phi_\gamma^{exp}(E)$: measured gamma-ray spectrum,
$\phi_\gamma^{cal}(E)$: calculated gamma-ray spectrum, and
$f(E)$: gamma-ray KERMA factors.

In Eq. (2-10), the lack of the experimental spectrum below the lowest energy E_0 is supplemented by considering the shape of a calculated gamma-ray spectrum, i.e., ratios of gamma-ray heating rates above E_0 to total gamma-ray heating rates were multiplyed as shown in Eq. (2-10). The factors are calculated for all the detector positions, and found to be nearly constant around 0.68. Hence the factor of 0.68 is commonly adopted to all the measured spectra.

Experimental Uncertainty

As to be explained in the next section, typical experimental uncertainties of the gamma-ray heating rate measured by TLDs range between 7 ~ 15 %. The gamma-ray spectra are normalized to the gamma-ray heating rates. About 10 % of uncertainties are introduced by the normalization procedure. All of the rest of experimental uncertainties, such as statistical errors, uncertainties of the response functions, determination of source D-T neutrons and subtraction of decay gamma-rays, are less than 5 %. Therefore, total experimental uncertainties are approximately 15 ~ 20 %. Note that only the statistical erorrs are indicated to the experimental data shown in the chapter 3.

2.3.8 Gamma-Ray Heating Rate by TLD

Experimental Method

Gamma-ray heating rate increases monotonously as a function of atomic numbers of probe materials. Basing on this principle, gamma-ray heating rates of materials can be deduced by interpolating the gamma-ray heating rates measured by several types of thermoluminescence dosimeters (TLDs) having different atomic numbers.[28] Gamma-ray heating rates in vanadium, iron and tungsten assembies were measured with applying the interpolation method. Three types of TLDs, Mg_2SiO_4 (MSO, effective atomic number Z_{eff} = 11.1), Sr_2SiO_4 (SSO, Z_{eff} = 32.5) and Ba_2SiO_4 (BSO, Z_{eff} = 49.9), were selected for the measurements. The atomic numbers of vanadium and iron, 23 and 26, respectively, were positioned between the effective atomic numbers of MSO and SSO. Although the BSO, whihc has fairly large atomic number of nearly 50, was used, the atomic number of

tungsten, 74, was still higher than that of BSO. Hnece, gamma-ray heating rates of tungsten were derived by extrapolations.

Irradiation

Four or six samples of each type of TLD were packed in an aluminum foil. The sample packets were inserted in the experimental channels and also put on the front surfaces of the assemblies. Irradiations were performed twice for short and long times to provide the optimum absorbed dose to the TLDs depending on the location. The short irradiation with source neutron yields of 0.5 ~ 1 x 10^{14} were for TLDs located near the D-T neutron source, while the long irradiation with source neutron yields of 1 ~ 2 x 10^{15} were for deeper positions far from the D-T neutron source.

Data Reduction

One week after the irradiation, thermoluminescence (TL) was measured by a TLD reader (Kasei Optonix, KYOKKO 2500). The measured TLs of four or six samples of each type of TLD are averaged. Neutron contributions to the response of TLDs were calculated by using neutron response functions and neutron energy spectra at each position, and were subtracted from the total responses. The neutron response functions were given by Yamaguchi et al. [29] Fractions of the neutron response to the total response were 20 ~ 50% at the front surface of the assemblies, and decrease to less than 5% at the deeper locations. The obtained TL was converted to gamma-ray heating rates of each type of TLD by correcting the differences of mass energy absorption coefficients of air and the TLD materials. Gamma-ray heating rates of vanadium and iron were derived by interpolations of the measured gamma-ray heating rates of MSO and SSO in terms of their effective atomic numbers. Uncertainties due to the interpolation procedure were considered to be small because the heating rates of MSO and SSO were nearly the same within ~ 10%. As for tungsten, gamma-ray heating rates measured by BSO were extrapolated with the help of calculated gamma-ray heating rates for BSO (Z_{eff}=49.9) and tungsten (Z=74). Finally, contributions of target gamma-rays which were emitted from the target by interactions of source D-T neutrons with the structural materials were calculated and subtracted from the measured gamma-ray heating rates. The fractions of target gamma-rays to the total gamma-ray heating rates were ~ 20 % at the front surface of the assemblies, and smaller than 3% at the positions deeper than 100 mm.

Experimental Error

Error sources of the measured gamma-ray heating rates are as follows.

Statistical deviation of four TLDs	5 - 15 %
Number of neutrons generated	2 - 3 %
Calibration of the TLD reader	5 %

In the subtraction of target gamma-rays and neutron response, the following uncertainties are added to the above errors according to the quadratic propagation of error.

Response functions for neutrons	30 %
Neutron energy spectra	10 %
Target gamma-ray	20 %

Overall errors for the obtained gamma-ray heating rates of vanadium and iron are ~ 10% except the positions at the front surface of the assemblies where errors are 20 ~ 25 %. For tungsten, the overall experimental errors are rather large about 20 % even in the experimental assembly due to the extrapolation.

3. Experimental Data

3.1 Beryllium

The first benchmark experiment on beryllium had been already conducted in 1988. The experimental data have been already reported in Ref. 6), and results of the experimental analysis have been discussed in Ref. 30). After that, a neutron spectrum between 1 eV and 10 keV, and dosimetry reaction rates of $^{6}Li(n,\alpha)^{3}T$, $^{7}Li(n,n\alpha)^{3}T$, $^{31}P(n,\gamma)^{32}P$, $^{32}S(n,p)^{32}P$ and $^{35}Cl(n,\alpha)^{32}P$ reactions were measured. Table 3.1.1 summarizes the atomic densities of the beryllium assembly.

The measured neutron spectrum between 1 eV and 10 keV is shown in Fig. 3.1.1 with previously obtained neutron spectra above 3 keV, and Table 3.1.2 summarizes the numerical data. Although experimental errors of the newly measured spectrum above 1 keV are rather large, the presently measured spectrum is combined smoothly with the previously measured data by PRC.

The measured dosimetry reaction rates are listed in Table 3.1.3. The tritium production rates by the $^{6}Li(n,\alpha)^{3}T$ and $^{7}Li(n,n\alpha)^{3}T$ reactions have been also measured in the previous experiment. Although the detector positions are different from the present and the previous experiment, both data are consistent each other. When the two non-threshold reaction rates, i.e., $^{6}Li(n,\alpha)^{3}T$ and $^{31}P(n,\gamma)^{32}P$ reactions, are compared with transport calculations with considering the impurities shown in Table 3.1.2, the experimental data are always smaller than the calculated results. This reason could be explained by possible unknown impurities introduced in the beryllium assembly. Most of the non-threshold reactions in the beryllium assembly are caused by thermal neutrons because the radiative neutron capture cross section of beryllium is extremely small and a great number of neutrons are accumulated in the thermal energy region. If impurities exist in the beryllium assembly, the thermal neutron flux is largely reduced by neutron capture reactions by the impurities. This impurity effect results in smaller experimental reaction rates for the non-threshold reactions.

The measured three threshold reactions, i.e., the $^{7}Li(n,n\alpha)^{3}T$, $^{32}S(n,p)^{32}P$ and $^{35}Cl(n,\alpha)^{32}P$ reactions, are almost in proportion with each other. The measured non-threshold reactions, i.e., $^{6}Li(n,\alpha)^{3}T$ and $^{31}P(n,\gamma)^{32}P$ reactions, are also in proportion with each other. The proportional characteristic indicates that the $^{32}S(n,p)^{32}P$ and $^{35}Cl(n,\alpha)^{32}P$ reactions and the $^{31}P(n,\gamma)^{32}P$ reaction can be used as reaction indeces for tritium production reactions, the $^{7}Li(n,n\alpha)^{3}T$ and $^{6}Li(n,\alpha)^{3}T$ reactions, respectively, required for fusion blanket benchmark experiments. The advantages of the indeces are (1) the simplicity for preparation of samples for the Cherenkov radiation counting compared with the samples for the tritium counting with a liquid scintillation counting system, and (ii) high counting rates of the ^{32}P measurement with the Cherenkov radiation counting method compared to the tritium measurement with the liquid scintillation counting method. In fact, the ^{32}P activity can be measured at all the detector positions owing to the high counting rate

while the tritium measurement of the $^{7}Li(n,n\alpha)^{3}T$ reaction is limited only up to the 52 mm depth in the beryllium assembly.

3.2 Vanadium

The leakage neutron spectrum measurement from spherical vanadium shells of 35 and 105 mm in thickness in the energy range above 0.07 MeV done by Möllendorff et al. was the unique existing benchmark experiment. [31] For validation of low energy neutron cross sections and secondary gamma-ray data for vanadium, there had been no benchmark experimental data. The experiment was performed under the IEA collaboration on the sub-task "Fusion Neutronics" for the Work Item #1 "Integral Experiment for advanced structural and breeder materials". Our benchmark experiment provides comprehensive experimental data, i.e., neutron energy spectra in the entire energy region, various dosimetry reaction rates, gamma-ray spectra and gamma-ray heating rates, needed for validation of nuclear data files. The experimental data related to low energy neutrons below 70 keV and secondary gamma-ray data are the first benchmark experimental data on vanadium. Results of experimental analysis are briefly reported in Ref. 32).

Table 3.2.1 summarises the atomic densities of the vanadium assembly and the surrounding graphite reflector. The measured neutron spectra by the three methods at the positions of 76 mm and 178 mm in depth are shown in Figs. 3.2.1 and 3.2.2. The numerical data of the spectra measured by the NE213, PRC and the SDT method are shown in Tables 3.2.2 ~ 3.2.4, respectively. Table 3.2.5 summarises integral neutron fluxes derived from the measured neutron spetra. The meausred dosimetry reaction rates are shown in Table 3.2.6. The measured gamma-ray spectra at the positions of 76 mm and 178 mm in depth are shown in Figs. 3.2.3 and 3.2.4. The numerical data of the spectra are shown in Table 3.2.7. Table 3.2.8 summarises the measured gamma-ray heating rates of vanadium.

3.3 Iron

The first benchmark experiment on iron was conducted in 1986, and neutron spectra > 2 MeV and dosimetry reaction rates in an iron assembly of 1000 mm in diameter and 950 m in thickness were measured. The results were reported in Ref. 33). Neutron spectra of 3 keV - 1 MeV in the same iron assembly were measured in 1990, and the results were published in Ref. 34). Then, the experiment was extended for lower energy neutrons and secondary gamma-rays. Neutron spectra below 10 keV were measured in 1993, and results of the experimental analysis were published in Ref. 20). Gamma-ray spectra and gamma-ray heating rates were measured in 1994, and results of the experimental analysis were published in Ref. 26). This report summarizes these

experimental data.

Table 3.3.1 summarizes the atomic densities of the iron assembly. The measured neutron spectra by the three methods at various positions are shown in Fig. 3.3.1. The numerical data of the spectra measured by the NE213, PRC and the SDT method are shown in Tables 3.3.2 ~ 3.3.4, respectively. Table 3.3.5 summarizes integral neutron fluxes derived from the measured neutron spectra. The measured neutron spectra in the energy range of 2 ~ 10 MeV by NE213 seems to be distorted by the unfolding process. Comparisons of the measured neutron spectra with calculations in the energy range are sometimes not meaningful. The integral fluxes are useful for numerical comparison of the measured and calculated neutron spectra. The measured dosimetry reaction rates are shown in Table 3.3.6.

The measured gamma-ray spectra at the positions of 100, 300, 500 and 700 mm in depth are shown in Figs. 3.3.2 ~ 3.3.5. The numerical data of the spectra are shown in Table 3.3.7. Table 3.3.8 summarizes the measured gamma-ray heating rates of iron. These experimental gamma-ray data on iron are useful for validating gamma-ray production cross section in evaluated nuclear data files at various incident neutron energy. According to the detailed experimental analysis, more than 90 % of observed gamma-rays at the 100 mm position are produced by neutrons of > 1 MeV mainly inducing the threshold reactions. At the 500 and 700 mm positions, contributions of neutrons of > 1 MeV on gamma-ray production are less than 10 % while most of gamma-rays are produced by low energy neutrons of 1 eV ~ 1 MeV mainly with the (n,γ) reactions.

3.4 Copper

A benchmark experiment on copper was performed in 1991. The experimental data have been summarized in Ref. 7), and also published with analytical results in Refs. 35) and 36). After that, low energy neutron spectra below 10 keV were measured. The experimental data of the low energy neutron spectra are included in this report.

Table 3.4.1 summarizes the material specifications of the copper assembly. Neutron spectra at four positions in the copper assembly measured by the SDT method are shown in Figs. 3.4.1 ~ 3.4.4 together with the previously obtained neutron spectra by NE213 and PRC. The neutron spectra measured by the three methods connect smoothly at the joint energy at ~ 5 keV and 1 MeV. Numerical data of the neutron spectra by the SDT method are shown in Table 3.4.2.

3.5 Tungsten

A benchmark experiment on tungsten was conducted in 1993. Experimental data for neutron spectra from 14 MeV to 3 keV, dosimetry reaction rates, gamma-ray spectra and gamma-ray heating rates were obtained. The results were reported briefly

in Ref. 37). All the experimental data are included in this report.

Table 3.5.1 summarizes the material specifications of the tungsten assembly. The tungsten is not pure, but an alloy with a small amount of nickel and copper. The measured neutron spectra by NE213 and PRC at three positions of 76, 228 and 380 mm in the tungsten assembly are shown in Figs. 3.5.1 ~ 3.5.3. The numerical data of the spectra measured by the NE213 and PRC are given in Tables 3.5.2 and 3.5.3, respectively. A measurement of neutron spectra below 10 keV by the SDT method was attempted. However, it could not be made because of too low neutron flux in the energy range. The measured dosimetry reaction rates are shown in Table 3.5.4.

The measured gamma-ray spectra at the three positions in the tungsten assembly are shown in Figs. 3.5.4 ~ 3.5.6. The numerical data of the spectra are given in Table 3.5.5. Table 3.5.6 summarizes the measured gamma-ray heating rates of tungsten. Most of the observed gamma-rays at the front surface of the assembly, 0 mm, are produced by high energy neutrons of > 1 MeV. At 76 mm, both halves of observed gamma-rays are produced by neutrons of > 1 MeV and 0.01 ~ 1 MeV. At 228 and 380 mm, low energy neutrons of 1 keV ~ 1 MeV contribute predominantly to produce secondary gamma-rays.

4. Summary

Efforts to acquire fusion neutronics experimental data have been continued on the clean benchmark experiment at FNS/JAERI. Experimental data for new materials, i.e., vanadium and tungsten, were obtained. Several experiments which had been performed previously were extended to complete more comprehensive experimental data set with introducing new experimental techniques. Especially, experimental data related to low energy neutrons and secondary gamma-rays were supplemented.

These experimental data have been contributed to benchmark test of recent evaluated nuclear data files, such as JENDL-3.2, JENDL Fusion File and FENDL/E-2.0. These data are expected to serve for further benchmark test of forthcoming evaluated nuclear data files, and then, for more accurate nuclear designs of fusion reactors.

Acknowledgment

The authors gratefully acknowledge the operating staff of FNS for their operation of FNS. They wish to express their gratitude to Drs. H. Maekawa and M. Sugimoto for their great support to the work.

The authors also gratefully acknowledge the co-experimentalists for their efforts to obtain the experimental data. Dr. Y. Verzilov, who was a visiting scientist of JAERI from Russia, contributed the tritium and ^{32}P measurements for the beryllium experiment by introducing new experimental techniques. Drs. I. Murata and Kokooo from Osaka university contributed to the vanadium experiment. Dr. K. Oishi contributed significantly for the iron experiment.

References

1) Nakamura T., Maekawa H., Ikeda Y. and Oyama Y.: "A DT Neutron Source for Fusion Neutronics Experiments at the JAERI", Proc. International. Ion Eng. Congress - ISIAT '83 & IAPT '83, Kyoto, Japan, Vol. 1, pp. 567-570 (1983).

2) Shibata K., et al.: "Japanese Evaluated Nuclear Data Library, Version-3 -- JENDL-3 --", JAERI 1319 (1990).

3) Ganesan S. and McLaughin P. K., "FENDL/E Evaluated Nuclear Data Library of Neutron Nuclear Interaction Cross-Sections and Photon Production Cross-Sections and Photon-Atom Interaction Cross Sections for Fusion Applications Version 1.0 of May 1994", IAEA-NDS-128, International Atomic Energy Agency (1995).

4) Maekawa H., et al.: "Fusion Blanket Benchmark Experiments on a 60 cm-thick Lithium-Oxide Cylindrical Assembly", JAERI-M 86-182 (1986).

5) Maekawa H., et al.: "Benchmark Experiments on a 60 cm-thick Graphite Cylindrical Assembly", JAERI-M 88-034 (1988).

6) Sub Working Group of Fusion Reactor Physics Subcommittee (Ed.): "Collection of Experimental Data for Fusion Neutronics Benchmark", JAERI-M 94-014 (1994).

7) Maekawa F., et al.: "Benchmark Experiment on a copper Slab Assembly Bombarded by D-T Neutrons", JAERI-M 94-038 (1994).

8) Konno C., et al.: "Bulk Shielding Experiments on Large SS316 Assemblies Bombarded by D-T Neutrons Volume I: Experiment", JAERI-Research 94-043 (1994).

9) Maekawa H., Ikeda Y., Oyama Y., Yamaguchi S. and Nakamura T.: "Neutron Yield Monitors for the Fusion Neutronics Source (FNS) -- for 80° Beam Line --", JAERI-M 83-219 (1983).

10) Briesmeister J. F. (Ed.): "MCNP - A General Monte Carlo N-Particle Transport Code, Version 4A", LA-12625-M, Los Alamos National Laboratory (1993).

11) Maekawa F., et al.: "Bulk Shielding Experiments on Large SS316 Assemblies Bombarded by D-T Neutrons Volume II: Analysis", JAERI-Research 94-044 (1994).

12) Oyama Y., Tanaka S., Tsuda K., Ikeda Y. and Maekawa H.: Nucl. Instrum. Meth., A256, 333 (1987).

13) FORIST Spectrum Unfolding Code: Radiation Shielding Information Center, Oak Ridge National Laboratory, PSR-92 (1975).

14) Nakashima H.: "Study on Shielding Design Methods for Fusion Reactors Using Benchmark Experiments", pp. 20-45, JAERI-M 92-025 (1992, in Japanese).

15) Bennett E. F.: "A Continuous Mode Data Acquisition Technique for Proton Recoil Proportional Counter Neutron Spectrometers", ANL/FPP/TM-239, Argonne National Laboratory (1989).

16) Bennett E. F.: "Induction Filtering for Proportional Counter Amplifiers", ANL/FPP/TM-234, Argonne National Laboratory (1989).

17) Konno C., Ikeda Y., Kosako K., Oyama Y., Maekawa H., Nakamura T. and Bennett E. F.: Fusion Eng. Des., 18, 297 (1991).

18) Maekawa F. and Oyama Y.: Nucl. Instrum. Meth., A372, 262 (1996).

19) Maekawa F. and Oyama Y.: "Measurement of Low Energy Neutron Spectrum below 10 keV Inside Various Media with the Slowing Down Time Method", Proc. 9th International Symposium on Reactor Dosimetry, Prague, Czech Republic, Sep. 2-6, 1996, to be published (1998).

20) Maekawa F. and Oyama Y.: Nucl. Sci. Eng., 125, 205 (1997).

21) Nakazawa M., Kobayashi K., Iwasaki S., Iguchi T., Sakurai K., Ikeda Y. and Nakagawa T.: "JENDL Dosimetry File", JAERI 1325 (1991).

22) Verzilov Y., Maekawa F. and Oyama Y.: J. Nucl. Sci. Technol., 33, 390 (1996).

23) Verzilov Y., Maekawa F., Oyama Y. and Maekawa H.: "A New Method of Extracting Tritium Produced in Neutron Irradiated Lithium-Containing Pellets for Liquid Scintillation Counting", JAERI-Research 94-042 (1994).

24) Pashchenko A. B.: "Summary Report for IAEA Consultants' Meeting on Selection of Evaluations for the FENDL/A-2 Activation Cross Section Library", INDC(NDS)-341, International Atomic Energy Agency (1996).

25) Verzilov Y., Maekawa F., Oyama Y. and Ikeda Y.: Fusion Eng. Des., 37, 95 (1997).

26) Maekawa F., Oyama Y., Konno C., Wada M. and Ikeda Y.: Nucl. Sci. Eng., 126, 187 (1997).

27) Saito K. and Moriuchi S.: Nucl. Instrum. Meth. 185, 299 (1981).

28) Tanaka S. and Sasamoto N: J. Nucl. Sci. Technol., 22, 109 (1985).

29) Yamaguchi S., et al.: Fusion Eng. Des., 10, 163 (1989).

30) Maekawa H., et al.: Fusion Technol., 19, 1949 (1991).

31) Möllendorff U., et al.: "A 14-MeV Neutron Transmission Experiment on Vanadium", Proc. 19th Symposium on Fusion Technology, Lisbon, September 16-21, 1996, pp. 1575-1578 (1997).

32) Maekawa F., et al.: "Benchmark Experiment on Vanadium Assembly with D-T Neutrons - In-situ Measurement -", Proc. '97 Symposium on Nuclear Data, JAERI/Tokai, Nov. 27-28, 1997, JAERI-Conf 98-003, pp. 168-173 (1998).

33) Oishi K., Ikeda Y., Konno C. and Nakamura T.: "Measurement and Analysis of Neutron Spectra in a Large Cylindrical Iron Assembly Irradiated by 14 MeV Neutrons", Proc. 7th International. Conference Radiation Shielding, Bournemouth, United Kingdom, Sept. 12-16, 1988, pp. 331-340, United Kingdom Atomic Energy Authority, Winfrith and the Organization for Economic Cooperation and Development, Nuclear Energy Agency (1988).

34) Konno C., Ikeda Y., Kosako K., Oyama Y., Maekawa H., Nakamura T. and Bennet E. F.: Fusion Eng. Des., 18, 297 (1991).

35) Konno C., Maekawa F., Oyama Y., Ikeda Y. and Maekawa H.: Fusion Eng. Des., 28, 745 (1995).

36) Maekawa F., Oyama Y., Konno C., Ikeda Y. and Maekawa H.: Fusion Eng. Des., 28, 753 (1995).

37) Maekawa F., Konno C., Oyama Y., Wada M., Uno Y. and Ikeda Y.: "Benchmark Experiment on Tungsten Assembly Bombarded with D-T Neutrons", Proc. International Conference on Nucl. Data for Science and Technology, Trieste, Italy, May 19-24, 1997, pp. 1218-1220 (1998).

Table 1 Summary of experimental data obtained so far in the clean benchmark experiment conducted at FNS.

Material	Neutron Spectrum			Reaction Rate					Gamma-Ray Spectrum	Gamma-Ray Heating
	NE213 Scintillator	P-Recoil Counter	Slowing Down Time	Foil Activation	Fission Chamber	Li-Pellet	Li-Glass Scintillator	^{32}P Counting	BC537 Scintillator	TLD
Li_2O	(1), (3)			(1), (3)	(1), (3)	(1), (3)	(1), (3)			
Be	(3)	(3)	●	(3)	(3)	(3), ●	(3)	●		
C	(2), (3)			(2), (3)	(2), (3)					
V	●	●	●	●					●	●
Fe	●	●	●	●					●	●
Cu	(4)	(4)	●	(4)					(4)	(4)
W	●	●		●					●	●
SS316	(5)	(5)	(5)	(5)	(5)				(5)	(5)

(1) JAERI-M 86-182
(2) JAERI-M 88-034
(3) JAERI-M 94-014
(4) JAERI-M 94-038
(5) JAERI-Research 94-043
● Experimental data are contained in this report.

Table 2.1.1 Dimensions of the experimental assemblies.

Material	Dimension [mm]
Beryllium	629 ϕ x 456 t quasi-cylinder
Vanadium	254 x 254 x 254 cube with a graphite reflector of 51 mm in thickness
Iron	1000 ϕ x 950 t cilinder
Copper	629 ϕ x 608 t quasi-cylinder
Tungsten	629 ϕ x 507 t quasi-cylinder

Table 2.3.1 Systematic errors in various energy range involved in the neutron spectra measured by the NE213 spectrometer. Errors expected in the range below 10 MeV originate from the response error of 14.8 MeV neutrons.

Energy range [MeV]	Efficiency	Energy Calibration	Neutron Source	Response Shape [fraction*1]	Total
>10	± 2 %	± 3 %	± 2 %	1	± 4 %
8.3 - 10.1	2	2	2	~ - 0.02	- 20 %*2
5.8 - 8.3	2	2	2	~ - 0.01	- 11%*2
4.1 - 5.8	2	2	2	~ - 0.001	- 3.4%*2
2.0 - 4.1	2	2	2	~ + 0.01	+ 3.5%*2
1.1 - 2.0	2	2	2	~ + 0.01	+ 3.5%*2

*1 Ratio of the error due to the response to the peak flux around 14 MeV.

*2 Example in the case of $\Phi_{peak}/\Phi(E_n) \sim 10$.

Table 2.3.2 Typical qualities of the measured neutron spectra by the SDT method in the four experimental assemblies.

Medium	Energy resolution below 1 keV in FWHM [%]	Correction factors for effective cross sections [%]	Overall experimental uncertainty	
			< 1 keV [%]	1-10 keV [%]
Be	130	12	7 ~ 12	12 ~ 26
V	50 ~ 100	2 ~ 10	11 ~ 40	-
Fe, Cu	50 ~ 200	1 ~ 20	6 ~ 18	20 ~ 63

Table 2.3.3 Dosimetry Reactions used in the foil activation method.

Reaction	Half-Life	Abundance (%)	γ-ray Energy (keV)	γ-ray Branching (%)	Threshold Energy (MeV)
$^{27}Al(n,\alpha)^{24}Na$	15.02 h	100.0	1368.6	100.0	5
$^{56}Fe(n,p)^{56}Mn$	2.579 h	91.72	846.8	98.9	5
$^{90}Zr(n,2n)^{89}Zr$	3.268 d	51.45	909.2	99.01	12
$^{93}Nb(n,2n)^{92m}Nb$	10.15 d	100.0	934.5	99.0	9
$^{115}In(n,n')^{115m}In$	4.486 h	95.7	336.3	45.8	0.34
$^{186}W(n,\gamma)^{187}W$	23.85 h	28.4	479.5	23.4	---
$^{197}Au(n,\gamma)^{198}Au$	2.694 d	100.0	411.8	95.5	---

Table 2.3.4 Characteristics of the compounds used in the ^{32}P measurement.

Reaction	Threshold Energy (MeV)	Compound	Purity (%)	Isotopic Content (%)
$^{31}P(n,\gamma)^{32}P$	---	$NH_4PH_2O_2$	99.9	^{31}P - 100.0
$^{32}S(n,p)^{32}P$	2.3	$CH_3SO_2CH_3$	99.9	^{32}S - 95.02 ^{33}S - 0.75 ^{34}S - 4.22 ^{36}S - 0.02
$^{35}Cl(n,\alpha)^{32}P$	3.7	NH_4Cl	99.6	^{35}Cl - 75.47 ^{37}Cl - 24.23

Table 3.1.1 Material specification for the beryllium assembly.

Atomic Density [x10^{24}atoms/cm^3]	
Be	1.2152 x 10^{-1}
C	7.7109 x 10^{-5}
O	4.9713 x 10^{-4}
Al	2.9013 x 10^{-5}
Fe	2.4678 x 10^{-5}

Table 3.1.2 Neutron spectrum in the beryllium assembly measured by the SDT method in the unit of [n / cm^2 / lethargy / source].

Neutron Energy [MeV]	Flux at z=127mm	Absolute Error
1.26e-06	2.35e-05	1.63e-06
2.00e-06	2.31e-05	1.60e-06
3.16e-06	2.29e-05	1.60e-06
5.01e-06	2.32e-05	1.62e-06
7.94e-06	2.31e-05	1.62e-06
1.26e-05	2.39e-05	1.69e-06
2.00e-05	2.37e-05	1.70e-06
3.16e-05	2.38e-05	1.73e-06
5.01e-05	2.42e-05	1.79e-06
7.94e-05	2.43e-05	1.85e-06
1.26e-04	2.51e-05	2.28e-06
2.00e-04	2.52e-05	2.38e-06
3.16e-04	2.59e-05	2.58e-06
5.01e-04	2.61e-05	2.81e-06
7.94e-04	2.71e-05	3.22e-06
1.26e-03	2.68e-05	3.57e-06
2.00e-03	2.83e-05	4.36e-06
3.16e-03	2.94e-05	5.29e-06
5.01e-03	3.16e-05	6.77e-06
7.94e-03	3.16e-05	8.15e-06

Table 3.1.3 Measured dosimetry reaction rates in the beryllium assembly in the unit of [reactions / atom / source]. Numbers in the parenthesis are percentage errors.

Position [mm]	Reaction				
	^{6}Li(n,α)T	^{7}Li(n,n'α)T	^{31}P(n,γ)^{32}P	^{32}S(n,p)^{32}P	^{35}Cl(n,α)^{32}P
-1		6.93e-29 (4.5)		5.53e-29 (3.8)	2.79e-29 (3.8)
52	2.00e-25 (4.5)	5.06e-29 (10.0)	4.82e-29 (3.8)	4.00e-29 (3.8)	2.00e-29 (3.8)
157	3.49e-25 (4.5)		8.27e-29 (3.8)	1.36e-29 (3.8)	6.73e-29 (3.8)
261	2.74e-25 (4.5)		6.34e-29 (3.8)	4.16e-30 (3.8)	2.07e-30 (3.8)
366	1.31e-25 (4.5)		3.03e-29 (3.8)	1.20e-30 (3.8)	6.00e-31 (3.8)
470	9.47e-27 (4.5)		2.36e-30 (3.8)	2.96e-31 (3.8)	1.52e-31 (3.8)

Table 3.2.1 Material specification for the vanadium assembly.

	Vanadium	Graphite
Chemical Composition	V 99.777 wt% Al 0.073 wt% Si 0.108 wt% Fe 0.042 wt%	C 100 wt%
Weight Density	6.033 [g/cm^3]	1.625 [g/cm^3]

Table 3.2.2 Neutron spectra in the vanadium assembly measured by the NE213 spectrometer in the unit of [n / cm^2 / lethargy / source].

Neutron Energy [MeV]	Flux at z= 76 mm	Absolute Error	Window [%]	Flux at z= 178 mm	Absolute Error	Window [%]
1.553e+00	5.17e-05	2.44e-06	32.5	1.65e-05	8.26e-07	31.2
1.633e+00	5.05e-05	2.47e-06	31.9	1.71e-05	8.00e-07	29.4
1.717e+00	4.72e-05	2.17e-06	32.3	1.72e-05	7.44e-07	28.5
1.805e+00	4.36e-05	1.95e-06	33.0	1.68e-05	8.14e-07	27.9
1.897e+00	4.10e-05	2.11e-06	32.8	1.62e-05	8.52e-07	27.3
1.995e+00	4.03e-05	2.19e-06	31.8	1.57e-05	7.88e-07	26.9
2.097e+00	4.12e-05	2.10e-06	30.4	1.54e-05	7.60e-07	26.1
2.204e+00	4.30e-05	2.05e-06	28.4	1.54e-05	7.67e-07	25.0
2.317e+00	4.41e-05	1.98e-06	26.6	1.53e-05	7.53e-07	24.2
2.436e+00	4.33e-05	1.94e-06	25.5	1.47e-05	6.82e-07	23.9
2.561e+00	4.05e-05	2.01e-06	25.4	1.36e-05	6.75e-07	24.1
2.692e+00	3.69e-05	1.86e-06	26.4	1.23e-05	6.25e-07	24.8
2.830e+00	3.38e-05	1.73e-06	27.4	1.11e-05	5.65e-07	25.8
2.975e+00	3.13e-05	1.81e-06	28.1	1.01e-05	5.54e-07	26.7
3.128e+00	2.91e-05	1.76e-06	28.5	9.34e-06	4.88e-07	27.1
3.288e+00	2.69e-05	1.69e-06	28.3	8.74e-06	4.60e-07	26.7
3.457e+00	2.50e-05	1.54e-06	27.6	8.42e-06	4.26e-07	25.6
3.634e+00	2.39e-05	1.31e-06	26.8	8.36e-06	3.87e-07	24.5
3.820e+00	2.32e-05	1.18e-06	26.1	8.31e-06	3.68e-07	23.5
4.016e+00	2.23e-05	1.26e-06	25.3	7.97e-06	3.71e-07	23.0
4.222e+00	2.05e-05	1.36e-06	24.6	7.22e-06	3.69e-07	22.8
4.439e+00	1.83e-05	1.34e-06	23.9	6.28e-06	3.55e-07	23.0
4.666e+00	1.63e-05	1.28e-06	23.3	5.37e-06	3.37e-07	23.0
4.906e+00	1.45e-05	1.31e-06	22.7	4.63e-06	3.34e-07	22.7
5.157e+00	1.26e-05	1.36e-06	22.2	4.08e-06	3.34e-07	22.2
5.422e+00	1.04e-05	1.43e-06	21.7	3.70e-06	3.41e-07	21.7
5.700e+00	8.41e-06	1.51e-06	21.1	3.45e-06	3.55e-07	21.1
5.992e+00	7.36e-06	1.55e-06	20.6	3.33e-06	3.63e-07	20.6
6.299e+00	7.93e-06	1.69e-06	20.0	3.31e-06	3.86e-07	20.0
6.622e+00	9.75e-06	1.88e-06	19.5	3.31e-06	4.22e-07	19.5
6.961e+00	1.11e-05	1.94e-06	19.0	3.16e-06	4.38e-07	19.0
7.318e+00	1.06e-05	2.20e-06	18.5	2.86e-06	4.87e-07	18.5
7.694e+00	7.84e-06	2.57e-06	18.0	2.63e-06	5.63e-07	18.0
8.088e+00	3.26e-06	2.80e-06	17.6	2.61e-06	6.05e-07	17.6
8.503e+00	9.21e-08	3.22e-06	17.2	2.91e-06	6.77e-07	17.2
8.939e+00	1.96e-06	4.10e-06	16.8	3.19e-06	8.57e-07	16.8
9.397e+00	7.46e-06	4.53e-06	16.4	2.88e-06	9.29e-07	16.4
9.879e+00	1.16e-05	4.62e-06	15.9	2.86e-06	9.41e-07	15.9
1.039e+01	1.13e-05	5.22e-06	15.5	3.55e-06	1.08e-06	15.5
1.092e+01	8.56e-06	5.20e-06	15.1	3.94e-06	1.05e-06	15.1
1.148e+01	8.78e-06	5.17e-06	14.8	4.17e-06	1.04e-06	14.8
1.207e+01	1.05e-05	6.38e-06	14.5	4.51e-06	1.24e-06	14.5
1.268e+01	8.31e-06	8.42e-06	14.4	4.56e-06	1.58e-06	14.4
1.334e+01	5.04e-05	1.17e-05	14.4	1.06e-05	2.20e-06	14.4
1.402e+01	2.29e-04	1.35e-05	13.2	3.96e-05	2.48e-06	13.2
1.474e+01	4.02e-04	3.09e-05	13.2	7.01e-05	5.64e-06	13.2
1.549e+01	2.97e-04	9.26e-06	13.2	5.68e-05	1.73e-06	13.2
1.629e+01	1.32e-04	1.57e-05	13.2	3.06e-05	2.90e-06	12.6
1.712e+01	7.31e-05	8.94e-06	13.8	1.74e-05	1.60e-06	12.6
1.800e+01	3.29e-05	2.09e-06	14.4	7.06e-06	3.42e-07	12.5

Table 3.2.3 Neutron spectra in the vanadium assembly measured by the PRC in the unit of [n / cm^2 / lethargy / source]. (1/2)

Neutron Energy [MeV]	Flux at z=76mm	Absolute Error	Neutron Ennergy [MeV]	Flux at z=178mm	Absolute Error
2.003e-02	6.61e-06	2.51e-06	2.003e-02	1.497e-06	8.430e-07
2.098e-02	6.92e-06	2.48e-06	2.098e-02	3.892e-06	8.480e-07
2.197e-02	4.70e-06	2.53e-06	2.197e-02	4.711e-06	8.550e-07
2.301e-02	6.85e-06	2.55e-06	2.301e-02	3.667e-06	8.600e-07
2.410e-02	4.95e-06	2.61e-06	2.410e-02	3.585e-06	8.720e-07
2.524e-02	-1.75e-06	2.65e-06	2.524e-02	3.736e-06	8.800e-07
2.644e-02	1.04e-06	2.72e-06	2.644e-02	3.554e-06	8.960e-07
2.769e-02	5.83e-06	2.78e-06	2.769e-02	2.688e-06	9.040e-07
2.901e-02	7.04e-06	2.85e-06	2.901e-02	2.753e-06	9.230e-07
3.039e-02	7.18e-06	2.90e-06	3.039e-02	1.909e-06	9.360e-07
3.183e-02	5.64e-06	2.94e-06	3.183e-02	2.355e-06	9.590e-07
3.334e-02	1.06e-05	2.98e-06	3.334e-02	3.990e-06	9.750e-07
3.493e-02	9.82e-06	3.03e-06	3.493e-02	7.049e-06	9.900e-07
3.659e-02	8.39e-06	3.06e-06	3.659e-02	5.657e-06	1.000e-06
3.833e-02	8.85e-06	3.15e-06	3.833e-02	4.031e-06	1.020e-06
4.016e-02	8.99e-06	3.19e-06	4.016e-02	6.655e-06	1.030e-06
4.207e-02	9.57e-06	3.26e-06	4.207e-02	6.454e-06	1.050e-06
4.408e-02	1.07e-05	3.32e-06	4.408e-02	6.237e-06	1.070e-06
4.618e-02	1.24e-05	3.41e-06	4.618e-02	6.023e-06	1.100e-06
4.838e-02	1.30e-05	3.51e-06	4.838e-02	6.249e-06	1.130e-06
5.068e-02	1.71e-05	3.63e-06	5.068e-02	1.015e-05	1.170e-06
5.310e-02	2.90e-05	3.72e-06	5.310e-02	1.447e-05	1.210e-06
5.564e-02	2.73e-05	3.83e-06	5.564e-02	1.658e-05	1.240e-06
5.829e-02	1.80e-05	3.91e-06	5.829e-02	9.478e-06	1.270e-06
6.108e-02	1.15e-05	4.06e-06	6.108e-02	5.430e-06	1.320e-06
6.399e-02	6.14e-06	4.26e-06	6.399e-02	4.972e-06	1.380e-06
6.705e-02	1.55e-05	4.45e-06	6.705e-02	5.249e-06	1.440e-06
7.025e-02	3.03e-05	4.62e-06	7.025e-02	8.137e-06	1.510e-06
7.361e-02	1.47e-05	4.81e-06	7.361e-02	1.079e-05	1.570e-06
7.713e-02	1.25e-05	4.98e-06	7.713e-02	7.240e-06	1.650e-06
8.082e-02	2.32e-05	5.27e-06	8.082e-02	6.350e-06	1.730e-06
8.468e-02	2.74e-05	5.49e-06	8.468e-02	1.618e-05	1.810e-06
8.873e-02	4.30e-05	5.69e-06	8.873e-02	2.226e-05	1.890e-06
9.297e-02	5.09e-05	5.88e-06	9.297e-02	2.289e-05	1.960e-06
9.742e-02	3.53e-05	6.13e-06	9.742e-02	2.064e-05	2.040e-06
1.017e-01	6.06e-05	5.56e-06	1.033e-01	3.386e-05	2.490e-06
1.066e-01	5.15e-05	5.34e-06	1.082e-01	3.513e-05	2.370e-06
1.117e-01	3.31e-05	5.10e-06	1.134e-01	4.063e-05	2.260e-06
1.170e-01	3.69e-05	4.95e-06	1.189e-01	2.928e-05	2.160e-06
1.226e-01	3.20e-05	4.83e-06	1.245e-01	2.447e-05	2.080e-06
1.285e-01	4.50e-05	4.72e-06	1.305e-01	2.292e-05	2.020e-06
1.346e-01	4.99e-05	4.64e-06	1.367e-01	2.371e-05	1.970e-06
1.411e-01	4.95e-05	4.51e-06	1.433e-01	2.505e-05	1.930e-06
1.478e-01	5.70e-05	4.42e-06	1.502e-01	2.690e-05	1.890e-06
1.549e-01	5.17e-05	4.34e-06	1.574e-01	2.889e-05	1.860e-06
1.623e-01	5.20e-05	4.25e-06	1.649e-01	2.678e-05	1.810e-06
1.701e-01	5.51e-05	4.20e-06	1.728e-01	2.403e-05	1.790e-06
1.783e-01	4.13e-05	4.10e-06	1.811e-01	2.064e-05	1.760e-06
1.868e-01	3.64e-05	4.10e-06	1.897e-01	1.869e-05	1.750e-06
1.958e-01	3.96e-05	4.07e-06	1.988e-01	1.831e-05	1.750e-06
2.051e-01	4.33e-05	4.07e-06	2.084e-01	2.191e-05	1.740e-06
2.150e-01	4.40e-05	4.04e-06	2.183e-01	2.509e-05	1.730e-06
2.253e-01	5.84e-05	4.02e-06	2.288e-01	2.807e-05	1.720e-06
2.361e-01	4.91e-05	4.00e-06	2.398e-01	2.569e-05	1.700e-06
2.474e-01	4.73e-05	3.99e-06	2.513e-01	2.546e-05	1.700e-06
2.592e-01	5.49e-05	3.97e-06	2.633e-01	3.076e-05	1.680e-06
2.717e-01	6.58e-05	3.95e-06	2.759e-01	3.153e-05	1.670e-06
2.847e-01	5.77e-05	3.93e-06	2.892e-01	2.654e-05	1.660e-06
2.983e-01	5.37e-05	3.93e-06	3.030e-01	2.487e-05	1.660e-06
3.126e-01	4.89e-05	3.98e-06	3.176e-01	2.118e-05	1.690e-06
3.276e-01	5.21e-05	4.04e-06	3.328e-01	2.565e-05	1.730e-06
3.433e-01	5.72e-05	4.16e-06	3.487e-01	2.936e-05	1.770e-06
3.598e-01	5.81e-05	4.31e-06	3.655e-01	3.110e-05	1.820e-06
3.771e-01	6.38e-05	4.41e-06	3.830e-01	3.010e-05	1.870e-06
3.951e-01	6.33e-05	4.56e-06	4.013e-01	3.025e-05	1.920e-06
4.141e-01	6.68e-05	4.67e-06	4.206e-01	3.280e-05	1.980e-06
4.339e-01	7.36e-05	4.83e-06	4.408e-01	3.124e-05	2.040e-06
4.547e-01	7.43e-05	4.95e-06	4.619e-01	3.343e-05	2.090e-06
4.766e-01	6.76e-05	5.12e-06	4.841e-01	3.565e-05	2.150e-06

Table 3.2.3 Continued. (2/2)

Neutron Energy [MeV]	Flux at z=76mm	Absolute Error	Neutron Ennergy [MeV]	Flux at z=178mm	Absolute Error
4.994e-01	7.10e-05	5.27e-06	5.073e-01	3.160e-05	2.210e-06
5.234e-01	7.85e-05	5.43e-06	5.316e-01	3.213e-05	2.270e-06
5.485e-01	7.96e-05	5.61e-06	5.571e-01	3.614e-05	2.340e-06
5.748e-01	9.10e-05	5.73e-06	5.838e-01	3.440e-05	2.410e-06
6.023e-01	8.17e-05	5.91e-06	6.118e-01	3.832e-05	2.470e-06
6.312e-01	7.45e-05	6.06e-06	6.412e-01	4.095e-05	2.540e-06
6.615e-01	8.14e-05	6.29e-06	6.719e-01	3.712e-05	2.610e-06
6.933e-01	7.53e-05	6.49e-06	7.042e-01	3.791e-05	2.680e-06
7.265e-01	7.33e-05	6.74e-06	7.379e-01	3.579e-05	2.760e-06
7.614e-01	7.33e-05	7.02e-06	7.733e-01	3.844e-05	2.840e-06
7.979e-01	8.72e-05	7.29e-06	8.104e-01	4.210e-05	2.910e-06
8.362e-01	8.38e-05	7.55e-06	8.493e-01	3.608e-05	3.010e-06
8.763e-01	9.08e-05	7.86e-06	8.901e-01	3.222e-05	3.100e-06
9.183e-01	7.83e-05	8.21e-06	9.328e-01	3.541e-05	3.250e-06
9.624e-01	8.77e-05	8.59e-06	9.775e-01	3.159e-05	3.380e-06
1.009e+00	1.07e-04	9.02e-06	1.024e+00	4.053e-05	3.560e-06

Table 3.2.4 Neutron spectra in the vanadium assembly measured by the SDT method in the unit of [n / cm^2 / lethargy / source].

Neutron Energy [MeV]	Flux at z=76mm	Absolute Error	Flux at z=178mm	Absolute Error
1.179e-06	8.58e-10	1.14e-10	1.20e-09	1.72e-10
1.638e-06	1.80e-09	2.18e-10	3.40e-09	4.14e-10
2.276e-06	3.73e-09	4.27e-10	5.60e-09	6.59e-10
3.162e-06	5.35e-09	6.10e-10	9.02e-09	1.04e-09
4.394e-06	9.48e-09	1.07e-09	1.53e-08	1.76e-09
6.105e-06	1.61e-08	1.84e-09	2.43e-08	2.82e-09
8.483e-06	2.41e-08	2.83e-09	3.91e-08	4.65e-09
1.179e-05	3.11e-08	3.88e-09	6.26e-08	7.89e-09
1.638e-05	6.55e-08	8.55e-09	8.91e-08	1.18e-08
2.276e-05	8.54e-08	1.19e-08	1.24e-07	1.76e-08
3.162e-05	1.24e-07	1.88e-08	1.90e-07	2.96e-08
4.394e-05	1.85e-07	3.10e-08	2.75e-07	4.75e-08
6.105e-05	2.90e-07	5.39e-08	3.42e-07	6.67e-08
8.483e-05	3.93e-07	8.66e-08	5.80e-07	1.31e-07
1.179e-04	5.88e-07	1.49e-07	7.60e-07	1.98e-07
1.638e-04	9.97e-07	3.00e-07	1.22e-06	3.73e-07
2.276e-04	1.81e-06	6.47e-07	2.02e-06	7.52e-07
3.162e-04	3.11e-06	1.39e-06	3.47e-06	1.58e-06

Table 3.2.5 Integral neutron fluxes in the vanadium assembly derived from the measured neutron spectra in the unit of [n / cm^2 / source].

Energy Range	z=76mm	Error	z=178mm	Error
> 10 MeV	6.317e-05	7 %	1.265e-05	7 %
2-10 MeV	3.223e-05	15 %	1.134e-05	10 %
0.1-1 MeV	1.415e-04	5 %	6.954e-05	5 %
20-100 keV	2.387e-05	7 %	1.256e-05	7 %
10-100 eV	3.861e-07	20 %	5.473e-07	20 %
1-10 eV	2.202e-08	12 %	3.221e-08	12 %

Table 3.2.6 Measured dosimetry reaction rates in the vanadium assembly in the unit of [reactions / atom / source].

Reaction	z=0mm	Error	z=76mm	Error	z=178mm	Error
$^{27}Al(n,\alpha)^{24}Na$	2.32e-29	7.73e-31	6.42e-30	2.17e-31	1.34e-30	4.37e-32
$^{93}Nb(n,2n)^{92m}Nb$	1.00e-28	3.51e-30	2.55e-29	8.42e-31	5.27e-30	1.86e-31
$^{115}In(n,n')^{115m}In$	3.40e-29	1.11e-30	2.68e-29	8.91e-31	9.16e-30	3.13e-31
$^{197}Au(n,\gamma)^{198}Au$			1.62e-28	5.26e-30	1.56e-28	5.30e-30

Table 3.2.7 Gamma-ray spectra in the vanadium assembly measured by the BC-537 spectrometer in the unit of [photons / cm^2 / lethargy / source]. (1/2)

Photon Energy [MeV]	Flux at z=76mm	Absolute Error	Window [%]	Flux at z=178mm	Absolute Error	Window [%]
3.311e-01	5.505e-05	2.942e-06	26.5	2.177e-05	1.136e-06	25.7
3.467e-01	4.969e-05	2.194e-06	27.5	1.926e-05	8.398e-07	26.9
3.631e-01	4.568e-05	2.141e-06	27.6	1.697e-05	8.507e-07	27.4
3.802e-01	4.096e-05	2.071e-06	27.3	1.451e-05	7.745e-07	27.4
3.981e-01	3.589e-05	1.822e-06	27.1	1.244e-05	6.633e-07	27.4
4.169e-01	3.251e-05	1.667e-06	26.7	1.155e-05	6.091e-07	26.8
4.365e-01	3.187e-05	1.593e-06	26.1	1.178e-05	5.617e-07	26.0
4.571e-01	3.330e-05	1.620e-06	25.5	1.244e-05	5.669e-07	25.3
4.786e-01	3.559e-05	1.678e-06	24.9	1.302e-05	5.970e-07	24.6
5.012e-01	3.756e-05	1.692e-06	24.6	1.319e-05	5.955e-07	24.4
5.248e-01	3.795e-05	1.713e-06	24.6	1.275e-05	5.779e-07	24.5
5.495e-01	3.599e-05	1.755e-06	24.8	1.174e-05	5.923e-07	24.9
5.754e-01	3.235e-05	1.651e-06	25.2	1.055e-05	5.586e-07	25.4
6.026e-01	2.898e-05	1.553e-06	25.5	9.588e-06	5.205e-07	25.9
6.310e-01	2.742e-05	1.477e-06	25.8	8.983e-06	4.942e-07	26.2
6.607e-01	2.734e-05	1.404e-06	26.0	8.656e-06	4.591e-07	26.3
6.918e-01	2.733e-05	1.377e-06	26.0	8.534e-06	4.445e-07	26.3
7.244e-01	2.669e-05	1.348e-06	25.8	8.609e-06	4.412e-07	25.9
7.586e-01	2.602e-05	1.329e-06	25.4	8.908e-06	4.456e-07	25.4
7.943e-01	2.629e-05	1.326e-06	24.8	9.391e-06	4.527e-07	24.7
8.318e-01	2.791e-05	1.367e-06	24.1	9.948e-06	4.710e-07	24.0
8.710e-01	3.029e-05	1.445e-06	23.4	1.042e-05	4.946e-07	23.2
9.120e-01	3.210e-05	1.474e-06	23.0	1.067e-05	4.971e-07	22.8
9.550e-01	3.200e-05	1.457e-06	23.1	1.055e-05	4.899e-07	22.9
1.000e+00	2.966e-05	1.402e-06	23.6	9.996e-06	4.759e-07	23.4
1.047e+00	2.628e-05	1.350e-06	24.3	9.112e-06	4.646e-07	24.0
1.097e+00	2.366e-05	1.321e-06	25.0	8.201e-06	4.525e-07	24.8
1.148e+00	2.268e-05	1.272e-06	25.3	7.555e-06	4.277e-07	25.4
1.202e+00	2.315e-05	1.287e-06	25.0	7.364e-06	4.237e-07	25.5
1.259e+00	2.472e-05	1.346e-06	24.0	7.684e-06	4.368e-07	24.8
1.318e+00	2.751e-05	1.500e-06	22.6	8.514e-06	4.750e-07	23.6
1.380e+00	3.169e-05	1.631e-06	20.8	9.880e-06	5.197e-07	21.9
1.445e+00	3.741e-05	1.848e-06	19.0	1.192e-05	6.042e-07	20.0
1.514e+00	4.425e-05	1.952e-06	17.5	1.463e-05	6.288e-07	18.0
1.585e+00	4.983e-05	2.116e-06	16.5	1.713e-05	7.208e-07	16.7
1.660e+00	5.036e-05	2.142e-06	16.1	1.782e-05	7.276e-07	16.1
1.738e+00	4.517e-05	2.002e-06	16.4	1.605e-05	6.909e-07	16.3
1.820e+00	3.754e-05	1.799e-06	17.2	1.299e-05	6.195e-07	17.1
1.906e+00	3.002e-05	1.572e-06	18.4	1.011e-05	5.453e-07	18.2
1.995e+00	2.364e-05	1.316e-06	19.8	8.126e-06	4.542e-07	19.4
2.089e+00	1.957e-05	1.093e-06	21.0	7.052e-06	3.884e-07	20.4
2.188e+00	1.799e-05	1.004e-06	21.9	6.603e-06	3.588e-07	21.0
2.291e+00	1.744e-05	9.540e-07	22.5	6.388e-06	3.397e-07	21.4
2.399e+00	1.694e-05	8.969e-07	22.7	6.193e-06	3.194e-07	21.7
2.512e+00	1.667e-05	8.860e-07	22.5	6.033e-06	3.140e-07	21.7
2.630e+00	1.706e-05	9.058e-07	21.9	5.987e-06	3.177e-07	21.5

Table 3.2.7 Continued. (2/2)

Photon Energy [MeV]	Flux at z=76mm	Absolute Error	Window [%]	Flux at z=178mm	Absolute Error	Window [%]
2.754e+00	1.820e-05	9.391e-07	21.1	6.118e-06	3.243e-07	21.1
2.884e+00	1.990e-05	9.772e-07	20.3	6.442e-06	3.316e-07	20.4
3.020e+00	2.157e-05	1.012e-06	19.5	6.936e-06	3.415e-07	19.6
3.162e+00	2.266e-05	1.040e-06	19.2	7.589e-06	3.560e-07	18.9
3.311e+00	2.303e-05	1.068e-06	19.1	8.282e-06	3.767e-07	18.6
3.467e+00	2.278e-05	1.112e-06	19.3	8.670e-06	3.986e-07	18.7
3.631e+00	2.220e-05	1.068e-06	20.3	8.425e-06	3.856e-07	20.2
3.802e+00	2.194e-05	9.309e-07	21.7	7.623e-06	3.284e-07	21.7
3.981e+00	2.224e-05	1.074e-06	22.7	6.621e-06	3.749e-07	23.2
4.169e+00	2.249e-05	1.269e-06	23.7	5.880e-06	4.493e-07	24.6
4.365e+00	2.180e-05	1.114e-06	24.9	5.763e-06	3.983e-07	25.7
4.571e+00	1.992e-05	8.269e-07	25.3	6.212e-06	2.924e-07	25.7
4.786e+00	1.758e-05	7.806e-07	25.3	6.625e-06	2.674e-07	25.7
5.012e+00	1.591e-05	7.092e-07	25.5	6.371e-06	2.659e-07	25.7
5.248e+00	1.527e-05	7.194e-07	25.7	5.473e-06	2.909e-07	25.7
5.495e+00	1.493e-05	7.752e-07	25.7	4.625e-06	3.064e-07	25.7
5.754e+00	1.394e-05	6.603e-07	25.7	4.415e-06	2.740e-07	25.7
6.026e+00	1.240e-05	6.963e-07	25.7	4.604e-06	2.896e-07	25.7
6.310e+00	1.127e-05	6.514e-07	25.7	4.450e-06	2.689e-07	25.7
6.607e+00	1.091e-05	5.627e-07	25.7	3.682e-06	2.352e-07	25.7
6.918e+00	1.051e-05	6.078e-07	25.7	2.812e-06	2.425e-07	25.7
7.244e+00	9.275e-06	4.867e-07	25.7	2.373e-06	1.937e-07	25.7
7.586e+00	7.528e-06	4.079e-07	25.7	2.260e-06	1.623e-07	25.7
7.943e+00	6.079e-06	3.992e-07	25.7	2.077e-06	1.554e-07	25.7
8.318e+00	5.154e-06	3.731e-07	25.7	1.733e-06	1.363e-07	25.7
8.710e+00	4.412e-06	4.063e-07	25.7	1.392e-06	1.227e-07	25.7
9.120e+00	3.629e-06	4.787e-07	25.7	1.134e-06	1.157e-07	25.7
9.550e+00	2.827e-06	5.159e-07	25.7	9.221e-07	1.129e-07	25.7
1.000e+01	2.054e-06	4.729e-07	25.7	7.392e-07	1.074e-07	25.7
1.047e+01	1.372e-06	4.043e-07	25.7	6.034e-07	9.629e-08	25.7
1.097e+01	9.282e-07	4.439e-07	25.7	5.103e-07	8.242e-08	25.7
1.148e+01	8.276e-07	4.787e-07	25.7	4.294e-07	7.031e-08	25.7
1.202e+01	9.513e-07	4.146e-07	25.7	3.365e-07	6.313e-08	25.7
1.259e+01	1.010e-06	3.413e-07	25.7	2.317e-07	5.620e-08	25.7
1.318e+01	8.262e-07	2.659e-07	25.7	1.337e-07	4.241e-08	25.7
1.380e+01	4.914e-07	1.648e-07	25.7	6.174e-08	2.444e-08	25.7
1.445e+01	2.062e-07	7.235e-08	25.7	2.175e-08	1.016e-08	25.7
1.514e+01	5.930e-08	2.156e-08	25.7	5.562e-09	2.925e-09	25.7

Table 3.2.8 Measured gamma-ray heating rates of vanadium in the unit of [Gy / source neutron].

	z=0mm	Error	z=76mm	Error	z=178mm	Error
Gamma_Heat	7.42E-16	1.51E-16	7.25E-16	6.75E-17	2.23E-16	2.14E-17

Table 3.3.1 Material specification for the iron assembly.

Atomic Density [x10^{24} atoms/cm^3]			
Fe	0.083490	C	0.000727
Si	0.000249	Mn	0.000716

Table 3.3.2 Neutron spectra in the iron assembly measured by the NE213 spectrometer in the unit of [n / cm^2 / lethargy / source]. (1/3)

Neutron Energy [MeV]	Flux at z=16mm	Abs. Error	Window [%]	Flux at z=41mm	Abs. Error	Window [%]	Flux at z=66mm	Abs. Error	Window [%]
2.0	2.34e-5	2.26e-6	36.1	2.69e-5	1.70e-6	36.1	2.74e-5	1.32e-6	36.1
2.2	2.86e-5	2.28e-6	34.6	3.01e-5	1.71e-6	34.6	2.85e-5	1.29e-6	34.6
2.4	3.33e-5	2.21e-6	33.2	3.41e-5	1.68e-6	33.2	3.08e-5	1.26e-6	33.2
2.6	3.43e-5	2.12e-6	31.8	3.54e-5	1.63e-6	31.8	3.13e-5	1.23e-6	31.8
2.8	3.22e-5	2.10e-6	30.7	3.38e-5	1.61e-6	30.7	2.95e-5	1.21e-6	30.7
3.0	2.90e-5	2.67e-6	29.7	3.08e-5	1.87e-6	29.7	2.70e-5	1.34e-6	29.7
3.2	2.68e-5	3.24e-6	28.7	2.82e-5	2.17e-6	28.7	2.51e-5	1.51e-6	28.7
3.4	2.54e-5	3.17e-6	27.8	2.63e-5	2.12e-6	27.8	2.38e-5	1.48e-6	27.8
3.6	2.34e-5	2.62e-6	27.0	2.47e-5	1.82e-6	27.0	2.25e-5	1.29e-6	27.0
3.8	2.04e-5	2.21e-6	26.2	2.31e-5	1.59e-6	26.2	2.10e-5	1.16e-6	26.2
4.0	1.75e-5	2.33e-6	25.4	2.19e-5	1.64e-6	25.4	1.93e-5	1.19e-6	25.4
4.2	1.58e-5	2.62e-6	24.7	2.10e-5	1.79e-6	24.7	1.78e-5	1.27e-6	24.7
4.4	1.50e-5	2.74e-6	24.1	1.98e-5	1.84e-6	24.1	1.65e-5	1.28e-6	24.1
4.6	1.39e-5	2.72e-6	23.6	1.76e-5	1.84e-6	23.6	1.53e-5	1.27e-6	23.6
4.8	1.17e-5	2.80e-6	23.0	1.44e-5	1.87e-6	23.0	1.37e-5	1.29e-6	23.0
5.0	8.55e-6	2.94e-6	22.5	1.07e-5	1.94e-6	22.5	1.15e-5	1.34e-6	22.5
5.2	5.67e-6	3.05e-6	22.1	7.65e-6	2.00e-6	22.1	9.08e-6	1.38e-6	22.1
5.4	4.42e-6	3.23e-6	21.7	6.18e-6	2.11e-6	21.7	7.28e-6	1.44e-6	21.7
5.6	5.55e-6	3.44e-6	21.3	6.77e-6	2.23e-6	21.3	6.78e-6	1.52e-6	21.3
5.8	8.78e-6	3.56e-6	21.0	9.06e-6	2.29e-6	21.0	7.66e-6	1.56e-6	21.0
6.0	1.29e-5	3.68e-6	20.6	1.19e-5	2.36e-6	20.6	9.42e-6	1.60e-6	20.6
6.2	1.62e-5	3.96e-6	20.2	1.40e-5	2.53e-6	20.2	1.13e-5	1.70e-6	20.2
6.4	1.76e-5	4.36e-6	19.9	1.45e-5	2.78e-6	19.9	1.24e-5	1.85e-6	19.9
6.6	1.65e-5	4.66e-6	19.5	1.34e-5	2.95e-6	19.5	1.27e-5	1.96e-6	19.5
6.8	1.36e-5	4.74e-6	19.2	1.15e-5	3.01e-6	19.2	1.22e-5	2.00e-6	19.2
7.0	9.67e-6	4.85e-6	18.9	9.76e-6	3.05e-6	18.9	1.12e-5	2.03e-6	18.9
7.2	5.97e-6	5.22e-6	18.6	8.91e-6	3.26e-6	18.6	1.02e-5	2.17e-6	18.6
7.4	3.39e-6	5.82e-6	18.4	8.83e-6	3.62e-6	18.4	9.51e-6	2.38e-6	18.4
7.6	2.16e-6	6.39e-6	18.1	8.86e-6	3.97e-6	18.1	9.21e-6	2.59e-6	18.1
7.8	1.85e-6	6.82e-6	17.9	8.25e-6	4.25e-6	17.9	9.09e-6	2.74e-6	17.9
8.0	1.72e-6	7.13e-6	17.7	6.73e-6	4.43e-6	17.7	8.84e-6	2.84e-6	17.7
8.2	1.37e-6	7.46e-6	17.5	4.82e-6	4.60e-6	17.5	8.30e-6	2.95e-6	17.5
8.4	9.76e-7	8.02e-6	17.3	3.44e-6	4.90e-6	17.3	7.53e-6	3.15e-6	17.3
8.6	1.02e-6	8.94e-6	17.1	3.40e-6	5.43e-6	17.1	6.78e-6	3.49e-6	17.1
8.8	1.78e-6	1.01e-5	16.9	4.84e-6	6.13e-6	16.9	6.26e-6	3.93e-6	16.9
9.0	3.03e-6	1.12e-5	16.7	7.25e-6	6.77e-6	16.7	6.03e-6	4.33e-6	16.7
9.2	4.12e-6	1.19e-5	16.6	9.75e-6	7.16e-6	16.6	5.99e-6	4.58e-6	16.6
9.4	4.43e-6	1.21e-5	16.4	1.14e-5	7.30e-6	16.4	6.00e-6	4.66e-6	16.4
9.6	3.62e-6	1.21e-5	16.2	1.16e-5	7.32e-6	16.2	6.03e-6	4.66e-6	16.2
9.8	1.77e-6	1.23e-5	16.0	9.97e-6	7.41e-6	16.0	6.07e-6	4.70e-6	16.0
10.0	-7.53e-7	-7.53e-7	15.8	6.72e-6	7.71e-6	15.8	6.08e-6	4.90e-6	15.8
10.2	-3.53e-6	-3.53e-6	15.7	2.35e-6	8.17e-6	15.7	5.87e-6	5.20e-6	15.7
10.4	-6.25e-6	-6.25e-6	15.5	-2.39e-6	-2.39e-6	15.5	5.16e-6	5.46e-6	15.5
10.6	-8.76e-6	-8.76e-6	15.3	-6.76e-6	-6.76e-6	15.3	3.70e-6	5.56e-6	15.3
10.8	-1.11e-5	-1.11e-5	15.1	-1.02e-5	-1.02e-5	15.1	1.45e-6	5.56e-6	15.1
11.0	-1.31e-5	-1.31e-5	14.9	-1.23e-5	-1.23e-5	14.9	-1.38e-6	-1.38e-6	14.9
11.2	-1.44e-5	-1.44e-5	14.8	-1.30e-5	-1.30e-5	14.8	-4.22e-6	-4.22e-6	14.8
11.4	-1.44e-5	-1.44e-5	14.6	-1.22e-5	-1.22e-5	14.6	-6.34e-6	-6.34e-6	14.6
11.6	-1.23e-5	-1.23e-5	14.5	-1.00e-5	-1.00e-5	14.5	-6.98e-6	-6.98e-6	14.5
11.8	-7.48e-6	-7.48e-6	14.4	-6.86e-6	-6.86e-6	14.4	-5.63e-6	-5.63e-6	14.4
12.0	-4.12e-7	-4.12e-7	14.4	-3.17e-6	-3.17e-6	14.4	-2.26e-6	-2.26e-6	14.4
12.2	7.78e-6	2.01e-5	14.4	5.12e-7	1.21e-5	14.4	2.74e-6	7.61e-6	14.4
12.4	1.61e-5	2.15e-5	14.4	4.15e-6	1.31e-5	14.4	8.82e-6	8.23e-6	14.4
12.6	2.54e-5	2.20e-5	14.4	8.88e-6	1.34e-5	14.4	1.58e-5	8.50e-6	14.4
12.8	3.95e-5	2.18e-5	14.4	1.76e-5	1.32e-5	14.4	2.46e-5	8.50e-6	14.4
13.0	6.60e-5	2.25e-5	14.4	3.50e-5	1.36e-5	14.4	3.73e-5	8.73e-6	14.4
13.2	1.15e-4	2.51e-5	14.4	6.68e-5	1.51e-5	14.4	5.67e-5	9.59e-6	14.4
13.4	1.95e-4	2.85e-5	14.4	1.18e-4	1.71e-5	14.4	8.57e-5	1.07e-5	14.4
13.6	3.11e-4	3.12e-5	14.4	1.90e-4	1.88e-5	14.4	1.26e-4	1.17e-5	14.4
13.8	4.61e-4	3.32e-5	14.4	2.82e-4	2.02e-5	14.4	1.76e-4	1.25e-5	14.4
14.0	6.32e-4	3.63e-5	14.4	3.87e-4	2.22e-5	14.4	2.34e-4	1.40e-5	14.4
14.2	8.05e-4	4.16e-5	14.4	4.92e-4	2.55e-5	14.4	2.92e-4	1.65e-5	14.4
14.4	9.58e-4	4.77e-5	14.4	5.85e-4	2.95e-5	14.4	3.43e-4	1.94e-5	14.4
14.6	1.07e-3	5.21e-5	14.4	6.53e-4	3.20e-5	14.4	3.81e-4	2.14e-5	14.4
14.8	1.13e-3	5.18e-5	14.4	6.87e-4	3.18e-5	14.4	4.01e-4	2.13e-5	14.4
15.0	1.13e-3	4.63e-5	14.0	6.85e-4	2.85e-5	14.1	4.02e-4	1.91e-5	14.3
15.2	1.07e-3	3.64e-5	13.0	6.47e-4	2.24e-5	13.1	3.83e-4	1.51e-5	13.4
15.4	9.66e-4	2.47e-5	12.2	5.83e-4	1.51e-5	12.2	3.50e-4	1.00e-5	12.5
15.6	8.34e-4	1.61e-5	12.2	5.02e-4	9.85e-6	12.2	3.06e-4	6.06e-6	12.5
15.8	6.91e-4	1.71e-5	12.2	4.15e-4	1.04e-5	12.2	2.59e-4	6.35e-6	12.5
16.0	5.55e-4	2.27e-5	12.5	3.32e-4	1.39e-5	12.6	2.12e-4	8.87e-6	12.6
16.2	4.36e-4	2.66e-5	13.5	2.59e-4	1.64e-5	13.5	1.71e-4	1.08e-5	13.6
16.4	3.39e-4	2.76e-5	14.4	2.00e-4	1.70e-5	14.4	1.36e-4	1.14e-5	14.4
16.6	2.66e-4	2.60e-5	14.4	1.56e-4	1.60e-5	14.4	1.08e-4	1.08e-5	14.4
16.8	2.14e-4	2.26e-5	14.4	1.24e-4	1.40e-5	14.4	8.72e-5	9.54e-6	14.4
17.0	1.78e-4	1.85e-5	14.4	1.03e-4	1.14e-5	14.4	7.19e-5	7.89e-6	14.4
17.2	1.53e-4	1.44e-5	14.4	8.80e-5	8.90e-6	14.4	6.06e-5	6.19e-6	14.4
17.4	1.34e-4	1.08e-5	14.4	7.71e-5	6.67e-6	14.4	5.19e-5	4.66e-6	14.4
17.6	1.18e-4	7.84e-6	14.4	6.81e-5	4.85e-6	14.4	4.48e-5	3.42e-6	14.4
17.8	1.03e-4	5.62e-6	14.4	5.97e-5	3.48e-6	14.4	3.83e-5	2.46e-6	14.4
18.0	8.76e-5	4.02e-6	14.4	5.14e-5	2.48e-6	14.4	3.23e-5	1.75e-6	14.4

Table 3.3.2 Continued. (2/3)

Neutron Energy [MeV]	Flux at z=116mm	Abs, Error	Window [%]	Flux at z=216mm	Abs. Error	Window [%]	Flux at z=316mm	Abs. Error	Window [%]
2.0	1.78e-1	6.88e-3	36.1	5.02e-3	1.76e-4	35.0	1.52e-4	4.94e-6	32.0
2.2	1.78e-1	6.56e-3	34.6	4.75e-3	1.55e-4	34.1	1.43e-4	4.32e-6	31.1
2.4	1.83e-1	6.28e-3	33.2	4.64e-3	1.43e-4	33.1	1.26e-4	3.79e-6	30.7
2.6	1.79e-1	6.11e-3	31.8	4.41e-3	1.34e-4	31.8	1.08e-4	3.27e-6	30.1
2.8	1.67e-1	5.93e-3	30.7	4.01e-3	1.28e-4	30.7	9.27e-5	2.98e-6	29.6
3.0	1.54e-1	6.20e-3	29.7	3.62e-3	1.28e-4	29.7	8.10e-5	2.82e-6	29.3
3.2	1.44e-1	6.65e-3	28.7	3.33e-3	1.31e-4	28.7	7.28e-5	2.73e-6	28.7
3.4	1.35e-1	6.51e-3	27.8	3.14e-3	1.27e-4	27.8	6.70e-5	2.61e-6	27.8
3.6	1.26e-1	5.85e-3	27.0	2.94e-3	1.18e-4	27.0	6.22e-5	2.40e-6	27.0
3.8	1.15e-1	5.39e-3	26.2	2.73e-3	1.10e-4	26.2	5.80e-5	2.24e-6	26.2
4.0	1.04e-1	5.41e-3	25.4	2.52e-3	1.08e-4	25.4	5.46e-5	2.18e-6	25.4
4.2	9.47e-2	5.60e-3	24.7	2.33e-3	1.09e-4	24.7	5.18e-5	2.19e-6	24.7
4.4	8.81e-2	5.66e-3	24.1	2.15e-3	1.10e-4	24.1	4.88e-5	2.19e-6	24.1
4.6	8.20e-2	5.66e-3	23.6	1.97e-3	1.10e-4	23.6	4.51e-5	2.18e-6	23.6
4.8	7.46e-2	5.76e-3	23.0	1.79e-3	1.11e-4	23.0	4.04e-5	2.18e-6	23.0
5.0	6.61e-2	5.92e-3	22.5	1.61e-3	1.12e-4	22.5	3.54e-5	2.20e-6	22.5
5.2	5.87e-2	6.02e-3	22.1	1.48e-3	1.14e-4	22.1	3.10e-5	2.23e-6	22.1
5.4	5.47e-2	6.23e-3	21.7	1.39e-3	1.17e-4	21.7	2.79e-5	2.28e-6	21.7
5.6	5.45e-2	6.55e-3	21.3	1.37e-3	1.21e-4	21.3	2.68e-5	2.36e-6	21.3
5.8	5.73e-2	6.69e-3	21.0	1.40e-3	1.23e-4	21.0	2.77e-5	2.39e-6	21.0
6.0	6.17e-2	6.79e-3	20.6	1.46e-3	1.24e-4	20.6	2.97e-5	2.42e-6	20.6
6.2	6.54e-2	7.08e-3	20.2	1.52e-3	1.28e-4	20.2	3.15e-5	2.50e-6	20.2
6.4	6.64e-2	7.63e-3	19.9	1.54e-3	1.35e-4	19.9	3.20e-5	2.64e-6	19.9
6.6	6.35e-2	8.12e-3	19.5	1.48e-3	1.43e-4	19.5	3.09e-5	2.76e-6	19.5
6.8	5.71e-2	8.23e-3	19.2	1.36e-3	1.45e-4	19.2	2.88e-5	2.80e-6	19.2
7.0	4.93e-2	8.33e-3	18.9	1.19e-3	1.47e-4	18.9	2.65e-5	2.82e-6	18.9
7.2	4.24e-2	8.83e-3	18.6	1.01e-3	1.55e-4	18.6	2.48e-5	2.95e-6	18.6
7.4	3.81e-2	9.67e-3	18.4	8.69e-4	1.67e-4	18.4	2.38e-5	3.19e-6	18.4
7.6	3.65e-2	1.05e-2	18.1	7.80e-4	1.81e-4	18.1	2.34e-5	3.42e-6	18.1
7.8	3.70e-2	1.11e-2	17.9	7.35e-4	1.92e-4	17.9	2.30e-5	3.59e-6	17.9
8.0	3.82e-2	1.15e-2	17.7	7.17e-4	1.98e-4	17.7	2.24e-5	3.70e-6	17.7
8.2	3.93e-2	1.19e-2	17.5	7.12e-4	2.05e-4	17.5	2.17e-5	3.80e-6	17.5
8.4	3.98e-2	1.27e-2	17.3	7.21e-4	2.17e-4	17.3	2.11e-5	4.01e-6	17.3
8.6	3.97e-2	1.40e-2	17.1	7.47e-4	2.39e-4	17.1	2.08e-5	4.41e-6	17.1
8.8	3.95e-2	1.57e-2	16.9	7.92e-4	2.68e-4	16.9	2.07e-5	4.91e-6	16.9
9.0	3.95e-2	1.72e-2	16.7	8.47e-4	2.93e-4	16.7	2.07e-5	5.36e-6	16.7
9.2	4.00e-2	1.82e-2	16.6	9.01e-4	3.08e-4	16.6	2.07e-5	5.63e-6	16.6
9.4	4.04e-2	1.85e-2	16.4	9.42e-4	3.12e-4	16.4	2.05e-5	5.72e-6	16.4
9.6	4.03e-2	1.86e-2	16.2	9.59e-4	3.12e-4	16.2	2.02e-5	5.72e-6	16.2
9.8	3.91e-2	1.87e-2	16.0	9.48e-4	3.16e-4	16.0	1.98e-5	5.78e-6	16.0
10.0	3.70e-2	1.94e-2	15.8	9.06e-4	3.30e-4	15.8	1.92e-5	5.99e-6	15.8
10.2	3.41e-2	2.05e-2	15.7	8.37e-4	3.49e-4	15.7	1.82e-5	6.33e-6	15.7
10.4	3.02e-2	2.14e-2	15.5	7.56e-4	3.64e-4	15.5	1.68e-5	6.62e-6	15.5
10.6	2.47e-2	2.19e-2	15.3	6.80e-4	3.67e-4	15.3	1.48e-5	6.72e-6	15.3
10.8	1.68e-2	2.19e-2	15.1	6.21e-4	3.64e-4	15.1	1.25e-5	6.67e-6	15.1
11.0	6.67e-3	2.18e-2	14.9	5.80e-4	3.60e-4	14.9	1.02e-5	6.59e-6	14.9
11.2	-3.92e-3	-3.92e-3	14.8	5.49e-4	3.61e-4	14.8	8.59e-6	6.56e-6	14.8
11.4	-1.24e-2	-1.24e-2	14.6	5.14e-4	3.67e-4	14.6	8.34e-6	6.62e-6	14.6
11.6	-1.60e-2	-1.60e-2	14.5	4.72e-4	3.80e-4	14.5	1.00e-5	6.82e-6	14.5
11.8	-1.33e-2	-1.33e-2	14.4	4.33e-4	4.05e-4	14.4	1.37e-5	7.24e-6	14.4
12.0	-4.11e-3	-4.11e-3	14.4	4.24e-4	4.45e-4	14.4	1.90e-5	7.90e-6	14.4
12.2	1.09e-2	2.99e-2	14.4	4.84e-4	4.94e-4	14.4	2.52e-5	8.72e-6	14.4
12.4	3.19e-2	3.23e-2	14.4	6.67e-4	5.32e-4	14.4	3.18e-5	9.39e-6	14.4
12.6	6.10e-2	3.30e-2	14.4	1.05e-3	5.44e-4	14.4	3.88e-5	9.68e-6	14.4
12.8	1.03e-1	3.28e-2	14.4	1.73e-3	5.40e-4	14.4	4.78e-5	9.67e-6	14.4
13.0	1.67e-1	3.36e-2	14.4	2.84e-3	5.51e-4	14.4	6.17e-5	9.93e-6	14.4
13.2	2.60e-1	3.71e-2	14.4	4.50e-3	6.06e-4	14.4	8.42e-5	1.08e-5	14.4
13.4	3.91e-1	4.18e-2	14.4	6.80e-3	6.82e-4	14.4	1.18e-4	1.19e-5	14.4
13.6	5.59e-1	4.56e-2	14.4	9.74e-3	7.44e-4	14.4	1.66e-4	1.29e-5	14.4
13.8	7.60e-1	4.89e-2	14.4	1.32e-2	8.00e-4	14.4	2.25e-4	1.39e-5	14.4
14.0	9.78e-1	5.44e-2	14.4	1.69e-2	8.97e-4	14.4	2.92e-4	1.59e-5	14.4
14.2	1.19e+0	6.35e-2	14.4	2.04e-2	1.06e-3	14.4	3.57e-4	1.91e-5	14.4
14.4	1.38e+0	7.48e-2	14.4	2.33e-2	1.25e-3	14.4	4.13e-4	2.27e-5	14.4
14.6	1.51e+0	8.20e-2	14.4	2.52e-2	1.38e-3	14.4	4.52e-4	2.51e-5	14.4
14.8	1.57e+0	8.20e-2	14.4	2.59e-2	1.39e-3	14.4	4.67e-4	2.52e-5	14.4
15.0	1.55e+0	7.34e-2	14.3	2.53e-2	1.24e-3	14.4	4.57e-4	2.26e-5	14.4
15.2	1.47e+0	5.75e-2	13.4	2.36e-2	9.72e-4	13.5	4.25e-4	1.77e-5	13.5
15.4	1.32e+0	3.88e-2	12.6	2.09e-2	6.50e-4	12.8	3.76e-4	1.16e-5	12.8
15.6	1.15e+0	2.32e-2	12.6	1.78e-2	3.75e-4	12.8	3.17e-4	6.57e-6	12.8
15.8	9.53e-1	2.38e-2	12.6	1.46e-2	3.76e-4	12.8	2.56e-4	6.87e-6	12.8
16.0	7.70e-1	3.37e-2	12.6	1.16e-2	5.50e-4	12.8	1.99e-4	1.02e-5	12.8
16.2	6.08e-1	4.10e-2	13.6	8.98e-3	6.85e-4	13.7	1.51e-4	1.26e-5	13.7
16.4	4.78e-1	4.35e-2	14.4	6.95e-3	7.34e-4	14.4	1.14e-4	1.35e-5	14.4
16.6	3.78e-1	4.16e-2	14.4	5.45e-3	7.10e-4	14.4	8.64e-5	1.30e-5	14.4
16.8	3.07e-1	3.68e-2	14.4	4.40e-3	6.31e-4	14.4	6.79e-5	1.15e-5	14.4
17.0	2.57e-1	3.05e-2	14.4	3.70e-3	5.28e-4	14.4	5.59e-5	9.58e-6	14.4
17.2	2.21e-1	2.40e-2	14.4	3.22e-3	4.18e-4	14.4	4.82e-5	7.57e-6	14.4
17.4	1.94e-1	1.81e-2	14.4	2.86e-3	3.16e-4	14.4	4.27e-5	5.74e-6	14.4
17.6	1.71e-1	1.33e-2	14.4	2.55e-3	2.32e-4	14.4	3.82e-5	4.21e-6	14.4
17.8	1.48e-1	9.52e-3	14.4	2.26e-3	1.66e-4	14.4	3.39e-5	3.03e-6	14.4
18.0	1.26e-1	6.79e-3	14.4	1.95e-3	1.18e-4	14.4	2.94e-5	2.16e-6	14.4

Table 3.3.2 Continued. (3/3)

Neutron Energy [MeV]	Flux at z=416mm	Abs. Error	Window [%]	Flux at z=516mm	Abs. Error	Window [%]	Flux at z=716mm	Abs. Error	Window [%]
2.0	5.00e-6	1.46e-7	29.5	1.17e-6	2.84e-8	27.9	3.91e-8	1.33e-9	28.8
2.2	4.68e-6	1.32e-7	28.8	1.07e-6	2.69e-8	27.1	3.06e-8	9.43-10	29.6
2.4	3.49e-6	1.04e-7	28.6	6.03e-7	1.75e-8	26.9	2.17e-8	6.69-10	30.1
2.6	2.62e-6	8.27e-8	28.7	3.76e-7	1.29e-8	27.8	1.60e-8	5.30-10	30.3
2.8	2.17e-6	7.27e-8	29.0	3.18e-7	1.13e-8	28.6	1.25e-8	4.69-10	30.3
3.0	1.90e-6	6.56e-8	29.2	2.81e-7	9.97e-9	29.2	1.00e-8	5.04-10	29.7
3.2	1.74e-6	6.06e-8	28.7	2.61e-7	8.76e-9	28.7	8.92e-9	5.74-10	28.7
3.4	1.64e-6	5.66e-8	27.8	2.50e-7	8.04e-9	27.8	8.85e-9	5.75-10	27.8
3.6	1.52e-6	5.20e-8	27.0	2.38e-7	7.44e-9	27.0	9.05e-9	5.16-10	27.0
3.8	1.38e-6	4.85e-8	26.2	2.25e-7	6.93e-9	26.2	9.20e-9	4.73-10	26.2
4.0	1.25e-6	4.65e-8	25.4	2.13e-7	6.58e-9	25.4	9.30e-9	5.12-10	25.4
4.2	1.14e-6	4.59e-8	24.7	1.99e-7	6.39e-9	24.7	9.36e-9	5.66-10	24.7
4.4	1.05e-6	4.57e-8	24.1	1.83e-7	6.20e-9	24.1	9.31e-9	5.81-10	24.1
4.6	9.69e-7	4.54e-8	23.6	1.66e-7	6.03e-9	23.6	9.04e-9	5.67-10	23.6
4.8	9.04e-7	4.55e-8	23.0	1.51e-7	5.94e-9	23.0	8.57e-9	5.63-10	23.0
5.0	8.48e-7	4.57e-8	22.5	1.40e-7	5.85e-9	22.5	7.94e-9	5.83-10	22.5
5.2	7.97e-7	4.58e-8	22.1	1.32e-7	5.72e-9	22.1	7.21e-9	6.05-10	22.1
5.4	7.56e-7	4.66e-8	21.7	1.27e-7	5.69e-9	21.7	6.53e-9	6.27-10	21.7
5.6	7.25e-7	4.77e-8	21.3	1.23e-7	5.72e-9	21.3	6.09e-9	6.44-10	21.3
5.8	7.04e-7	4.84e-8	21.0	1.20e-7	5.72e-9	21.0	6.01e-9	6.45-10	21.0
6.0	6.89e-7	4.87e-8	20.6	1.15e-7	5.66e-9	20.6	6.21e-9	6.49-10	20.6
6.2	6.76e-7	4.97e-8	20.2	1.09e-7	5.59e-9	20.2	6.36e-9	6.74-10	20.2
6.4	6.60e-7	5.20e-8	19.9	1.01e-7	5.70e-9	19.9	6.18e-9	7.13-10	19.9
6.6	6.42e-7	5.41e-8	19.5	9.36e-8	5.81e-9	19.5	5.53e-9	7.45-10	19.5
6.8	6.20e-7	5.47e-8	19.2	8.54e-8	5.92e-9	19.2	4.56e-9	7.56-10	19.2
7.0	5.93e-7	5.50e-8	18.9	7.77e-8	5.89e-9	18.9	3.52e-9	7.67-10	18.9
7.2	5.59e-7	5.78e-8	18.6	7.14e-8	6.10e-9	18.6	2.72e-9	8.09-10	18.6
7.4	5.19e-7	6.23e-8	18.4	6.70e-8	6.46e-9	18.4	2.37e-9	8.77-10	18.4
7.6	4.81e-7	6.66e-8	18.1	6.42e-8	6.85e-9	18.1	2.46e-9	9.47-10	18.1
7.8	4.50e-7	6.93e-8	17.9	6.18e-8	7.16e-9	17.9	2.85e-9	1.01e-9	17.9
8.0	4.30e-7	7.10e-8	17.7	5.91e-8	7.37e-9	17.7	3.27e-9	1.05e-9	17.7
8.2	4.19e-7	7.33e-8	17.5	5.60e-8	7.53e-9	17.5	3.57e-9	1.08e-9	17.5
8.4	4.14e-7	7.76e-8	17.3	5.35e-8	7.86e-9	17.3	3.73e-9	1.09e-9	17.3
8.6	4.17e-7	8.50e-8	17.1	5.24e-8	8.52e-9	17.1	3.82e-9	1.12e-9	17.1
8.8	4.26e-7	9.41e-8	16.9	5.33e-8	9.42e-9	16.9	3.90e-9	1.21e-9	16.9
9.0	4.43e-7	1.02e-7	16.7	5.55e-8	1.02e-8	16.7	3.90e-9	1.34e-9	16.7
9.2	4.64e-7	1.07e-7	16.6	5.79e-8	1.07e-8	16.6	3.74e-9	1.45e-9	16.6
9.4	4.81e-7	1.09e-7	16.4	5.94e-8	1.07e-8	16.4	3.37e-9	1.49e-9	16.4
9.6	4.89e-7	1.09e-7	16.2	5.93e-8	1.08e-8	16.2	2.87e-9	1.48e-9	16.2
9.8	4.85e-7	1.11e-7	16.0	5.78e-8	1.09e-8	16.0	2.41e-9	1.46e-9	16.0
10.0	4.73e-7	1.15e-7	15.8	5.53e-8	1.14e-8	15.8	2.13e-9	1.47e-9	15.8
10.2	4.58e-7	1.21e-7	15.7	5.28e-8	1.19e-8	15.7	2.12e-9	1.51e-9	15.7
10.4	4.43e-7	1.26e-7	15.5	5.07e-8	1.24e-8	15.5	2.38e-9	1.57e-9	15.5
10.6	4.31e-7	1.26e-7	15.3	4.90e-8	1.24e-8	15.3	2.81e-9	1.62e-9	15.3
10.8	4.20e-7	1.25e-7	15.1	4.76e-8	1.22e-8	15.1	3.29e-9	1.67e-9	15.1
11.0	4.09e-7	1.23e-7	14.9	4.62e-8	1.20e-8	14.9	3.67e-9	1.73e-9	14.9
11.2	3.99e-7	1.22e-7	14.8	4.47e-8	1.20e-8	14.8	3.81e-9	1.80e-9	14.8
11.4	3.96e-7	1.24e-7	14.6	4.31e-8	1.20e-8	14.6	3.69e-9	1.86e-9	14.6
11.6	4.09e-7	1.27e-7	14.5	4.18e-8	1.24e-8	14.5	3.38e-9	1.94e-9	14.5
11.8	4.44e-7	1.35e-7	14.4	4.07e-8	1.31e-8	14.4	3.04e-9	2.07e-9	14.4
12.0	5.03e-7	1.47e-7	14.4	4.00e-8	1.44e-8	14.4	2.86e-9	2.29e-9	14.4
12.2	5.83e-7	1.62e-7	14.4	4.02e-8	1.59e-8	14.4	2.95e-9	2.59e-9	14.4
12.4	6.86e-7	1.74e-7	14.4	4.25e-8	1.71e-8	14.4	3.34e-9	2.89e-9	14.4
12.6	8.23e-7	1.77e-7	14.4	4.95e-8	1.75e-8	14.4	4.01e-9	3.11e-9	14.4
12.8	1.02e-6	1.74e-7	14.4	6.51e-8	1.72e-8	14.4	5.00e-9	3.26e-9	14.4
13.0	1.33e-6	1.77e-7	14.4	9.41e-8	1.75e-8	14.4	6.44e-9	3.41e-9	14.4
13.2	1.80e-6	1.96e-7	14.4	1.41e-7	1.93e-8	14.4	8.54e-9	3.62e-9	14.4
13.4	2.44e-6	2.22e-7	14.4	2.09e-7	2.18e-8	14.4	1.15e-8	3.76e-9	14.4
13.6	3.27e-6	2.44e-7	14.4	2.99e-7	2.39e-8	14.4	1.55e-8	3.79e-9	14.4
13.8	4.24e-6	2.61e-7	14.4	4.05e-7	2.58e-8	14.4	2.03e-8	4.16e-9	14.4
14.0	5.26e-6	2.90e-7	14.4	5.19e-7	2.88e-8	14.4	2.56e-8	5.20e-9	14.4
14.2	6.21e-6	3.38e-7	14.4	6.28e-7	3.39e-8	14.4	3.07e-8	6.84e-9	14.4
14.4	7.00e-6	3.94e-7	14.4	7.20e-7	3.96e-8	14.4	3.50e-8	8.54e-9	14.4
14.6	7.51e-6	4.33e-7	14.4	7.83e-7	4.36e-8	14.4	3.78e-8	9.71e-9	14.4
14.8	7.70e-6	4.34e-7	14.4	8.09e-7	4.37e-8	14.4	3.88e-8	9.94e-9	14.4
15.0	7.55e-6	3.90e-7	14.4	7.96e-7	3.92e-8	14.4	3.78e-8	9.09e-9	14.4
15.2	7.10e-6	3.07e-7	13.5	7.48e-7	3.08e-8	13.5	3.52e-8	7.28e-9	14.4
15.4	6.43e-6	2.03e-7	12.7	6.72e-7	2.04e-8	12.7	3.13e-8	4.88e-9	14.4
15.6	5.62e-6	1.18e-7	12.7	5.80e-7	1.20e-8	12.7	2.67e-8	2.59e-9	14.4
15.8	4.75e-6	1.20e-7	12.7	4.83e-7	1.23e-8	12.7	2.21e-8	2.15e-9	14.4
16.0	3.93e-6	1.74e-7	12.7	3.91e-7	1.78e-8	12.7	1.77e-8	3.54e-9	14.4
16.2	3.19e-6	2.16e-7	13.6	3.10e-7	2.19e-8	13.7	1.40e-8	4.73e-9	14.4
16.4	2.58e-6	2.32e-7	14.4	2.44e-7	2.35e-8	14.4	1.10e-8	5.31e-9	14.4
16.6	2.09e-6	2.23e-7	14.4	1.94e-7	2.25e-8	14.4	8.62e-9	5.32e-9	14.4
16.8	1.73e-6	1.98e-7	14.4	1.58e-7	1.99e-8	14.4	6.82e-9	4.90e-9	14.4
17.0	1.45e-6	1.65e-7	14.4	1.33e-7	1.66e-8	14.4	5.43e-9	4.21e-9	14.4
17.2	1.24e-6	1.31e-7	14.4	1.15e-7	1.31e-8	14.4	4.33e-9	3.43e-9	14.4
17.4	1.07e-6	9.92e-8	14.4	1.01e-7	9.88e-9	14.4	3.43e-9	2.65e-9	14.4
17.6	9.17e-7	7.29e-8	14.4	8.96e-8	7.22e-9	14.4	2.67e-9	1.96e-9	14.4
17.8	7.80e-7	5.23e-8	14.4	7.86e-8	5.17e-9	14.4	2.03e-9	1.38e-9	14.4
18.0	6.51e-7	3.71e-8	14.4	6.77e-8	3.67e-9	14.4	1.50e-9	9.32-10	14.4

Table 3.3.3 Neutron spectra in the iron assembly measured by the PRC in the unit of [n / cm^2 / lethargy / source]. (1/4)

Neutron Energy [MeV]	Flux at z=110mm	Absolute Error	Neutron Energy [MeV]	Flux at z=210mm	Absolute Error	Neutron Energy [MeV]	Flux at z=310mm	Absolute Error
3.09e-03	5.94e-02	1.68e-02	3.05e-03	1.79e-03	1.01e-03	3.01e-03	1.02e-04	6.19e-05
3.23e-03	1.90e-02	1.60e-02	3.18e-03	3.48e-03	9.65e-04	3.14e-03	2.32e-04	5.95e-05
3.37e-03	9.48e-03	1.56e-02	3.32e-03	2.74e-03	9.39e-04	3.27e-03	2.21e-04	5.79e-05
3.51e-03	3.37e-02	1.52e-02	3.46e-03	3.44e-03	8.92e-04	3.42e-03	1.48e-04	5.53e-05
3.67e-03	5.32e-02	1.48e-02	3.62e-03	1.62e-03	8.81e-04	3.56e-03	1.99e-04	5.42e-05
3.83e-03	9.96e-03	1.44e-02	3.78e-03	1.90e-03	8.50e-04	3.72e-03	1.84e-04	5.29e-05
4.00e-03	2.74e-02	1.41e-02	3.94e-03	2.58e-03	8.40e-04	3.89e-03	1.20e-04	5.18e-05
4.18e-03	3.18e-02	1.38e-02	4.12e-03	2.10e-03	8.22e-04	4.06e-03	2.25e-04	5.06e-05
4.36e-03	3.83e-02	1.36e-02	4.30e-03	3.07e-03	8.09e-04	4.24e-03	2.23e-04	4.97e-05
4.56e-03	2.67e-02	1.33e-02	4.49e-03	2.00e-03	7.93e-04	4.43e-03	2.20e-04	4.87e-05
4.76e-03	2.53e-02	1.32e-02	4.69e-03	2.73e-03	7.81e-04	4.62e-03	2.17e-04	4.81e-05
4.98e-03	3.71e-02	1.29e-02	4.90e-03	3.33e-03	7.72e-04	4.83e-03	2.50e-04	4.72e-05
5.20e-03	4.32e-02	1.28e-02	5.12e-03	2.34e-03	7.61e-04	5.05e-03	2.26e-04	4.67e-05
5.44e-03	4.01e-02	1.25e-02	5.36e-03	2.08e-03	7.52e-04	5.28e-03	2.15e-04	4.59e-05
5.68e-03	3.18e-02	1.25e-02	5.60e-03	3.63e-03	7.45e-04	5.52e-03	1.77e-04	4.56e-05
5.94e-03	2.25e-02	1.24e-02	5.85e-03	2.69e-03	7.39e-04	5.77e-03	2.41e-04	4.50e-05
6.21e-03	3.17e-02	1.23e-02	6.12e-03	2.19e-03	7.34e-04	6.03e-03	2.25e-04	4.48e-05
6.49e-03	3.21e-02	1.23e-02	6.40e-03	2.58e-03	7.27e-04	6.30e-03	1.69e-04	4.45e-05
6.79e-03	7.75e-03	1.23e-02	6.69e-03	1.83e-03	7.27e-04	6.59e-03	1.14e-04	4.44e-05
7.10e-03	2.39e-02	1.22e-02	7.00e-03	8.84e-04	7.26e-04	6.89e-03	1.48e-04	4.43e-05
7.43e-03	2.54e-02	1.23e-02	7.32e-03	1.37e-03	7.25e-04	7.21e-03	1.04e-04	4.43e-05
7.77e-03	1.39e-02	1.23e-02	7.66e-03	6.65e-04	7.30e-04	7.54e-03	6.40e-05	4.45e-05
8.13e-03	3.64e-02	1.24e-02	8.01e-03	1.70e-03	7.38e-04	7.89e-03	8.00e-05	4.49e-05
8.51e-03	2.94e-02	1.26e-02	8.38e-03	1.92e-03	7.52e-04	8.25e-03	1.73e-04	4.56e-05
8.90e-03	3.52e-02	1.28e-02	8.77e-03	2.56e-03	7.61e-04	8.64e-03	1.64e-04	4.64e-05
9.31e-03	5.42e-02	1.29e-02	9.17e-03	3.90e-03	7.78e-04	9.04e-03	2.41e-04	4.71e-05
9.74e-03	4.13e-02	1.31e-02	9.60e-03	3.38e-03	7.83e-04	9.46e-03	2.98e-04	4.78e-05
1.02e-02	3.80e-02	1.33e-02	1.00e-02	3.01e-03	7.97e-04	9.89e-03	2.41e-04	4.84e-05
1.07e-02	2.44e-02	1.35e-02	1.05e-02	4.12e-03	8.05e-04	1.04e-02	3.93e-04	4.89e-05
1.12e-02	2.46e-02	1.37e-02	1.10e-02	4.48e-03	8.17e-04	1.08e-02	3.56e-04	4.95e-05
1.17e-02	6.72e-02	1.39e-02	1.15e-02	4.94e-03	8.28e-04	1.13e-02	3.35e-04	5.01e-05
1.22e-02	4.59e-02	1.41e-02	1.21e-02	4.40e-03	8.35e-04	1.19e-02	3.96e-04	5.07e-05
1.28e-02	5.78e-02	1.43e-02	1.26e-02	4.93e-03	8.47e-04	1.24e-02	3.30e-04	5.14e-05
1.34e-02	4.90e-02	1.44e-02	1.32e-02	4.80e-03	8.58e-04	1.30e-02	3.81e-04	5.20e-05
1.40e-02	4.60e-02	1.47e-02	1.38e-02	4.86e-03	8.70e-04	1.36e-02	4.57e-04	5.28e-05
1.47e-02	4.79e-02	1.49e-02	1.45e-02	3.88e-03	8.80e-04	1.43e-02	4.41e-04	5.33e-05
1.54e-02	8.00e-02	1.51e-02	1.52e-02	5.44e-03	8.92e-04	1.49e-02	4.50e-04	5.41e-05
1.61e-02	6.22e-02	1.53e-02	1.59e-02	6.12e-03	9.07e-04	1.56e-02	4.92e-04	5.47e-05
1.69e-02	7.98e-02	1.55e-02	1.66e-02	5.62e-03	9.16e-04	1.64e-02	5.27e-04	5.54e-05
1.77e-02	6.34e-02	1.57e-02	1.74e-02	5.70e-03	9.32e-04	1.71e-02	3.95e-04	5.61e-05
1.85e-02	6.09e-02	1.59e-02	1.82e-02	7.00e-03	9.42e-04	1.79e-02	5.69e-04	5.68e-05
1.94e-02	7.79e-02	1.61e-02	1.91e-02	8.05e-03	9.55e-04	1.88e-02	7.08e-04	5.76e-05
2.03e-02	8.83e-02	1.63e-02	2.00e-02	8.83e-03	9.61e-04	1.97e-02	7.36e-04	5.78e-05
2.13e-02	1.37e-01	1.65e-02	2.09e-02	1.04e-02	9.72e-04	2.06e-02	9.61e-04	5.81e-05
2.23e-02	1.58e-01	1.65e-02	2.19e-02	1.43e-02	9.72e-04	2.16e-02	1.23e-03	5.81e-05
2.33e-02	2.41e-01	1.64e-02	2.30e-02	2.20e-02	9.70e-04	2.26e-02	1.75e-03	5.75e-05
2.44e-02	2.78e-01	1.63e-02	2.40e-02	2.49e-02	9.52e-04	2.37e-02	2.11e-03	5.62e-05
2.56e-02	2.14e-01	1.61e-02	2.52e-02	2.23e-02	9.37e-04	2.48e-02	1.95e-03	5.46e-05
2.68e-02	8.93e-02	1.62e-02	2.64e-02	1.43e-02	9.22e-04	2.60e-02	1.25e-03	5.37e-05
2.81e-02	4.45e-02	1.63e-02	2.76e-02	6.40e-03	9.30e-04	2.72e-02	6.53e-04	5.37e-05
2.94e-02	5.33e-02	1.68e-02	2.89e-02	1.34e-03	9.45e-04	2.85e-02	2.68e-04	5.43e-05
3.08e-02	3.69e-02	1.71e-02	3.03e-02	2.71e-03	9.72e-04	2.99e-02	1.47e-04	5.55e-05
3.23e-02	5.55e-02	1.75e-02	3.18e-02	3.41e-03	9.91e-04	3.13e-02	3.44e-04	5.67e-05
3.38e-02	5.80e-02	1.79e-02	3.33e-02	5.39e-03	1.01e-03	3.28e-02	2.97e-04	5.81e-05
3.54e-02	7.22e-02	1.82e-02	3.49e-02	4.43e-03	1.04e-03	3.43e-02	3.96e-04	5.90e-05
3.71e-02	1.33e-01	1.86e-02	3.65e-02	6.27e-03	1.06e-03	3.59e-02	4.56e-04	6.03e-05
3.88e-02	6.35e-02	1.89e-02	3.82e-02	8.79e-03	1.07e-03	3.77e-02	5.03e-04	6.12e-05
4.07e-02	9.88e-02	1.92e-02	4.01e-02	8.34e-03	1.10e-03	3.95e-02	6.54e-04	6.23e-05
4.26e-02	1.32e-01	1.97e-02	4.20e-02	6.80e-03	1.11e-03	4.13e-02	6.41e-04	6.33e-05
4.47e-02	1.11e-01	1.99e-02	4.40e-02	1.10e-02	1.13e-03	4.33e-02	6.76e-04	6.44e-05
4.68e-02	1.58e-01	2.03e-02	4.61e-02	1.23e-02	1.15e-03	4.54e-02	7.48e-04	6.54e-05
4.90e-02	1.50e-01	2.06e-02	4.83e-02	9.17e-03	1.17e-03	4.75e-02	7.64e-04	6.64e-05
5.14e-02	1.35e-01	2.09e-02	5.06e-02	1.13e-02	1.19e-03	4.98e-02	7.78e-04	6.76e-05
5.38e-02	1.52e-01	2.13e-02	5.30e-02	1.08e-02	1.21e-03	5.22e-02	8.14e-04	6.87e-05
5.64e-02	1.42e-01	2.18e-02	5.55e-02	1.19e-02	1.23e-03	5.47e-02	8.20e-04	6.99e-05
5.91e-02	1.78e-01	2.21e-02	5.82e-02	1.21e-02	1.26e-03	5.73e-02	1.03e-03	7.09e-05
6.19e-02	2.00e-01	2.25e-02	6.09e-02	1.79e-02	1.27e-03	6.00e-02	1.14e-03	7.18e-05
6.48e-02	2.23e-01	2.28e-02	6.38e-02	1.92e-02	1.29e-03	6.29e-02	1.29e-03	7.25e-05
6.79e-02	2.44e-01	2.31e-02	6.69e-02	1.99e-02	1.30e-03	6.59e-02	1.41e-03	7.31e-05

Table 3.3.3 Continued. (2/4)

Neutron Energy [MeV]	Flux at z=110mm	Absolute Error	Neutron Energy [MeV]	Flux at z=210mm	Absolute Error	Neutron Energy [MeV]	Flux at z=310mm	Absolute Error
7.12e-02	2.64e-01	2.35e-02	7.01e-02	1.99e-02	1.32e-03	6.90e-02	1.38e-03	7.39e-05
7.46e-02	2.59e-01	2.37e-02	7.34e-02	1.95e-02	1.33e-03	7.23e-02	1.41e-03	7.46e-05
7.82e-02	2.69e-01	2.41e-02	7.70e-02	1.82e-02	1.35e-03	7.58e-02	1.56e-03	7.56e-05
8.19e-02	2.25e-01	2.44e-02	8.06e-02	1.93e-02	1.37e-03	7.94e-02	1.58e-03	7.60e-05
8.58e-02	1.78e-01	2.49e-02	8.45e-02	1.46e-02	1.39e-03	8.32e-02	1.26e-03	7.70e-05
8.99e-02	1.89e-01	2.55e-02	8.85e-02	1.57e-02	1.42e-03	8.72e-02	8.83e-04	7.83e-05
9.42e-02	2.42e-01	2.60e-02	9.28e-02	1.63e-02	1.45e-03	9.13e-02	1.01e-03	8.00e-05
9.87e-02	2.27e-01	2.65e-02	9.72e-02	2.16e-02	1.47e-03	9.57e-02	1.37e-03	8.13e-05
1.03e-01	2.48e-01	2.70e-02	1.02e-01	2.01e-02	1.50e-03	1.00e-01	1.45e-03	8.28e-05
1.08e-01	2.93e-01	2.76e-02	1.07e-01	2.31e-02	1.52e-03	1.05e-01	1.62e-03	8.35e-05
1.14e-01	3.48e-01	2.81e-02	1.12e-01	2.50e-02	1.55e-03	1.10e-01	1.93e-03	8.46e-05
1.19e-01	4.27e-01	2.88e-02	1.17e-01	3.38e-02	1.57e-03	1.15e-01	2.26e-03	8.56e-05
1.25e-01	4.54e-01	2.97e-02	1.23e-01	3.97e-02	1.61e-03	1.21e-01	2.60e-03	8.70e-05
1.31e-01	4.66e-01	3.06e-02	1.29e-01	3.87e-02	1.64e-03	1.27e-01	2.87e-03	8.84e-05
1.37e-01	3.93e-01	3.16e-02	1.35e-01	3.01e-02	1.69e-03	1.33e-01	2.31e-03	9.02e-05
1.44e-01	3.34e-01	3.27e-02	1.41e-01	2.35e-02	1.75e-03	1.39e-01	1.72e-03	9.27e-05
1.50e-01	4.27e-01	3.34e-02	1.50e-01	2.36e-02	2.01e-03	1.46e-01	1.78e-03	9.55e-05
1.57e-01	3.80e-01	3.20e-02	1.57e-01	3.55e-02	1.93e-03	1.50e-01	1.62e-03	1.17e-04
1.64e-01	4.45e-01	3.11e-02	1.64e-01	4.02e-02	1.85e-03	1.57e-01	1.94e-03	1.12e-04
1.72e-01	4.64e-01	3.03e-02	1.72e-01	3.78e-02	1.78e-03	1.64e-01	2.52e-03	1.08e-04
1.80e-01	5.35e-01	2.95e-02	1.80e-01	3.89e-02	1.73e-03	1.72e-01	2.67e-03	1.04e-04
1.89e-01	5.54e-01	2.89e-02	1.89e-01	3.31e-02	1.69e-03	1.80e-01	2.66e-03	1.00e-04
1.98e-01	3.91e-01	2.83e-02	1.98e-01	2.62e-02	1.66e-03	1.89e-01	2.09e-03	9.73e-05
2.08e-01	4.50e-01	2.80e-02	2.08e-01	3.28e-02	1.63e-03	1.98e-01	1.62e-03	9.53e-05
2.18e-01	5.40e-01	2.76e-02	2.18e-01	3.65e-02	1.61e-03	2.08e-01	2.06e-03	9.35e-05
2.28e-01	4.65e-01	2.73e-02	2.28e-01	3.35e-02	1.59e-03	2.18e-01	2.39e-03	9.17e-05
2.39e-01	5.05e-01	2.71e-02	2.39e-01	3.44e-02	1.57e-03	2.28e-01	2.07e-03	9.00e-05
2.50e-01	5.30e-01	2.69e-02	2.50e-01	4.41e-02	1.55e-03	2.39e-01	2.26e-03	8.87e-05
2.62e-01	6.01e-01	2.67e-02	2.62e-01	4.62e-02	1.52e-03	2.50e-01	2.47e-03	8.73e-05
2.75e-01	6.67e-01	2.65e-02	2.75e-01	4.75e-02	1.50e-03	2.62e-01	2.87e-03	8.56e-05
2.88e-01	7.36e-01	2.62e-02	2.88e-01	5.29e-02	1.47e-03	2.75e-01	3.15e-03	8.39e-05
3.02e-01	8.43e-01	2.59e-02	3.02e-01	6.71e-02	1.43e-03	2.88e-01	3.30e-03	8.17e-05
3.16e-01	8.97e-01	2.55e-02	3.16e-01	5.95e-02	1.40e-03	3.02e-01	3.91e-03	7.90e-05
3.32e-01	8.76e-01	2.50e-02	3.32e-01	5.39e-02	1.36e-03	3.16e-01	3.89e-03	7.63e-05
3.48e-01	9.22e-01	2.46e-02	3.48e-01	6.40e-02	1.33e-03	3.32e-01	3.50e-03	7.34e-05
3.64e-01	9.59e-01	2.42e-02	3.64e-01	6.54e-02	1.29e-03	3.48e-01	3.45e-03	7.08e-05
3.82e-01	8.58e-01	2.38e-02	3.82e-01	5.06e-02	1.25e-03	3.64e-01	3.42e-03	6.84e-05
4.00e-01	7.41e-01	2.35e-02	4.00e-01	3.85e-02	1.23e-03	3.82e-01	2.94e-03	6.61e-05
4.19e-01	6.31e-01	2.33e-02	4.19e-01	3.66e-02	1.22e-03	4.00e-01	2.20e-03	6.47e-05
4.39e-01	6.79e-01	2.32e-02	4.39e-01	4.06e-02	1.21e-03	4.19e-01	1.85e-03	6.34e-05
4.60e-01	8.24e-01	2.33e-02	4.60e-01	4.76e-02	1.20e-03	4.39e-01	2.09e-03	6.25e-05
4.82e-01	8.00e-01	2.33e-02	4.82e-01	4.84e-02	1.19e-03	4.60e-01	2.44e-03	6.17e-05
5.06e-01	8.69e-01	2.36e-02	5.06e-01	4.85e-02	1.20e-03	4.82e-01	2.44e-03	6.11e-05
5.30e-01	8.70e-01	2.41e-02	5.30e-01	4.87e-02	1.21e-03	5.06e-01	2.59e-03	6.09e-05
5.55e-01	8.51e-01	2.45e-02	5.55e-01	5.06e-02	1.22e-03	5.30e-01	2.48e-03	6.09e-05
5.82e-01	9.65e-01	2.49e-02	5.82e-01	5.68e-02	1.22e-03	5.55e-01	2.64e-03	6.10e-05
6.10e-01	1.15e+00	2.51e-02	6.10e-01	7.02e-02	1.21e-03	5.82e-01	2.88e-03	6.02e-05
6.39e-01	1.31e+00	2.51e-02	6.39e-01	6.97e-02	1.18e-03	6.10e-01	3.35e-03	5.87e-05
6.70e-01	1.20e+00	2.50e-02	6.70e-01	5.78e-02	1.15e-03	6.39e-01	3.45e-03	5.64e-05
7.02e-01	1.02e+00	2.49e-02	7.02e-01	4.85e-02	1.12e-03	6.70e-01	2.73e-03	5.37e-05
7.35e-01	8.56e-01	2.51e-02	7.35e-01	3.73e-02	1.12e-03	7.02e-01	2.05e-03	5.15e-05
7.71e-01	7.73e-01	2.53e-02	7.71e-01	3.15e-02	1.12e-03	7.35e-01	1.60e-03	5.04e-05
8.08e-01	7.64e-01	2.57e-02	8.08e-01	3.14e-02	1.12e-03	7.71e-01	1.35e-03	4.96e-05
8.46e-01	7.44e-01	2.61e-02	8.46e-01	3.11e-02	1.13e-03	8.08e-01	1.19e-03	4.92e-05
8.87e-01	7.68e-01	2.65e-02	8.87e-01	3.26e-02	1.13e-03	8.46e-01	1.14e-03	4.90e-05
9.30e-01	8.46e-01	2.67e-02	9.30e-01	3.30e-02	1.12e-03	8.87e-01	1.20e-03	4.84e-05
9.74e-01	8.66e-01	2.68e-02	9.74e-01	3.14e-02	1.11e-03	9.30e-01	1.20e-03	4.78e-05
1.02e+00	7.70e-01	2.68e-02	1.02e+00	2.74e-02	1.10e-03	9.74e-01	1.13e-03	4.65e-05
						1.02e+00	8.67e-04	4.56e-05

Table 3.3.3 Continued. (3/4)

Neutron Energy [MeV]	Flux at z=410mm	Absolute Error	Neutron Energy [MeV]	Flux at z=610mm	Absolute Error	Neutron Energy [MeV]	Flux at z=810mm	Absolute Error
2.96e-03	1.68e-05	4.73e-06	2.92e-03	2.49e-06	6.09e-07	2.88e-03	1.70e-07	7.82e-08
3.09e-03	1.30e-05	4.53e-06	3.05e-03	2.00e-06	5.82e-07	3.01e-03	1.87e-07	7.55e-08
3.23e-03	8.06e-06	4.38e-06	3.18e-03	1.62e-06	5.61e-07	3.14e-03	3.44e-07	7.27e-08
3.37e-03	1.13e-05	4.24e-06	3.32e-03	1.72e-06	5.49e-07	3.27e-03	3.06e-07	7.06e-08
3.51e-03	1.76e-05	4.14e-06	3.46e-03	2.66e-06	5.28e-07	3.42e-03	2.52e-07	6.81e-08
3.67e-03	8.34e-06	4.01e-06	3.62e-03	2.41e-06	5.16e-07	3.56e-03	3.14e-07	6.62e-08
3.83e-03	1.80e-05	3.94e-06	3.78e-03	2.38e-06	4.98e-07	3.72e-03	3.30e-07	6.50e-08
4.00e-03	1.42e-05	3.85e-06	3.94e-03	2.83e-06	4.89e-07	3.89e-03	3.29e-07	6.32e-08
4.18e-03	1.23e-05	3.77e-06	4.12e-03	2.33e-06	4.77e-07	4.06e-03	4.05e-07	6.16e-08
4.36e-03	1.99e-05	3.70e-06	4.30e-03	2.16e-06	4.68e-07	4.24e-03	3.67e-07	6.02e-08
4.56e-03	1.88e-05	3.63e-06	4.49e-03	2.46e-06	4.62e-07	4.43e-03	3.13e-07	5.90e-08
4.76e-03	1.49e-05	3.56e-06	4.69e-03	2.72e-06	4.53e-07	4.62e-03	3.56e-07	5.82e-08
4.98e-03	1.77e-05	3.51e-06	4.90e-03	2.37e-06	4.47e-07	4.83e-03	3.95e-07	5.73e-08
5.20e-03	1.63e-05	3.48e-06	5.12e-03	3.38e-06	4.41e-07	5.05e-03	3.89e-07	5.63e-08
5.44e-03	1.52e-05	3.42e-06	5.36e-03	3.73e-06	4.32e-07	5.28e-03	3.77e-07	5.57e-08
5.68e-03	2.17e-05	3.40e-06	5.60e-03	2.75e-06	4.26e-07	5.52e-03	4.28e-07	5.50e-08
5.94e-03	1.04e-05	3.35e-06	5.85e-03	2.84e-06	4.23e-07	5.77e-03	4.33e-07	5.42e-08
6.21e-03	1.11e-05	3.35e-06	6.12e-03	2.31e-06	4.17e-07	6.03e-03	3.45e-07	5.35e-08
6.49e-03	1.36e-05	3.33e-06	6.40e-03	2.16e-06	4.17e-07	6.30e-03	3.81e-07	5.30e-08
6.79e-03	1.30e-05	3.31e-06	6.69e-03	1.76e-06	4.14e-07	6.59e-03	2.41e-07	5.27e-08
7.10e-03	5.59e-06	3.32e-06	7.00e-03	2.11e-06	4.11e-07	6.89e-03	2.35e-07	5.26e-08
7.43e-03	7.79e-06	3.32e-06	7.32e-03	1.61e-06	4.11e-07	7.21e-03	1.36e-07	5.24e-08
7.77e-03	3.83e-06	3.35e-06	7.66e-03	3.19e-07	4.14e-07	7.54e-03	1.48e-07	5.28e-08
8.13e-03	1.29e-05	3.39e-06	8.01e-03	1.05e-06	4.20e-07	7.89e-03	1.96e-07	5.32e-08
8.51e-03	1.54e-05	3.44e-06	8.38e-03	1.95e-06	4.26e-07	8.25e-03	3.14e-07	5.40e-08
8.90e-03	1.80e-05	3.49e-06	8.77e-03	2.79e-06	4.32e-07	8.64e-03	3.87e-07	5.46e-08
9.31e-03	2.10e-05	3.54e-06	9.17e-03	2.67e-06	4.38e-07	9.04e-03	3.89e-07	5.54e-08
9.74e-03	2.02e-05	3.59e-06	9.60e-03	4.05e-06	4.44e-07	9.46e-03	2.98e-07	5.62e-08
1.02e-02	2.01e-05	3.63e-06	1.00e-02	4.27e-06	4.47e-07	9.89e-03	4.70e-07	5.70e-08
1.07e-02	2.37e-05	3.69e-06	1.05e-02	4.03e-06	4.53e-07	1.04e-02	5.56e-07	5.77e-08
1.12e-02	2.41e-05	3.73e-06	1.10e-02	3.12e-06	4.59e-07	1.08e-02	6.40e-07	5.82e-08
1.17e-02	3.54e-05	3.76e-06	1.15e-02	4.77e-06	4.62e-07	1.13e-02	7.24e-07	5.86e-08
1.22e-02	3.37e-05	3.80e-06	1.21e-02	5.06e-06	4.68e-07	1.19e-02	6.49e-07	5.92e-08
1.28e-02	2.90e-05	3.84e-06	1.26e-02	5.71e-06	4.71e-07	1.24e-02	5.91e-07	5.97e-08
1.34e-02	2.41e-05	3.88e-06	1.32e-02	4.78e-06	4.77e-07	1.30e-02	6.98e-07	6.04e-08
1.40e-02	2.95e-05	3.95e-06	1.38e-02	4.99e-06	4.80e-07	1.36e-02	9.16e-07	6.08e-08
1.47e-02	3.66e-05	3.99e-06	1.45e-02	5.44e-06	4.86e-07	1.43e-02	8.57e-07	6.12e-08
1.54e-02	3.49e-05	4.04e-06	1.52e-02	6.31e-06	4.89e-07	1.49e-02	7.05e-07	6.16e-08
1.61e-02	3.86e-05	4.07e-06	1.59e-02	6.38e-06	4.95e-07	1.56e-02	7.37e-07	6.23e-08
1.69e-02	4.84e-05	4.13e-06	1.66e-02	5.77e-06	4.98e-07	1.64e-02	9.77e-07	6.28e-08
1.77e-02	4.19e-05	4.15e-06	1.74e-02	6.48e-06	5.04e-07	1.71e-02	1.01e-06	6.31e-08
1.85e-02	4.59e-05	4.19e-06	1.82e-02	8.12e-06	5.07e-07	1.79e-02	9.81e-07	6.35e-08
1.94e-02	4.86e-05	4.23e-06	1.91e-02	8.21e-06	5.10e-07	1.88e-02	1.12e-06	6.39e-08
2.03e-02	5.86e-05	4.25e-06	2.00e-02	9.23e-06	5.10e-07	1.97e-02	1.27e-06	6.40e-08
2.13e-02	9.40e-05	4.26e-06	2.09e-02	1.18e-05	5.10e-07	2.06e-02	1.62e-06	6.38e-08
2.23e-02	1.16e-04	4.19e-06	2.19e-02	1.74e-05	5.04e-07	2.16e-02	2.20e-06	6.27e-08
2.33e-02	1.50e-04	4.09e-06	2.30e-02	2.11e-05	4.89e-07	2.26e-02	2.84e-06	6.11e-08
2.44e-02	1.55e-04	3.96e-06	2.40e-02	2.44e-05	4.71e-07	2.37e-02	3.33e-06	5.84e-08
2.56e-02	1.06e-04	3.86e-06	2.52e-02	2.05e-05	4.50e-07	2.48e-02	3.16e-06	5.54e-08
2.68e-02	5.44e-05	3.80e-06	2.64e-02	1.29e-05	4.38e-07	2.60e-02	2.05e-06	5.29e-08
2.81e-02	2.53e-05	3.84e-06	2.76e-02	5.54e-06	4.35e-07	2.72e-02	9.67e-07	5.19e-08
2.94e-02	1.80e-05	3.91e-06	2.89e-02	2.16e-06	4.38e-07	2.85e-02	3.45e-07	5.20e-08
3.08e-02	1.60e-05	4.00e-06	3.03e-02	1.94e-06	4.47e-07	2.99e-02	2.10e-07	5.31e-08
3.23e-02	1.94e-05	4.07e-06	3.18e-02	1.94e-06	4.56e-07	3.13e-02	2.26e-07	5.42e-08
3.38e-02	2.04e-05	4.16e-06	3.33e-02	2.55e-06	4.68e-07	3.28e-02	2.31e-07	5.55e-08
3.54e-02	2.67e-05	4.25e-06	3.49e-02	3.76e-06	4.77e-07	3.43e-02	5.38e-07	5.65e-08
3.71e-02	3.63e-05	4.34e-06	3.65e-02	4.72e-06	4.83e-07	3.59e-02	5.20e-07	5.75e-08
3.88e-02	3.70e-05	4.39e-06	3.82e-02	5.06e-06	4.92e-07	3.77e-02	5.64e-07	5.82e-08
4.07e-02	3.91e-05	4.48e-06	4.01e-02	5.88e-06	4.98e-07	3.95e-02	6.46e-07	5.91e-08
4.26e-02	4.68e-05	4.54e-06	4.20e-02	5.71e-06	5.04e-07	4.13e-02	6.54e-07	5.99e-08
4.47e-02	5.10e-05	4.61e-06	4.40e-02	5.01e-06	5.13e-07	4.33e-02	7.76e-07	6.06e-08
4.68e-02	5.01e-05	4.70e-06	4.61e-02	6.35e-06	5.22e-07	4.54e-02	8.47e-07	6.13e-08
4.90e-02	4.87e-05	4.74e-06	4.83e-02	7.90e-06	5.28e-07	4.75e-02	9.12e-07	6.22e-08
5.14e-02	5.27e-05	4.84e-06	5.06e-02	7.40e-06	5.34e-07	4.98e-02	8.40e-07	6.26e-08
5.38e-02	5.65e-05	4.90e-06	5.30e-02	6.55e-06	5.40e-07	5.22e-02	8.75e-07	6.36e-08
5.64e-02	5.51e-05	4.97e-06	5.55e-02	7.02e-06	5.49e-07	5.47e-02	8.24e-07	6.44e-08
5.91e-02	6.30e-05	5.05e-06	5.82e-02	8.81e-06	5.55e-07	5.73e-02	9.88e-07	6.52e-08
6.19e-02	9.04e-05	5.10e-06	6.09e-02	1.08e-05	5.64e-07	6.00e-02	1.19e-06	6.57e-08
6.48e-02	9.84e-05	5.14e-06	6.38e-02	1.22e-05	5.64e-07	6.29e-02	1.40e-06	6.60e-08
6.79e-02	1.02e-04	5.17e-06	6.69e-02	1.39e-05	5.67e-07	6.59e-02	1.72e-06	6.63e-08

Table 3.3.3 Continued. (4/4)

Neutron Energy [MeV]	Flux at z=410mm	Absolute Error	Neutron Energy [MeV]	Flux at z=610mm	Absolute Error	Neutron Energy [MeV]	Flux at z=810mm	Absolute Error
7.12e-02	8.81e-05	5.20e-06	7.01e-02	1.24e-05	5.64e-07	6.90e-02	1.48e-06	6.62e-08
7.46e-02	9.24e-05	5.25e-06	7.34e-02	1.28e-05	5.67e-07	7.23e-02	1.31e-06	6.63e-08
7.82e-02	1.03e-04	5.29e-06	7.70e-02	1.38e-05	5.70e-07	7.58e-02	1.67e-06	6.66e-08
8.19e-02	9.08e-05	5.34e-06	8.06e-02	1.25e-05	5.73e-07	7.94e-02	1.79e-06	6.65e-08
8.58e-02	6.99e-05	5.42e-06	8.45e-02	1.09e-05	5.76e-07	8.32e-02	1.53e-06	6.65e-08
8.99e-02	6.19e-05	5.50e-06	8.85e-02	8.22e-06	5.82e-07	8.72e-02	1.10e-06	6.68e-08
9.42e-02	9.29e-05	5.60e-06	9.28e-02	9.04e-06	5.91e-07	9.13e-02	1.02e-06	6.75e-08
9.87e-02	9.54e-05	5.67e-06	9.72e-02	1.08e-05	6.00e-07	9.57e-02	1.25e-06	6.82e-08
1.03e-01	9.04e-05	5.74e-06	1.02e-01	1.19e-05	6.03e-07	1.00e-01	1.45e-06	6.89e-08
1.08e-01	1.03e-04	5.80e-06	1.07e-01	1.35e-05	6.06e-07	1.05e-01	1.49e-06	6.92e-08
1.14e-01	1.37e-04	5.87e-06	1.12e-01	1.56e-05	6.12e-07	1.10e-01	1.72e-06	6.96e-08
1.19e-01	1.79e-04	5.93e-06	1.17e-01	1.97e-05	6.12e-07	1.15e-01	2.13e-06	6.94e-08
1.25e-01	1.90e-04	6.00e-06	1.23e-01	2.32e-05	6.15e-07	1.21e-01	2.66e-06	6.95e-08
1.31e-01	1.67e-04	6.06e-06	1.29e-01	2.32e-05	6.15e-07	1.27e-01	2.86e-06	6.89e-08
1.37e-01	1.26e-04	6.20e-06	1.35e-01	1.69e-05	6.21e-07	1.33e-01	2.43e-06	6.87e-08
1.44e-01	1.16e-04	6.32e-06	1.41e-01	1.29e-05	6.30e-07	1.39e-01	1.63e-06	6.90e-08
1.50e-01	1.40e-04	6.51e-06	1.48e-01	1.46e-05	6.42e-07	1.46e-01	1.42e-06	7.00e-08
1.58e-01	1.57e-04	6.64e-06	1.57e-01	1.39e-05	4.47e-07	1.50e-01	1.37e-06	5.48e-08
1.64e-01	1.46e-04	4.52e-06	1.64e-01	1.78e-05	4.26e-07	1.57e-01	1.45e-06	5.21e-08
1.72e-01	1.63e-04	4.34e-06	1.72e-01	1.81e-05	4.05e-07	1.64e-01	1.91e-06	4.97e-08
1.80e-01	1.59e-04	4.16e-06	1.80e-01	1.69e-05	3.87e-07	1.72e-01	2.20e-06	4.69e-08
1.89e-01	1.18e-04	4.04e-06	1.89e-01	1.36e-05	3.72e-07	1.80e-01	1.96e-06	4.44e-08
1.98e-01	8.71e-05	3.96e-06	1.98e-01	1.08e-05	3.63e-07	1.89e-01	1.45e-06	4.23e-08
2.08e-01	1.06e-04	3.90e-06	2.08e-01	1.20e-05	3.54e-07	1.98e-01	1.12e-06	4.09e-08
2.18e-01	1.30e-04	3.83e-06	2.18e-01	1.44e-05	3.42e-07	2.08e-01	1.27e-06	3.98e-08
2.28e-01	1.42e-04	3.75e-06	2.28e-01	1.41e-05	3.33e-07	2.18e-01	1.44e-06	3.87e-08
2.39e-01	1.38e-04	3.67e-06	2.39e-01	1.36e-05	3.24e-07	2.28e-01	1.49e-06	3.75e-08
2.50e-01	1.44e-04	3.60e-06	2.50e-01	1.48e-05	3.18e-07	2.39e-01	1.47e-06	3.63e-08
2.62e-01	1.70e-04	3.51e-06	2.62e-01	1.83e-05	3.06e-07	2.50e-01	1.58e-06	3.51e-08
2.75e-01	1.88e-04	3.42e-06	2.75e-01	1.95e-05	2.94e-07	2.62e-01	1.90e-06	3.37e-08
2.88e-01	2.03e-04	3.30e-06	2.88e-01	1.94e-05	2.80e-07	2.75e-01	2.02e-06	3.21e-08
3.02e-01	2.30e-04	3.16e-06	3.02e-01	2.24e-05	2.65e-07	2.88e-01	1.99e-06	3.02e-08
3.16e-01	2.17e-04	3.03e-06	3.16e-01	2.04e-05	2.49e-07	3.02e-01	2.20e-06	2.81e-08
3.32e-01	1.90e-04	2.89e-06	3.32e-01	1.65e-05	2.34e-07	3.16e-01	1.99e-06	2.62e-08
3.48e-01	1.89e-04	2.77e-06	3.48e-01	1.66e-05	2.20e-07	3.32e-01	1.48e-06	2.42e-08
3.64e-01	1.83e-04	2.65e-06	3.64e-01	1.54e-05	2.08e-07	3.48e-01	1.46e-06	2.25e-08
3.82e-01	1.49e-04	2.54e-06	3.82e-01	1.22e-05	1.96e-07	3.64e-01	1.37e-06	2.10e-08
4.00e-01	1.08e-04	2.46e-06	4.00e-01	8.02e-06	1.88e-07	3.82e-01	1.02e-06	1.95e-08
4.19e-01	9.41e-05	2.41e-06	4.19e-01	7.07e-06	1.81e-07	4.00e-01	6.69e-07	1.85e-08
4.39e-01	1.04e-04	2.37e-06	4.39e-01	7.68e-06	1.77e-07	4.19e-01	5.26e-07	1.78e-08
4.60e-01	1.21e-04	2.33e-06	4.60e-01	8.34e-06	1.72e-07	4.39e-01	5.74e-07	1.73e-08
4.82e-01	1.23e-04	2.29e-06	4.82e-01	8.89e-06	1.68e-07	4.60e-01	6.81e-07	1.68e-08
5.06e-01	1.25e-04	2.27e-06	5.06e-01	8.47e-06	1.65e-07	4.82e-01	6.73e-07	1.63e-08
5.30e-01	1.18e-04	2.25e-06	5.30e-01	8.15e-06	1.61e-07	5.06e-01	6.17e-07	1.58e-08
5.55e-01	1.23e-04	2.24e-06	5.55e-01	8.43e-06	1.58e-07	5.30e-01	6.31e-07	1.54e-08
5.82e-01	1.42e-04	2.18e-06	5.82e-01	9.49e-06	1.51e-07	5.55e-01	6.30e-07	1.48e-08
6.10e-01	1.62e-04	2.10e-06	6.10e-01	1.05e-05	1.41e-07	5.82e-01	6.66e-07	1.42e-08
6.39e-01	1.58e-04	1.97e-06	6.39e-01	9.54e-06	1.27e-07	6.10e-01	7.55e-07	1.29e-08
6.70e-01	1.23e-04	1.83e-06	6.70e-01	6.75e-06	1.14e-07	6.39e-01	6.82e-07	1.15e-08
7.02e-01	8.62e-05	1.71e-06	7.02e-01	4.19e-06	1.02e-07	6.70e-01	4.47e-07	9.92e-09
7.35e-01	6.38e-05	1.64e-06	7.35e-01	2.78e-06	9.63e-08	7.02e-01	2.70e-07	8.59e-09
7.71e-01	4.84e-05	1.59e-06	7.71e-01	2.10e-06	9.12e-08	7.35e-01	1.63e-07	7.89e-09
8.08e-01	4.33e-05	1.56e-06	8.08e-01	1.86e-06	8.94e-08	7.71e-01	1.12e-07	7.41e-09
8.46e-01	4.69e-05	1.53e-06	8.46e-01	1.78e-06	8.52e-08	8.08e-01	9.23e-08	7.09e-09
8.87e-01	4.47e-05	1.48e-06	8.87e-01	1.93e-06	8.22e-08	8.46e-01	9.25e-08	6.77e-09
9.30e-01	3.95e-05	1.42e-06	9.30e-01	1.74e-06	7.59e-08	8.87e-01	9.54e-08	6.39e-09
9.74e-01	3.43e-05	1.37e-06	9.74e-01	1.39e-06	7.05e-08	9.30e-01	8.63e-08	5.90e-09
1.02e+00	2.82e-05	1.32e-06	1.02e+00	1.00e-06	6.60e-08	9.74e-01	6.53e-08	5.31e-09
						1.02e+00	5.08e-08	4.85e-09

Table 3.3.4 Neutron spectra in the iron assembly measured by the SDT method in the unit of [n / cm^2 / lethargy / source]. (1/2)

Neutron Energy [MeV]	Flux at z=110mm	Absolute Error	Flux at z=210mm	Absolute Error	Flux at z=310mm	Absolute Error
2.82e-07	4.18e-05	7.04e-06	6.09e-06	5.65e-07	1.62e-06	1.36e-07
3.55e-07	2.25e-04	2.02e-05	2.84e-05	1.82e-06	1.28e-06	1.21e-07
4.47e-07	2.14e-04	2.03e-05	2.72e-05	1.79e-06	4.25e-06	2.94e-07
5.62e-07	5.24e-04	3.91e-05	7.01e-05	4.10e-06	5.34e-06	3.60e-07
7.08e-07	6.94e-04	4.98e-05	9.21e-05	5.31e-06	7.46e-06	4.83e-07
8.91e-07	6.35e-04	4.79e-05	9.12e-05	5.32e-06	1.08e-05	6.72e-07
1.12e-06	1.17e-03	7.89e-05	1.60e-04	8.97e-06	1.41e-05	8.57e-07
1.41e-06	1.31e-03	8.78e-05	1.78e-04	9.99e-06	1.65e-05	9.96e-07
1.78e-06	1.54e-03	1.03e-04	2.13e-04	1.19e-05	2.13e-05	1.27e-06
2.24e-06	1.64e-03	1.10e-04	2.40e-04	1.34e-05	2.37e-05	1.41e-06
2.82e-06	2.43e-03	1.55e-04	3.23e-04	1.79e-05	2.92e-05	1.72e-06
3.55e-06	2.77e-03	1.77e-04	3.57e-04	1.98e-05	3.32e-05	1.96e-06
4.47e-06	3.08e-03	1.97e-04	3.95e-04	2.19e-05	3.68e-05	2.17e-06
5.62e-06	3.27e-03	2.11e-04	4.46e-04	2.48e-05	4.30e-05	2.53e-06
7.08e-06	4.13e-03	2.62e-04	5.46e-04	3.02e-05	4.46e-05	2.64e-06
8.91e-06	3.97e-03	2.59e-04	5.31e-04	2.97e-05	5.44e-05	3.20e-06
1.12e-05	4.84e-03	3.11e-04	6.04e-04	3.37e-05	5.93e-05	3.51e-06
1.41e-05	4.93e-03	3.22e-04	6.33e-04	3.56e-05	6.77e-05	4.01e-06
1.78e-05	4.80e-03	3.23e-04	6.68e-04	3.78e-05	6.54e-05	3.94e-06
2.24e-05	6.13e-03	4.03e-04	7.63e-04	4.32e-05	6.46e-05	3.96e-06
2.82e-05	6.48e-03	4.32e-04	8.30e-04	4.73e-05	7.23e-05	4.45e-06
3.55e-05	7.59e-03	5.04e-04	8.57e-04	4.94e-05	7.93e-05	4.91e-06
4.47e-05	7.83e-03	5.30e-04	8.78e-04	5.12e-05	8.43e-05	5.28e-06
5.62e-05	7.05e-03	5.00e-04	9.07e-04	5.35e-05	8.15e-05	5.24e-06
7.08e-05	7.39e-03	5.34e-04	9.33e-04	5.58e-05	9.03e-05	5.85e-06
8.91e-05	8.09e-03	5.90e-04	9.95e-04	6.02e-05	9.08e-05	6.02e-06
1.12e-04	8.00e-03	6.05e-04	1.01e-03	6.25e-05	9.51e-05	6.42e-06
1.41e-04	8.21e-03	6.36e-04	1.14e-03	7.13e-05	1.00e-04	6.89e-06
1.78e-04	9.09e-03	7.12e-04	1.16e-03	7.40e-05	9.96e-05	7.08e-06
2.24e-04	8.58e-03	7.05e-04	1.06e-03	6.99e-05	9.04e-05	6.74e-06
2.82e-04	9.17e-03	7.69e-04	1.04e-03	7.04e-05	8.39e-05	6.55e-06
3.55e-04	9.86e-03	8.42e-04	1.23e-03	8.37e-05	1.04e-04	8.05e-06
4.47e-04	1.07e-02	9.24e-04	1.29e-03	9.02e-05	1.15e-04	9.05e-06
5.62e-04	1.29e-02	1.11e-03	1.34e-03	9.61e-05	1.18e-04	9.54e-06
7.08e-04	1.34e-02	1.19e-03	1.35e-03	9.99e-05	1.25e-04	1.04e-05
8.91e-04	1.36e-02	1.27e-03	1.55e-03	1.17e-04	1.29e-04	1.10e-05
1.12e-03	1.51e-02	1.43e-03	1.65e-03	1.29e-04	1.61e-04	1.38e-05
1.41e-03	1.88e-02	1.80e-03	1.88e-03	1.51e-04	1.69e-04	1.51e-05
1.78e-03	2.01e-02	1.98e-03	2.05e-03	1.72e-04	1.81e-04	1.67e-05
2.24e-03	1.95e-02	2.02e-03	2.24e-03	1.95e-04	1.82e-04	1.75e-05
2.82e-03	1.90e-02	2.07e-03	2.20e-03	2.02e-04	2.03e-04	2.01e-05
3.55e-03	2.09e-02	2.35e-03	2.17e-03	2.09e-04	2.10e-04	2.16e-05
4.47e-03	2.30e-02	2.71e-03	2.59e-03	2.58e-04	2.46e-04	2.65e-05
5.62e-03	2.20e-02	2.72e-03	2.39e-03	2.52e-04	1.72e-04	2.04e-05
7.08e-03	2.81e-02	3.51e-03	2.94e-03	3.25e-04	2.35e-04	2.79e-05
8.91e-03	3.60e-02	4.64e-03	3.28e-03	3.84e-04	2.67e-04	3.32e-05

Table 3.3.4 Continued. (2/2)

Neutron Energy [MeV]	Flux at z=410mm	Absolute Error	Flux at z=610mm	Absolute Error	Flux at z=810mm	Absolute Error
2.82e-07	1.09e-07	8.71e-09	1.90e-08	1.57e-09	3.38e-09	2.99e-10
3.55e-07	2.61e-07	1.73e-08	4.15e-08	2.89e-09	5.69e-09	4.45e-10
4.47e-07	2.88e-07	1.92e-08	6.46e-08	4.21e-09	9.88e-09	6.91e-10
5.62e-07	5.27e-07	3.24e-08	9.44e-08	5.88e-09	1.27e-08	8.60e-10
7.08e-07	7.00e-07	4.21e-08	1.15e-07	7.09e-09	1.78e-08	1.16e-09
8.91e-07	8.60e-07	5.11e-08	1.51e-07	9.09e-09	2.12e-08	1.37e-09
1.12e-06	1.28e-06	7.36e-08	2.28e-07	1.33e-08	2.99e-08	1.86e-09
1.41e-06	1.50e-06	8.62e-08	2.62e-07	1.53e-08	3.44e-08	2.13e-09
1.78e-06	1.95e-06	1.11e-07	3.13e-07	1.82e-08	4.32e-08	2.63e-09
2.24e-06	2.15e-06	1.22e-07	3.90e-07	2.24e-08	4.82e-08	2.94e-09
2.82e-06	2.53e-06	1.43e-07	4.57e-07	2.62e-08	6.03e-08	3.62e-09
3.55e-06	2.94e-06	1.67e-07	5.35e-07	3.05e-08	6.56e-08	3.97e-09
4.47e-06	3.23e-06	1.83e-07	5.96e-07	3.41e-08	7.99e-08	4.78e-09
5.62e-06	3.85e-06	2.18e-07	6.11e-07	3.52e-08	8.50e-08	5.12e-09
7.08e-06	4.17e-06	2.37e-07	7.26e-07	4.17e-08	9.38e-08	5.67e-09
8.91e-06	4.76e-06	2.70e-07	8.14e-07	4.69e-08	1.06e-07	6.43e-09
1.12e-05	4.83e-06	2.76e-07	8.51e-07	4.94e-08	1.14e-07	6.96e-09
1.41e-05	5.25e-06	3.02e-07	8.88e-07	5.19e-08	1.24e-07	7.58e-09
1.78e-05	5.43e-06	3.15e-07	9.83e-07	5.76e-08	1.36e-07	8.37e-09
2.24e-05	6.13e-06	3.57e-07	1.05e-06	6.22e-08	1.41e-07	8.77e-09
2.82e-05	6.58e-06	3.86e-07	1.09e-06	6.54e-08	1.32e-07	8.45e-09
3.55e-05	6.69e-06	3.97e-07	1.12e-06	6.76e-08	1.57e-07	1.00e-08
4.47e-05	7.09e-06	4.26e-07	1.20e-06	7.35e-08	1.65e-07	1.07e-08
5.62e-05	7.22e-06	4.40e-07	1.26e-06	7.77e-08	1.65e-07	1.10e-08
7.08e-05	7.66e-06	4.72e-07	1.33e-06	8.36e-08	1.77e-07	1.19e-08
8.91e-05	7.59e-06	4.78e-07	1.31e-06	8.45e-08	1.70e-07	1.18e-08
1.12e-04	8.08e-06	5.17e-07	1.33e-06	8.77e-08	1.74e-07	1.24e-08
1.41e-04	8.02e-06	5.26e-07	1.45e-06	9.63e-08	1.73e-07	1.27e-08
1.78e-04	8.47e-06	5.65e-07	1.29e-06	8.99e-08	2.07e-07	1.51e-08
2.24e-04	7.62e-06	5.29e-07	1.24e-06	8.91e-08	1.88e-07	1.44e-08
2.82e-04	7.80e-06	5.56e-07	1.42e-06	1.03e-07	1.72e-07	1.39e-08
3.55e-04	8.74e-06	6.30e-07	1.48e-06	1.09e-07	1.86e-07	1.53e-08
4.47e-04	9.33e-06	6.89e-07	1.58e-06	1.19e-07	2.25e-07	1.84e-08
5.62e-04	1.04e-05	7.78e-07	1.82e-06	1.39e-07	2.17e-07	1.86e-08
7.08e-04	1.13e-05	8.67e-07	1.97e-06	1.54e-07	2.68e-07	2.28e-08
8.91e-04	1.26e-05	9.91e-07	2.14e-06	1.71e-07	2.83e-07	2.47e-08
1.12e-03	1.33e-05	1.08e-06	2.30e-06	1.90e-07	2.93e-07	2.64e-08
1.41e-03	1.41e-05	1.19e-06	2.37e-06	2.03e-07	3.28e-07	3.01e-08
1.78e-03	1.28e-05	1.13e-06	2.63e-06	2.32e-07	3.50e-07	3.31e-08
2.24e-03	1.49e-05	1.35e-06	2.77e-06	2.53e-07	3.49e-07	3.46e-08
2.82e-03	1.61e-05	1.52e-06	2.89e-06	2.75e-07	3.70e-07	3.81e-08
3.55e-03	1.72e-05	1.69e-06	2.86e-06	2.86e-07	3.44e-07	3.78e-08
4.47e-03	1.61e-05	1.68e-06	2.62e-06	2.78e-07	3.81e-07	4.28e-08
5.62e-03	1.67e-05	1.83e-06	3.20e-06	3.45e-07	3.60e-07	4.29e-08
7.08e-03	1.94e-05	2.20e-06	3.09e-06	3.54e-07	4.35e-07	5.22e-08
8.91e-03	2.28e-05	2.68e-06	4.13e-06	4.81e-07	5.21e-07	6.36e-08

Table 3.3.5 Integral neutron fluxes in the iron assembly derived from the measured neutron spectra in the unit of [n / cm^2 / source]. Numbers in the parenthesis are percentage errors.

Detector Position [mm]	Energy Range		
	0.1-1 MeV	10-100 keV	1-10 keV
110	1.57e-04 (5)	2.91e-05 (5)	5.12e-06 (11)
210	9.62e-05 (5)	2.46e-05 (5)	5.38e-06 (11)
310	5.43e-05 (5)	1.91e-05 (5)	4.67e-06 (11)
410	2.98e-05 (5)	1.33e-05 (5)	3.76e-06 (11)
610	9.27e-06 (5)	6.43e-06 (5)	2.22e-06 (11)
810	2.77e-06 (5)	2.54e-06 (5)	8.59e-07 (11)
Detector Position [mm]	Energy Range		
	0.1-1 keV	10-100 eV	1-10 eV
110	2.38e-06 (8)	1.50e-06 (6)	5.83e-07 (6)
210	2.80e-06 (8)	1.86e-06 (6)	7.80e-07 (6)
310	2.44e-06 (8)	1.74e-06 (6)	7.29e-07 (6)
410	2.13e-06 (8)	1.48e-06 (6)	6.53e-07 (6)
610	1.21e-06 (8)	8.51e-07 (6)	3.79e-07 (6)
810	4.82e-07 (8)	3.41e-07 (6)	1.49e-07 (6)

Table 3.3.6 Measured dosimetry reaction rates in the iron assembly in the unit of [reactions / atom / source]. Numbers in the parenthesis are percentage errors.

Detector Position [mm]	Reaction		
	$^{27}Al(n,a)^{24}Na$	$^{56}Fe(n,p)^{56}Mn$	$^{90}Zr(n,2n)^{89m+g}Zr$
0	2.51e-05 (2.7)	2.18e-05 (2.6)	1.96e-04 (2.7)
100	3.85e-06 (2.8)	3.38e-06 (2.7)	2.64e-05 (2.7)
200	6.29e-07 (2.8)	5.41e-07 (3.0)	4.14e-06 (2.7)
300	1.21e-07 (3.1)	1.06e-07 (3.0)	7.02e-07 (2.9)
400	2.20e-08 (3.5)	1.48e-08 (3.9)	1.49e-07 (3.6)
500	3.89e-09 (5.9)	3.51e-09 (5.6)	2.74e-08 (4.5)
700			5.57e-09 (8.9)
Detector Position [mm]	Reaction		
	$^{93}Nb(n,2n)^{92m}Nb$	$^{115}In(n,n')^{115m}In$	$^{197}Au(n,g)^{198}Au$
0	1.09e-04 (2.9)	3.24e-05 (2.6)	1.41e-04 (3.4)
100	1.08e-05 (3.0)	1.83e-05 (2.6)	6.21e-04 (3.0)
200	2.55e-06 (2.7)	5.12e-06 (2.9)	8.18e-04 (2.8)
300	4.63e-07 (3.2)	1.41e-06 (2.9)	7.42e-04 (3.1)
400	8.53e-08 (3.3)	3.89e-07 (3.4)	6.49e-04 (3.2)
500	1.55e-08 (4.7)	1.14e-07 (5.6)	5.10e-04 (3.2)
700		2.06e-08 (13.)	2.58e-04 (3.3)

Table 3.3.7 Gamma-ray spectra in the iron assembly measured by the BC-537 spectrometer in the unit of [photons / cm^2 / lethargy / source]. (1/2)

Photon Energy [MeV]	Flux at z=100mm	Absolute Error	Window [%]	Flux at z=300mm	Absolute Error	Window [%]
3.630e-01				2.030e-06	1.690e-07	26.8
3.800e-01				1.820e-06	1.520e-07	27.8
3.980e-01				2.080e-06	1.450e-07	27.5
4.170e-01	4.990e-05	2.440e-06	24.1	2.370e-06	1.420e-07	26.5
4.370e-01	4.770e-05	2.330e-06	23.0	2.540e-06	1.220e-07	26.0
4.570e-01	4.590e-05	2.260e-06	23.3	2.580e-06	1.060e-07	25.8
4.790e-01	4.430e-05	2.260e-06	24.1	2.480e-06	1.350e-07	25.7
5.010e-01	4.230e-05	2.170e-06	25.0	2.230e-06	1.770e-07	26.1
5.250e-01	3.930e-05	2.030e-06	26.1	1.900e-06	1.640e-07	26.7
5.490e-01	3.500e-05	2.010e-06	26.9	1.590e-06	1.090e-07	26.9
5.750e-01	3.020e-05	1.880e-06	26.8	1.380e-06	8.530e-08	26.8
6.030e-01	2.610e-05	1.730e-06	26.7	1.250e-06	8.640e-08	26.7
6.310e-01	2.350e-05	1.670e-06	26.6	1.210e-06	8.270e-08	26.5
6.610e-01	2.280e-05	1.570e-06	26.0	1.270e-06	8.440e-08	25.7
6.920e-01	2.480e-05	1.690e-06	24.8	1.450e-06	9.540e-08	24.4
7.240e-01	3.060e-05	1.780e-06	23.3	1.860e-06	1.030e-07	22.7
7.590e-01	4.050e-05	2.010e-06	21.8	2.490e-06	1.120e-07	20.7
7.940e-01	5.160e-05	2.470e-06	20.5	3.100e-06	1.440e-07	19.1
8.320e-01	5.800e-05	2.320e-06	20.4	3.290e-06	1.340e-07	18.7
8.710e-01	5.490e-05	2.430e-06	21.2	2.880e-06	1.260e-07	19.3
9.120e-01	4.290e-05	2.360e-06	22.4	2.110e-06	1.260e-07	20.9
9.550e-01	2.900e-05	1.570e-06	23.6	1.390e-06	8.220e-08	22.6
1.000e+00	2.010e-05	1.500e-06	23.8	9.810e-07	7.450e-08	24.2
1.047e+00	1.760e-05	1.230e-06	22.8	8.670e-07	6.100e-08	24.6
1.097e+00	1.930e-05	1.110e-06	21.3	9.060e-07	5.370e-08	24.2
1.148e+00	2.280e-05	1.210e-06	19.5	9.970e-07	5.410e-08	23.0
1.202e+00	2.680e-05	1.240e-06	18.3	1.100e-06	5.390e-08	21.8
1.259e+00	2.880e-05	1.290e-06	18.4	1.160e-06	5.700e-08	20.7
1.318e+00	2.720e-05	1.360e-06	19.7	1.140e-06	5.890e-08	20.3
1.380e+00	2.270e-05	1.180e-06	21.4	1.040e-06	5.620e-08	20.5
1.445e+00	1.800e-05	1.130e-06	23.3	9.290e-07	5.480e-08	20.9
1.514e+00	1.510e-05	9.600e-07	24.6	8.490e-07	5.080e-08	21.4
1.585e+00	1.430e-05	9.050e-07	25.5	8.200e-07	4.890e-08	21.7
1.660e+00	1.500e-05	8.780e-07	25.7	8.250e-07	4.770e-08	21.8
1.738e+00	1.630e-05	8.850e-07	25.7	8.370e-07	4.760e-08	21.9
1.820e+00	1.720e-05	9.110e-07	25.7	8.410e-07	4.750e-08	21.8
1.906e+00	1.690e-05	9.210e-07	25.5	8.300e-07	4.740e-08	21.8
1.995e+00	1.600e-05	8.720e-07	24.9	8.150e-07	4.650e-08	21.9
2.089e+00	1.510e-05	8.450e-07	23.8	8.080e-07	4.590e-08	21.8
2.188e+00	1.450e-05	8.470e-07	22.5	8.120e-07	4.660e-08	21.7
2.291e+00	1.410e-05	8.240e-07	21.2	8.250e-07	4.670e-08	21.5
2.399e+00	1.350e-05	6.970e-07	20.1	8.400e-07	4.630e-08	21.3
2.512e+00	1.370e-05	7.300e-07	19.6	8.510e-07	4.690e-08	21.1
2.630e+00	1.330e-05	7.450e-07	19.4	8.520e-07	4.760e-08	21.1
2.754e+00	1.280e-05	7.480e-07	19.2	8.420e-07	4.740e-08	21.1
2.884e+00	1.290e-05	7.470e-07	19.0	8.300e-07	4.690e-08	21.3
3.020e+00	1.380e-05	7.470e-07	18.8	8.280e-07	4.630e-08	21.4
3.162e+00	1.480e-05	7.620e-07	18.7	8.450e-07	4.670e-08	21.6
3.311e+00	1.510e-05	7.670e-07	18.9	8.780e-07	4.790e-08	21.7
3.467e+00	1.440e-05	7.780e-07	19.3	9.080e-07	4.930e-08	21.9
3.631e+00	1.340e-05	7.470e-07	20.5	9.050e-07	4.780e-08	22.8
3.802e+00	1.280e-05	6.400e-07	22.0	8.560e-07	4.400e-08	23.6
3.981e+00	1.260e-05	7.200e-07	23.3	7.870e-07	5.070e-08	24.4
4.169e+00	1.240e-05	8.710e-07	24.2	7.370e-07	6.190e-08	25.1
4.365e+00	1.170e-05	7.760e-07	25.3	7.310e-07	5.880e-08	25.7
4.571e+00	1.050e-05	5.630e-07	25.6	7.610e-07	4.600e-08	25.7
4.786e+00	9.110e-06	5.300e-07	25.6	7.810e-07	4.330e-08	25.7
5.012e+00	8.150e-06	5.100e-07	25.6	7.490e-07	4.540e-08	25.7
5.248e+00	7.710e-06	5.370e-07	25.7	6.670e-07	4.710e-08	25.7
5.495e+00	7.140e-06	5.980e-07	25.7	5.880e-07	5.010e-08	25.7
5.754e+00	5.910e-06	5.480e-07	25.7	5.630e-07	4.720e-08	25.7
6.026e+00	4.320e-06	5.780e-07	25.7	5.820e-07	4.090e-08	25.7
6.310e+00	3.210e-06	5.610e-07	25.7	6.010e-07	3.550e-08	25.1
6.607e+00	3.080e-06	4.920e-07	25.7	6.340e-07	3.250e-08	23.4
6.918e+00	3.760e-06	5.210e-07	25.4	7.500e-07	3.390e-08	21.3
7.244e+00	5.080e-06	4.820e-07	23.9	9.260e-07	3.910e-08	18.8
7.586e+00	7.070e-06	4.280e-07	22.0	1.010e-06	4.450e-08	16.5
7.943e+00	9.280e-06	4.430e-07	20.4	9.150e-07	4.020e-08	16.1
8.318e+00	1.040e-05	4.810e-07	19.3	7.050e-07	3.160e-08	17.8
8.710e+00	9.590e-06	4.720e-07	19.6	4.890e-07	2.780e-08	20.0
9.120e+00	7.540e-06	4.120e-07	21.2	3.230e-07	2.030e-08	22.5
9.550e+00	5.690e-06	3.610e-07	23.0	2.250e-07	1.610e-08	24.7
1.000e+01	4.620e-06	3.320e-07	24.7	1.710e-07	1.380e-08	25.7
1.047e+01	3.950e-06	2.930e-07	25.7	1.330e-07	1.190e-08	25.7
1.097e+01	3.260e-06	2.450e-07	25.7	9.870e-08	1.040e-08	25.7
1.148e+01	2.490e-06	2.040e-07	25.7	6.850e-08	9.280e-09	25.7
1.202e+01	1.720e-06	1.690e-07	25.7	4.300e-08	7.870e-09	25.7
1.259e+01	1.030e-06	1.310e-07	25.7	2.320e-08	5.780e-09	25.7
1.318e+01	5.140e-07	8.930e-08	25.7	1.020e-08	3.540e-09	25.7
1.380e+01	2.030e-07	4.920e-08	25.7	3.550e-09	1.760e-09	25.7
1.445e+01	6.190e-08	2.020e-08	25.7	9.130e-10	6.840e-10	25.7
1.514e+01	1.400e-08	5.810e-09	25.7	1.670e-10	1.940e-10	25.7

Table 3.3.7 Continued. (2/2)

Photon Energy [MeV]	Flux at z=100mm	Absolute Error	Window [%]	Flux at z=300mm	Absolute Error	Window [%]
3.630e-01				9.620e-08	5.690e-09	28.1
3.800e-01				9.250e-08	5.860e-09	28.2
3.980e-01	3.320e-07	2.370e-08	27.6	9.260e-08	6.070e-09	27.3
4.170e-01	3.800e-07	2.460e-08	26.5	9.990e-08	6.330e-09	26.0
4.370e-01	4.490e-07	2.350e-08	25.8	1.180e-07	6.410e-09	25.1
4.570e-01	5.260e-07	2.170e-08	25.4	1.470e-07	7.160e-09	24.7
4.790e-01	5.800e-07	2.980e-08	25.0	1.780e-07	8.900e-09	24.6
5.010e-01	5.840e-07	3.870e-08	24.9	1.920e-07	8.690e-09	24.8
5.250e-01	5.290e-07	3.430e-08	25.4	1.800e-07	7.780e-09	25.5
5.490e-01	4.340e-07	2.250e-08	25.8	1.430e-07	8.400e-09	26.1
5.750e-01	3.360e-07	1.860e-08	25.9	1.020e-07	6.750e-09	26.2
6.030e-01	2.650e-07	1.710e-08	26.0	7.220e-08	5.600e-09	26.2
6.310e-01	2.300e-07	1.530e-08	26.3	6.100e-08	5.210e-09	26.4
6.610e-01	2.240e-07	1.450e-08	26.3	6.040e-08	3.780e-09	26.5
6.920e-01	2.360e-07	1.460e-08	25.6	6.270e-08	3.670e-09	26.3
7.240e-01	2.630e-07	1.510e-08	24.6	6.550e-08	3.660e-09	26.0
7.590e-01	3.010e-07	1.610e-08	23.4	6.770e-08	3.680e-09	25.7
7.940e-01	3.460e-07	1.750e-08	22.3	6.910e-08	3.680e-09	25.5
8.320e-01	3.780e-07	1.780e-08	21.7	6.970e-08	3.690e-09	25.5
8.710e-01	3.760e-07	1.860e-08	21.9	6.870e-08	3.740e-09	25.5
9.120e-01	3.340e-07	1.840e-08	22.8	6.570e-08	3.730e-09	25.6
9.550e-01	2.680e-07	1.530e-08	23.8	6.110e-08	3.590e-09	25.8
1.000e+00	2.110e-07	1.400e-08	24.8	5.660e-08	3.470e-09	25.8
1.047e+00	1.790e-07	1.280e-08	25.4	5.370e-08	3.480e-09	25.8
1.097e+00	1.700e-07	1.210e-08	25.8	5.300e-08	3.520e-09	25.8
1.148e+00	1.750e-07	1.170e-08	25.7	5.390e-08	3.540e-09	25.7
1.202e+00	1.850e-07	1.160e-08	25.7	5.550e-08	3.570e-09	25.7
1.259e+00	1.970e-07	1.180e-08	25.7	5.730e-08	3.640e-09	25.7
1.318e+00	2.070e-07	1.200e-08	25.7	5.920e-08	3.720e-09	25.7
1.380e+00	2.130e-07	1.220e-08	25.7	6.110e-08	3.770e-09	25.7
1.445e+00	2.170e-07	1.220e-08	25.5	6.350e-08	3.780e-09	25.7
1.514e+00	2.210e-07	1.220e-08	25.4	6.630e-08	3.790e-09	25.7
1.585e+00	2.250e-07	1.220e-08	25.3	6.910e-08	3.840e-09	25.7
1.660e+00	2.300e-07	1.240e-08	25.3	7.110e-08	3.920e-09	25.7
1.738e+00	2.310e-07	1.270e-08	25.4	7.130e-08	4.010e-09	25.7
1.820e+00	2.280e-07	1.290e-08	25.5	6.990e-08	4.070e-09	25.7
1.906e+00	2.220e-07	1.300e-08	25.7	6.810e-08	4.120e-09	25.7
1.995e+00	2.150e-07	1.300e-08	25.7	6.670e-08	4.150e-09	25.7
2.089e+00	2.110e-07	1.310e-08	25.7	6.640e-08	4.190e-09	25.7
2.188e+00	2.120e-07	1.330e-08	25.7	6.710e-08	4.280e-09	25.7
2.291e+00	2.180e-07	1.350e-08	25.7	6.860e-08	4.360e-09	25.7
2.399e+00	2.260e-07	1.360e-08	25.7	7.070e-08	4.420e-09	25.7
2.512e+00	2.370e-07	1.390e-08	25.7	7.300e-08	4.520e-09	25.7
2.630e+00	2.470e-07	1.440e-08	25.7	7.540e-08	4.650e-09	25.7
2.754e+00	2.550e-07	1.460e-08	25.7	7.790e-08	4.740e-09	25.7
2.884e+00	2.600e-07	1.470e-08	25.7	8.050e-08	4.800e-09	25.7
3.020e+00	2.640e-07	1.510e-08	25.7	8.310e-08	4.950e-09	25.7
3.162e+00	2.680e-07	1.600e-08	25.7	8.580e-08	5.260e-09	25.7
3.311e+00	2.730e-07	1.720e-08	25.7	8.850e-08	5.680e-09	25.7
3.467e+00	2.780e-07	1.790e-08	25.7	9.090e-08	5.890e-09	25.7
3.631e+00	2.830e-07	1.720e-08	25.7	9.220e-08	5.670e-09	25.7
3.802e+00	2.880e-07	1.750e-08	25.7	9.260e-08	5.810e-09	25.7
3.981e+00	2.910e-07	2.280e-08	25.7	9.350e-08	7.550e-09	25.7
4.169e+00	2.960e-07	2.830e-08	25.7	9.720e-08	9.330e-09	25.7
4.365e+00	3.060e-07	2.720e-08	25.7	1.040e-07	8.990e-09	25.7
4.571e+00	3.240e-07	2.190e-08	25.7	1.120e-07	7.290e-09	25.7
4.786e+00	3.420e-07	2.130e-08	25.7	1.150e-07	7.030e-09	25.7
5.012e+00	3.500e-07	2.330e-08	25.7	1.110e-07	7.740e-09	25.7
5.248e+00	3.410e-07	2.590e-08	25.7	1.030e-07	8.670e-09	25.7
5.495e+00	3.260e-07	2.800e-08	25.7	1.010e-07	9.190e-09	25.7
5.754e+00	3.220e-07	2.600e-08	25.7	1.080e-07	8.570e-09	25.7
6.026e+00	3.320e-07	2.360e-08	25.7	1.180e-07	8.040e-09	25.7
6.310e+00	3.470e-07	2.190e-08	25.7	1.240e-07	7.600e-09	25.7
6.607e+00	3.740e-07	1.950e-08	24.2	1.300e-07	6.850e-09	24.1
6.918e+00	4.380e-07	1.830e-08	21.6	1.510e-07	6.500e-09	21.6
7.244e+00	5.380e-07	1.990e-08	18.8	1.850e-07	7.350e-09	18.6
7.586e+00	6.000e-07	2.260e-08	16.6	2.060e-07	8.230e-09	15.8
7.943e+00	5.320e-07	1.960e-08	16.6	1.830e-07	6.570e-09	13.8
8.318e+00	3.540e-07	1.350e-08	18.2	1.200e-07	4.320e-09	15.5
8.710e+00	1.880e-07	1.080e-08	20.7	5.880e-08	3.300e-09	17.8
9.120e+00	1.040e-07	7.010e-09	23.5	2.740e-08	1.650e-09	20.9
9.550e+00	7.460e-08	4.850e-09	25.7	1.770e-08	1.110e-09	23.7
1.000e+01	5.780e-08	4.090e-09	25.7	1.360e-08	8.210e-10	25.6
1.047e+01	4.070e-08	3.370e-09	25.7	9.130e-09	6.210e-10	25.6
1.097e+01	2.480e-08	2.540e-09	25.7	5.060e-09	4.310e-10	25.7
1.148e+01	1.350e-08	1.880e-09	25.7	2.390e-09	2.900e-10	25.7
1.202e+01	7.080e-09	1.460e-09	25.7	1.060e-09	2.070e-10	25.7
1.259e+01	3.890e-09	1.110e-09	25.7	4.780e-10	1.560e-10	25.7
1.318e+01	2.100e-09	7.680e-10	25.7	2.180e-10	1.040e-10	25.7
1.380e+01	9.830e-10	4.370e-10	25.7	8.970e-11	5.530e-11	25.7
1.445e+01	3.560e-10	1.850e-10	25.7	2.990e-11	2.170e-11	25.7
1.514e+01	9.340e-11	5.460e-11	25.7	7.350e-12	6.010e-12	25.7

Table 3.3.8 Measured gamma-ray heating rates of iron in the unit of [Gy / source neutron].

Detector Position [mm]	Gamma Heating	Error [%]	Detector Position [mm]	Gamma Heating	Error [%]
0	9.10e-16	25.7	400	1.36e-17	10.2
50	1.17e-15	10.8	500	7.18e-18	10.6
100	5.30e-16	10.5	600	4.92e-18	8.5
200	1.32e-16	9.3	700	3.08e-18	8.2
300	3.55e-17	10.0	800	2.00e-18	8.0

Table 3.4.1 Material specification for the copper assembly.

Copper	Purity: > 99.99%	Weight Density: 8.93 [g/cm^3]

Table 3.4.2 Neutron spectra in the copper assembly measured by the SDT method in the unit of [n / cm^2 / lethargy / source].

Neutron Energy [MeV]	Flux at z=76mm	Absolute Error	Flux at z=228mm	Absolute Error	Flux at z=380mm	Absolute Error	Flux at z=532mm	Absolute Error
2.82e-07	1.11e-09	1.63e-10	4.45e-10	9.54e-11	3.67e-10	8.77e-11	7.87e-10	1.32e-10
3.55e-07	2.28e-09	2.68e-10	4.98e-10	1.07e-10	3.77e-10	9.36e-11	1.49e-09	2.03e-10
4.47e-07	2.62e-09	3.05e-10	7.53e-10	1.41e-10	5.77e-10	1.24e-10	1.59e-09	2.20e-10
5.62e-07	3.09e-09	3.53e-10	1.24e-09	1.97e-10	1.09e-09	1.87e-10	1.81e-09	2.49e-10
7.08e-07	3.70e-09	4.14e-10	1.46e-09	2.28e-10	1.52e-09	2.38e-10	1.66e-09	2.48e-10
8.91e-07	4.51e-09	4.92e-10	2.69e-09	3.46e-10	2.42e-09	3.29e-10	2.75e-09	3.52e-10
1.12e-06	4.22e-09	4.88e-10	4.61e-09	5.12e-10	4.76e-09	5.31e-10	3.19e-09	4.04e-10
1.41e-06	5.11e-09	5.77e-10	6.36e-09	6.63e-10	4.69e-09	5.46e-10	4.11e-09	4.96e-10
1.78e-06	8.26e-09	8.34e-10	1.10e-08	1.02e-09	8.94e-09	8.86e-10	5.55e-09	6.29e-10
2.24e-06	1.09e-08	1.05e-09	1.43e-08	1.29e-09	1.22e-08	1.15e-09	6.72e-09	7.43e-10
2.82e-06	1.46e-08	1.35e-09	2.27e-08	1.90e-09	1.93e-08	1.68e-09	9.95e-09	1.01e-09
3.55e-06	1.93e-08	1.72e-09	2.91e-08	2.40e-09	2.52e-08	2.14e-09	1.20e-08	1.20e-09
4.47e-06	2.51e-08	2.18e-09	3.89e-08	3.12e-09	3.23e-08	2.69e-09	1.73e-08	1.63e-09
5.62e-06	2.99e-08	2.58e-09	4.92e-08	3.90e-09	4.15e-08	3.39e-09	1.63e-08	1.60e-09
7.08e-06	3.83e-08	3.24e-09	6.77e-08	5.26e-09	5.63e-08	4.50e-09	2.39e-08	2.21e-09
8.91e-06	4.47e-08	3.77e-09	8.63e-08	6.66e-09	6.32e-08	5.08e-09	2.70e-08	2.51e-09
1.12e-05	5.56e-08	4.65e-09	1.06e-07	8.15e-09	8.18e-08	6.51e-09	3.35e-08	3.06e-09
1.41e-05	6.75e-08	5.63e-09	1.21e-07	9.44e-09	1.01e-07	7.99e-09	4.14e-08	3.74e-09
1.78e-05	8.14e-08	6.79e-09	1.38e-07	1.08e-08	1.12e-07	9.01e-09	4.79e-08	4.34e-09
2.24e-05	1.03e-07	8.61e-09	1.68e-07	1.33e-08	1.26e-07	1.03e-08	5.26e-08	4.83e-09
2.82e-05	1.10e-07	9.35e-09	1.94e-07	1.56e-08	1.49e-07	1.23e-08	5.70e-08	5.33e-09
3.55e-05	1.29e-07	1.11e-08	2.24e-07	1.84e-08	1.71e-07	1.43e-08	6.82e-08	6.42e-09
4.47e-05	1.41e-07	1.25e-08	2.42e-07	2.04e-08	1.87e-07	1.61e-08	7.58e-08	7.28e-09
5.62e-05	1.73e-07	1.55e-08	2.71e-07	2.35e-08	1.97e-07	1.75e-08	8.04e-08	7.96e-09
7.08e-05	1.78e-07	1.67e-08	3.05e-07	2.73e-08	2.29e-07	2.10e-08	8.52e-08	8.73e-09
8.91e-05	1.97e-07	1.91e-08	3.37e-07	3.14e-08	2.47e-07	2.36e-08	1.03e-07	1.07e-08
1.12e-04	2.40e-07	2.40e-08	4.27e-07	4.55e-08	2.65e-07	3.05e-08	9.76e-08	1.08e-08
1.41e-04	2.50e-07	2.64e-08	4.41e-07	4.96e-08	2.47e-07	3.02e-08	1.11e-07	1.27e-08
1.78e-04	2.96e-07	3.28e-08	4.47e-07	5.30e-08	2.85e-07	3.59e-08	1.32e-07	1.57e-08
2.24e-04	3.02e-07	3.56e-08	4.61e-07	5.76e-08	3.34e-07	4.32e-08	1.64e-07	2.03e-08
2.82e-04	3.78e-07	4.71e-08	5.91e-07	7.73e-08	4.14e-07	5.58e-08	1.76e-07	2.31e-08
3.55e-04	4.43e-07	5.89e-08	5.99e-07	8.37e-08	4.15e-07	5.95e-08	1.92e-07	2.69e-08
4.47e-04	4.99e-07	7.14e-08	7.30e-07	1.07e-07	4.84e-07	7.31e-08	2.20e-07	3.26e-08
5.62e-04	6.33e-07	1.02e-07	9.60e-07	1.50e-07	6.82e-07	1.06e-07	2.52e-07	4.02e-08
7.08e-04	9.40e-07	1.60e-07	1.41e-06	2.37e-07	9.50e-07	1.60e-07	3.61e-07	6.07e-08
8.91e-04	1.32e-06	2.50e-07	1.83e-06	3.39e-07	1.33e-06	2.42e-07	5.73e-07	1.05e-07
1.12e-03	1.63e-06	3.43e-07	2.48e-06	5.13e-07	1.74e-06	3.56e-07	6.29e-07	1.29e-07
1.41e-03	1.77e-06	4.18e-07	2.50e-06	5.84e-07	1.77e-06	4.10e-07	7.26e-07	1.69e-07
1.78e-03	1.63e-06	4.32e-07	2.25e-06	5.83e-07	1.68e-06	4.29e-07	5.93e-07	1.52e-07
2.24e-03	2.19e-06	6.39e-07	3.37e-06	9.62e-07	1.64e-06	4.63e-07	6.08e-07	1.70e-07
2.82e-03	2.06e-06	6.58e-07	3.21e-06	1.02e-06	2.11e-06	6.47e-07	7.72e-07	2.37e-07
3.55e-03	2.92e-06	1.04e-06	4.26e-06	1.50e-06	2.82e-06	9.67e-07	9.52e-07	3.22e-07
4.47e-03	3.90e-06	1.57e-06	5.49e-06	2.20e-06	3.48e-06	1.35e-06	1.16e-06	4.38e-07
5.62e-03	6.02e-06	2.79e-06	8.36e-06	3.83e-06	4.24e-06	1.87e-06	1.76e-06	7.57e-07
7.08e-03	8.23e-06	4.57e-06	1.09e-05	5.93e-06	6.81e-06	3.53e-06	2.53e-06	1.28e-06
8.91e-03	9.20e-06	5.95e-06	1.14e-05	7.21e-06	6.83e-06	4.14e-06	2.13e-06	1.26e-06

Table 3.5.1 Material specification for the tungsten assembly.

Chemical Composition	W 94.8 wt% Cu 2.1 wt% Ni 3.1 wt%
Weight Density	18.05 [g/cm^3]

Table 3.5.2 Neutron spectra in the tungsten assembly measured by the NE213 spectrometer in the unit of [n / cm^2 / lethargy / source].

Neutron Energy [MeV]	Flux at z=76mm	Abs, Error	Window [%]	Flux at z=228mm	Abs. Error	Window [%]	Flux at z=380mm	Abs. Error	Window [%]
1.041e+0	6.11e-5	1.86e-6	42.5	5.73e-6	1.85e-7	34.9	3.13e-7	1.18e-8	37.1
1.095e+0	5.69e-5	1.87e-6	42.4	5.24e-6	1.99e-7	34.8	2.78e-7	1.06e-8	37.4
1.151e+0	5.28e-5	1.89e-6	42.2	4.73e-6	1.92e-7	34.9	2.54e-7	1.08e-8	37.0
1.210e+0	4.97e-5	1.79e-6	41.7	4.21e-6	1.52e-7	34.9	2.43e-7	9.57e-9	36.0
1.272e+0	4.81e-5	1.60e-6	40.8	3.70e-6	1.31e-7	35.0	2.44e-7	7.61e-9	34.6
1.337e+0	4.78e-5	1.48e-6	39.3	3.23e-6	1.28e-7	35.1	2.50e-7	7.17e-9	32.7
1.406e+0	4.86e-5	1.51e-6	37.5	2.86e-6	1.08e-7	35.4	2.52e-7	7.54e-9	30.9
1.478e+0	4.99e-5	1.53e-6	35.5	2.60e-6	9.33e-8	35.5	2.41e-7	7.42e-9	30.2
1.553e+0	5.09e-5	1.55e-6	33.8	2.42e-6	8.98e-8	35.3	2.13e-7	6.46e-9	31.0
1.633e+0	5.07e-5	1.53e-6	32.5	2.30e-6	7.92e-8	35.0	1.75e-7	5.65e-9	32.1
1.717e+0	4.88e-5	1.44e-6	32.0	2.19e-6	6.88e-8	34.7	1.39e-7	5.45e-9	33.4
1.805e+0	4.48e-5	1.35e-6	32.0	2.04e-6	6.34e-8	34.5	1.15e-7	4.52e-9	34.8
1.897e+0	3.97e-5	1.34e-6	32.6	1.88e-6	5.81e-8	34.2	1.02e-7	3.56e-9	35.5
1.995e+0	3.45e-5	1.21e-6	33.3	1.72e-6	5.31e-8	34.0	9.66e-8	3.43e-9	34.9
2.097e+0	3.00e-5	1.04e-6	33.8	1.58e-6	4.81e-8	33.8	9.26e-8	3.11e-9	34.1
2.204e+0	2.63e-5	9.42e-7	33.8	1.47e-6	4.39e-8	33.3	8.82e-8	2.61e-9	33.3
2.317e+0	2.34e-5	8.67e-7	33.5	1.39e-6	4.14e-8	32.7	8.29e-8	2.34e-9	32.3
2.436e+0	2.14e-5	7.74e-7	32.8	1.30e-6	3.88e-8	32.1	7.72e-8	2.18e-9	31.7
2.561e+0	2.00e-5	7.25e-7	32.0	1.21e-6	3.66e-8	31.6	7.10e-8	2.02e-9	31.4
2.692e+0	1.89e-5	6.87e-7	31.2	1.11e-6	3.43e-8	31.0	6.45e-8	1.94e-9	30.9
2.830e+0	1.77e-5	6.67e-7	30.5	9.95e-7	3.29e-8	30.4	5.82e-8	1.83e-9	30.3
2.975e+0	1.64e-5	6.96e-7	29.7	8.95e-7	3.26e-8	29.7	5.27e-8	1.76e-9	29.7
3.128e+0	1.53e-5	7.48e-7	29.0	8.18e-7	3.35e-8	29.0	4.82e-8	1.79e-9	29.0
3.288e+0	1.44e-5	7.63e-7	28.3	7.63e-7	3.32e-8	28.3	4.39e-8	1.76e-9	28.3
3.457e+0	1.35e-5	7.19e-7	27.6	7.18e-7	3.19e-8	27.6	3.96e-8	1.69e-9	27.6
3.634e+0	1.22e-5	6.59e-7	26.8	6.70e-7	3.02e-8	26.8	3.56e-8	1.60e-9	26.8
3.821e+0	1.06e-5	6.24e-7	26.1	6.15e-7	2.89e-8	26.1	3.26e-8	1.57e-9	26.1
4.016e+0	9.04e-6	6.20e-7	25.3	5.58e-7	2.89e-8	25.3	3.03e-8	1.59e-9	25.3
4.222e+0	7.89e-6	6.50e-7	24.5	5.01e-7	2.96e-8	24.5	2.85e-8	1.63e-9	24.5
4.439e+0	7.16e-6	6.83e-7	23.9	4.51e-7	3.05e-8	23.9	2.75e-8	1.68e-9	23.9
4.666e+0	6.59e-6	7.26e-7	23.3	4.06e-7	3.20e-8	23.3	2.72e-8	1.74e-9	23.3
4.906e+0	5.92e-6	7.72e-7	22.7	3.68e-7	3.37e-8	22.7	2.72e-8	1.83e-9	22.7
5.157e+0	5.10e-6	8.01e-7	22.2	3.40e-7	3.46e-8	22.2	2.65e-8	1.87e-9	22.2
5.422e+0	4.35e-6	8.57e-7	21.7	3.25e-7	3.65e-8	21.7	2.51e-8	1.93e-9	21.7
5.700e+0	3.85e-6	9.26e-7	21.1	3.07e-7	3.91e-8	21.1	2.32e-8	2.04e-9	21.1
5.992e+0	3.72e-6	9.68e-7	20.6	2.69e-7	4.07e-8	20.6	2.15e-8	2.08e-9	20.6
6.299e+0	3.95e-6	1.08e-6	20.0	2.33e-7	4.43e-8	20.0	2.07e-8	2.19e-9	20.0
6.622e+0	4.23e-6	1.21e-6	19.5	2.38e-7	4.92e-8	19.5	2.11e-8	2.39e-9	19.5
6.961e+0	4.40e-6	1.26e-6	19.0	2.83e-7	5.06e-8	19.0	2.13e-8	2.47e-9	19.0
7.318e+0	4.76e-6	1.43e-6	18.5	3.14e-7	5.76e-8	18.5	2.10e-8	2.73e-9	18.5
7.694e+0	5.29e-6	1.68e-6	18.0	2.99e-7	6.65e-8	18.0	2.12e-8	3.08e-9	18.0
8.088e+0	5.29e-6	1.81e-6	17.6	2.87e-7	7.04e-8	17.6	2.16e-8	3.28e-9	17.6
8.503e+0	4.98e-6	2.06e-6	17.2	3.29e-7	7.95e-8	17.2	2.19e-8	3.63e-9	17.2
8.939e+0	5.16e-6	2.60e-6	16.8	3.98e-7	9.84e-8	16.8	2.39e-8	4.41e-9	16.8
9.397e+0	5.83e-6	2.86e-6	16.4	4.54e-7	1.08e-7	16.4	2.58e-8	4.79e-9	16.4
9.879e+0	7.19e-6	2.96e-6	15.9	4.77e-7	1.11e-7	15.9	2.48e-8	4.97e-9	15.9
1.039e+1	8.84e-6	3.37e-6	15.5	4.79e-7	1.25e-7	15.5	2.44e-8	5.49e-9	15.5
1.092e+1	8.65e-6	3.35e-6	15.1	4.95e-7	1.22e-7	15.1	2.61e-8	5.36e-9	15.1
1.148e+1	8.88e-6	3.34e-6	14.8	5.64e-7	1.21e-7	14.8	2.89e-8	5.26e-9	14.8
1.207e+1	1.80e-5	3.96e-6	14.5	8.87e-7	1.42e-7	14.5	4.55e-8	6.04e-9	14.5
1.268e+1	4.71e-5	4.07e-6	14.4	2.09e-6	1.45e-7	14.4	1.00e-7	6.34e-9	14.4
1.334e+1	1.13e-4	5.05e-6	14.4	4.70e-6	1.76e-7	14.4	2.08e-7	7.43e-9	14.4
1.402e+1	1.88e-4	6.21e-6	14.4	6.95e-6	2.22e-7	14.4	3.06e-7	9.64e-9	14.4
1.474e+1	1.80e-4	6.42e-6	14.4	5.91e-6	2.50e-7	14.4	2.70e-7	1.25e-8	14.4
1.549e+1	9.98e-5	2.93e-6	14.4	2.92e-6	1.07e-7	14.4	1.24e-7	4.92e-9	14.4
1.629e+1	4.14e-5	3.20e-6	13.7	1.14e-6	1.20e-7	14.4	2.69e-8	6.18e-9	14.4
1.712e+1	2.41e-5	2.27e-6	13.1	6.29e-7	9.10e-8	14.4	1.10e-8	4.59e-9	14.4
1.800e+1	1.44e-5	5.29e-7	12.4	3.84e-7	2.38e-8	14.4	1.13e-8	1.24e-9	14.4

Table 3.5.3 Neutron spectra in the tungsten assembly measured by the PRC in the unit of [n / cm^2 / lethargy / source]. (1/2)

Neutron Energy [MeV]	Flux at z=76mm	Absolute Error	Neutron Energy [MeV]	Flux at z=228mm	Absolute Error	Neutron Energy [MeV]	Flux at z=380mm	Absolute Error
5.00e-03	1.52e-05	4.97e-06	3.11e-03	3.21e-06	1.90e-06	3.11e-03	8.26e-07	2.97e-07
5.23e-03	6.01e-06	4.97e-06	3.24e-03	5.25e-06	1.84e-06	3.24e-03	3.60e-07	2.87e-07
5.46e-03	1.04e-05	5.00e-06	3.38e-03	6.01e-06	1.81e-06	3.38e-03	9.03e-07	2.86e-07
5.71e-03	9.84e-06	5.09e-06	3.53e-03	2.41e-06	1.78e-06	3.53e-03	5.54e-07	2.82e-07
5.97e-03	8.83e-06	5.12e-06	3.68e-03	4.69e-06	1.74e-06	3.68e-03	7.03e-07	2.76e-07
6.24e-03	1.25e-05	5.21e-06	3.85e-03	3.27e-06	1.74e-06	3.85e-03	5.80e-07	2.76e-07
6.53e-03	5.47e-06	5.24e-06	4.02e-03	2.69e-06	1.71e-06	4.02e-03	6.77e-07	2.69e-07
6.83e-03	1.83e-05	5.30e-06	4.20e-03	2.93e-06	1.70e-06	4.20e-03	1.07e-06	2.68e-07
7.14e-03	1.68e-05	5.39e-06	4.38e-03	4.31e-06	1.69e-06	4.38e-03	4.93e-07	2.64e-07
7.47e-03	1.36e-05	5.39e-06	4.58e-03	6.05e-06	1.67e-06	4.58e-03	5.95e-07	2.62e-07
7.81e-03	1.54e-05	5.42e-06	4.78e-03	1.82e-06	1.66e-06	4.78e-03	6.92e-07	2.60e-07
8.17e-03	1.93e-05	5.42e-06	5.00e-03	2.60e-06	1.66e-06	5.00e-03	6.99e-07	2.61e-07
8.55e-03	6.90e-06	5.51e-06	5.23e-03	4.48e-06	1.69e-06	5.23e-03	2.63e-08	2.65e-07
8.94e-03	1.54e-05	5.54e-06	5.46e-03	4.34e-06	1.70e-06	5.46e-03	4.63e-07	2.69e-07
9.36e-03	1.76e-05	5.63e-06	5.71e-03	-4.26e-07	1.73e-06	5.71e-03	5.46e-07	2.74e-07
9.79e-03	1.57e-05	5.69e-06	5.97e-03	7.71e-07	1.76e-06	5.97e-03	8.37e-07	2.75e-07
1.03e-02	2.45e-05	5.69e-06	6.24e-03	3.56e-06	1.79e-06	6.24e-03	6.47e-07	2.78e-07
1.07e-02	1.93e-05	5.79e-06	6.53e-03	5.21e-06	1.82e-06	6.53e-03	6.30e-07	2.81e-07
1.12e-02	9.27e-06	5.79e-06	6.83e-03	6.61e-06	1.81e-06	6.83e-03	8.53e-07	2.84e-07
1.18e-02	1.42e-05	5.91e-06	7.14e-03	6.90e-06	1.84e-06	7.14e-03	6.75e-07	2.86e-07
1.23e-02	1.07e-05	5.97e-06	7.47e-03	1.19e-06	1.85e-06	7.47e-03	9.33e-07	2.90e-07
1.29e-02	1.42e-05	6.09e-06	7.81e-03	4.69e-06	1.87e-06	7.81e-03	1.12e-06	2.91e-07
1.35e-02	1.45e-05	6.12e-06	8.17e-03	2.94e-06	1.91e-06	8.17e-03	1.20e-06	2.94e-07
1.41e-02	1.70e-05	6.24e-06	8.55e-03	5.73e-06	1.92e-06	8.55e-03	8.84e-07	2.95e-07
1.48e-02	5.93e-07	6.36e-06	8.94e-03	7.94e-06	1.94e-06	8.94e-03	7.42e-07	3.00e-07
1.55e-02	5.37e-06	6.48e-06	9.36e-03	5.71e-06	1.96e-06	9.36e-03	1.18e-06	3.01e-07
1.62e-02	5.40e-06	6.63e-06	9.79e-03	7.89e-06	1.97e-06	9.79e-03	1.16e-06	3.06e-07
1.70e-02	-1.98e-06	6.82e-06	1.03e-02	6.63e-06	1.99e-06	1.03e-02	5.33e-07	3.06e-07
1.78e-02	1.63e-05	6.94e-06	1.07e-02	5.72e-06	1.99e-06	1.07e-02	1.13e-06	3.09e-07
1.86e-02	1.50e-05	7.06e-06	1.12e-02	4.68e-06	2.03e-06	1.12e-02	9.08e-07	3.15e-07
1.95e-02	2.23e-05	7.18e-06	1.18e-02	3.65e-06	2.04e-06	1.18e-02	1.02e-06	3.18e-07
2.04e-02	1.70e-05	7.30e-06	1.23e-02	4.25e-06	2.09e-06	1.23e-02	1.11e-06	3.21e-07
2.14e-02	2.81e-05	7.42e-06	1.29e-02	3.70e-06	2.11e-06	1.29e-02	6.14e-07	3.27e-07
2.24e-02	9.36e-06	7.57e-06	1.35e-02	4.26e-06	2.16e-06	1.35e-02	3.45e-07	3.30e-07
2.34e-02	1.90e-05	7.69e-06	1.41e-02	1.81e-06	2.20e-06	1.41e-02	3.83e-07	3.39e-07
2.45e-02	2.69e-05	7.88e-06	1.48e-02	3.91e-06	2.24e-06	1.48e-02	7.82e-07	3.45e-07
2.57e-02	2.79e-05	7.97e-06	1.55e-02	4.08e-06	2.28e-06	1.55e-02	1.00e-06	3.51e-07
2.69e-02	1.79e-05	8.12e-06	1.62e-02	8.45e-06	2.30e-06	1.62e-02	1.09e-06	3.54e-07
2.82e-02	2.08e-05	8.30e-06	1.70e-02	6.55e-06	2.36e-06	1.70e-02	1.02e-06	3.60e-07
2.95e-02	2.76e-05	8.42e-06	1.78e-02	6.71e-06	2.38e-06	1.78e-02	1.19e-06	3.67e-07
3.09e-02	3.15e-05	8.63e-06	1.86e-02	3.37e-06	2.41e-06	1.86e-02	1.00e-06	3.73e-07
3.24e-02	2.63e-05	8.78e-06	1.95e-02	1.29e-06	2.48e-06	1.95e-02	1.43e-06	3.79e-07
3.40e-02	2.57e-05	8.94e-06	2.04e-02	8.01e-06	2.52e-06	2.04e-02	1.71e-06	3.85e-07
3.56e-02	3.61e-05	9.12e-06	2.14e-02	1.56e-05	2.56e-06	2.14e-02	2.16e-06	3.88e-07
3.73e-02	3.51e-05	9.30e-06	2.24e-02	1.21e-05	2.58e-06	2.24e-02	1.88e-06	3.91e-07
3.90e-02	3.71e-05	9.48e-06	2.34e-02	6.07e-06	2.62e-06	2.34e-02	1.89e-06	3.94e-07
4.09e-02	5.50e-05	9.66e-06	2.45e-02	9.18e-06	2.66e-06	2.45e-02	1.28e-06	4.00e-07
4.29e-02	4.57e-05	9.78e-06	2.57e-02	1.23e-05	2.71e-06	2.57e-02	1.61e-06	4.06e-07
4.49e-02	6.49e-05	9.94e-06	2.69e-02	9.54e-06	2.74e-06	2.69e-02	2.26e-06	4.12e-07
4.70e-02	5.29e-05	1.01e-05	2.82e-02	1.06e-05	2.79e-06	2.82e-02	2.44e-06	4.15e-07
4.93e-02	5.90e-05	1.03e-05	2.95e-02	8.44e-06	2.84e-06	2.95e-02	2.58e-06	4.21e-07
5.16e-02	5.41e-05	1.05e-05	3.09e-02	1.64e-05	2.87e-06	3.09e-02	2.67e-06	4.24e-07
5.41e-02	4.46e-05	1.07e-05	3.24e-02	1.32e-05	2.92e-06	3.24e-02	3.00e-06	4.27e-07
5.67e-02	5.89e-05	1.09e-05	3.40e-02	1.53e-05	2.97e-06	3.40e-02	3.32e-06	4.30e-07
5.94e-02	7.00e-05	1.11e-05	3.56e-02	1.83e-05	3.00e-06	3.56e-02	3.11e-06	4.33e-07
6.22e-02	7.15e-05	1.13e-05	3.73e-02	1.54e-05	3.06e-06	3.73e-02	3.49e-06	4.36e-07
6.52e-02	7.25e-05	1.15e-05	3.90e-02	2.41e-05	3.06e-06	3.90e-02	3.81e-06	4.39e-07
6.83e-02	6.42e-05	1.18e-05	4.09e-02	2.65e-05	3.12e-06	4.09e-02	3.98e-06	4.39e-07
7.16e-02	6.68e-05	1.20e-05	4.29e-02	2.19e-05	3.12e-06	4.29e-02	4.19e-06	4.42e-07
7.50e-02	1.17e-04	1.23e-05	4.49e-02	2.11e-05	3.15e-06	4.49e-02	4.40e-06	4.39e-07
7.86e-02	1.27e-04	1.27e-05	4.70e-02	2.29e-05	3.18e-06	4.70e-02	4.36e-06	4.42e-07
8.23e-02	1.10e-04	1.31e-05	4.93e-02	3.10e-05	3.21e-06	4.93e-02	4.44e-06	4.42e-07
8.63e-02	1.04e-04	1.36e-05	5.16e-02	2.64e-05	3.24e-06	5.16e-02	4.10e-06	4.45e-07
9.04e-02	9.03e-05	1.41e-05	5.41e-02	2.11e-05	3.27e-06	5.41e-02	2.82e-06	4.48e-07
9.47e-02	8.11e-05	1.47e-05	5.67e-02	2.26e-05	3.30e-06	5.67e-02	3.18e-06	4.54e-07
9.92e-02	1.31e-04	1.53e-05	5.94e-02	2.27e-05	3.36e-06	5.94e-02	4.16e-06	4.60e-07

Table 3.5.3 Continued. (2/2)

Neutron Energy [MeV]	Flux at z=76mm	Absolute Error	Neutron Energy [MeV]	Flux at z=228mm	Absolute Error	Neutron Energy [MeV]	Flux at z=380mm	Absolute Error
1.04e-01	1.29e-04	1.58e-05	6.22e-02	2.31e-05	3.42e-06	6.22e-02	4.46e-06	4.57e-07
1.09e-01	1.08e-04	1.65e-05	6.52e-02	3.43e-05	3.45e-06	6.52e-02	4.80e-06	4.60e-07
1.14e-01	1.36e-04	1.71e-05	6.83e-02	2.97e-05	3.48e-06	6.83e-02	4.83e-06	4.63e-07
1.20e-01	1.53e-04	1.78e-05	7.16e-02	2.91e-05	3.51e-06	7.16e-02	5.36e-06	4.63e-07
1.25e-01	1.43e-04	1.85e-05	7.50e-02	4.02e-05	3.57e-06	7.50e-02	5.95e-06	4.66e-07
1.31e-01	1.37e-04	1.94e-05	7.86e-02	4.47e-05	3.63e-06	7.86e-02	5.47e-06	4.73e-07
1.38e-01	1.49e-04	2.02e-05	8.23e-02	3.81e-05	3.73e-06	8.23e-02	5.64e-06	4.76e-07
1.44e-01	1.84e-04	2.12e-05	8.63e-02	3.28e-05	3.82e-06	8.63e-02	5.54e-06	4.88e-07
			9.04e-02	3.90e-05	3.91e-06	9.04e-02	5.23e-06	4.94e-07
			9.47e-02	3.88e-05	4.03e-06	9.47e-02	5.59e-06	5.03e-07
			9.92e-02	3.77e-05	4.12e-06	9.92e-02	5.35e-06	5.12e-07
			1.04e-01	4.59e-05	4.24e-06	1.04e-01	5.42e-06	5.21e-07
			1.09e-01	3.72e-05	4.36e-06	1.09e-01	5.57e-06	5.30e-07
			1.14e-01	3.34e-05	4.48e-06	1.14e-01	5.18e-06	5.39e-07
			1.20e-01	4.12e-05	4.66e-06	1.20e-01	4.75e-06	5.54e-07
			1.25e-01	4.23e-05	4.79e-06	1.25e-01	4.59e-06	5.63e-07
			1.31e-01	3.63e-05	4.94e-06	1.31e-01	4.41e-06	5.79e-07
			1.38e-01	4.31e-05	5.12e-06	1.38e-01	4.58e-06	6.00e-07
			1.44e-01	5.28e-05	5.27e-06	1.44e-01	5.57e-06	6.12e-07
			1.53e-01	3.07e-05	2.10e-06	1.51e-01	4.16e-06	2.40e-07
			1.60e-01	3.12e-05	2.01e-06	1.58e-01	4.31e-06	2.27e-07
			1.68e-01	3.74e-05	1.91e-06	1.65e-01	4.39e-06	2.14e-07
			1.76e-01	3.49e-05	1.83e-06	1.73e-01	4.24e-06	2.03e-07
			1.84e-01	3.53e-05	1.75e-06	1.82e-01	4.17e-06	1.92e-07
			1.93e-01	3.43e-05	1.68e-06	1.90e-01	4.23e-06	1.83e-07
			2.02e-01	3.48e-05	1.62e-06	1.99e-01	3.87e-06	1.74e-07
			2.12e-01	3.18e-05	1.57e-06	2.09e-01	3.70e-06	1.67e-07
			2.22e-01	3.22e-05	1.51e-06	2.19e-01	3.70e-06	1.59e-07
			2.33e-01	3.54e-05	1.46e-06	2.29e-01	3.63e-06	1.53e-07
			2.44e-01	3.08e-05	1.42e-06	2.40e-01	3.51e-06	1.45e-07
			2.56e-01	3.12e-05	1.37e-06	2.52e-01	3.34e-06	1.39e-07
			2.68e-01	3.30e-05	1.33e-06	2.64e-01	3.35e-06	1.34e-07
			2.81e-01	2.95e-05	1.29e-06	2.77e-01	3.12e-06	1.28e-07
			2.94e-01	3.05e-05	1.25e-06	2.90e-01	2.70e-06	1.23e-07
			3.09e-01	2.99e-05	1.22e-06	3.04e-01	2.80e-06	1.18e-07
			3.23e-01	2.89e-05	1.18e-06	3.18e-01	2.76e-06	1.14e-07
			3.39e-01	2.77e-05	1.15e-06	3.34e-01	2.58e-06	1.09e-07
			3.55e-01	2.71e-05	1.11e-06	3.50e-01	2.49e-06	1.05e-07
			3.72e-01	2.75e-05	1.08e-06	3.66e-01	2.36e-06	1.01e-07
			3.90e-01	2.69e-05	1.05e-06	3.84e-01	2.29e-06	9.66e-08
			4.09e-01	2.79e-05	1.01e-06	4.02e-01	2.30e-06	9.25e-08
			4.28e-01	2.54e-05	9.80e-07	4.22e-01	2.09e-06	8.85e-08
			4.49e-01	2.43e-05	9.48e-07	4.42e-01	1.76e-06	8.50e-08
			4.70e-01	2.33e-05	9.30e-07	4.63e-01	1.83e-06	8.23e-08
			4.93e-01	2.20e-05	9.10e-07	4.85e-01	1.74e-06	7.94e-08
			5.17e-01	2.24e-05	8.87e-07	5.09e-01	1.68e-06	7.68e-08
			5.41e-01	2.25e-05	8.60e-07	5.33e-01	1.53e-06	7.37e-08
			5.67e-01	2.12e-05	8.35e-07	5.59e-01	1.53e-06	7.07e-08
			5.95e-01	1.97e-05	8.06e-07	5.85e-01	1.29e-06	6.80e-08
			6.23e-01	1.77e-05	7.81e-07	6.13e-01	1.18e-06	6.48e-08
			6.53e-01	1.82e-05	7.66e-07	6.43e-01	1.19e-06	6.31e-08
			6.84e-01	1.61e-05	7.50e-07	6.74e-01	1.02e-06	6.13e-08
			7.17e-01	1.54e-05	7.34e-07	7.06e-01	1.00e-06	5.96e-08
			7.51e-01	1.45e-05	7.18e-07	7.40e-01	9.09e-07	5.80e-08
			7.88e-01	1.23e-05	7.07e-07	7.75e-01	7.60e-07	5.61e-08
			8.25e-01	1.16e-05	6.92e-07	8.13e-01	6.85e-07	5.46e-08
			8.65e-01	1.14e-05	6.82e-07	8.51e-01	6.19e-07	5.35e-08
			9.06e-01	1.07e-05	6.63e-07	8.92e-01	5.79e-07	5.22e-08
			9.50e-01	8.66e-06	6.49e-07	9.35e-01	5.47e-07	5.00e-08
			9.95e-01	7.74e-06	6.39e-07	9.80e-01	4.85e-07	4.94e-08

Table 3.5.4 Measured dosimetry reaction rates in the tungsten assembly in the unit of [reactions / atom / source]. Numbers in the parenthesis are percentage errors.

Detector Position [mm]	Reaction		
	$^{27}Al(n,\alpha)^{24}Na$	$^{93}Nb(n,2n)^{92m}Nb$	$^{115}In(n,n')^{115m}In$
0	2.34e-29 (2.9)	1.01e-28 (2.9)	3.04e-29 (2.9)
76	4.27e-30 (3.1)	1.64e-29 (3.3)	1.47e-29 (3.0)
228	1.64e-31 (3.1)	6.00e-31 (3.2)	9.77e-31 (3.9)
380	6.60e-33 (4.7)	2.56e-32 (3.5)	4.71e-32 (7.2)
507	1.69e-33 (3.1)	4.72e-33 (3.2)	2.32e-32 (5.7)

Detector Position [mm]	Reaction	
	$^{186}W(n,\gamma)^{187}W$	$^{197}Au(n,\gamma)^{198}Au$
0	2.27e-29 (3.1)	7.26e-29 (3.8)
76	5.22e-29 (3.1)	1.51e-28 (4.7)
228	1.58e-29 (3.0)	4.41e-29 (4.9)
380	2.56e-30 (2.9)	8.23e-30 (7.7)
507	1.69e-30 (2.9)	1.07e-29 (4.8)

Table 3.5.5 Gamma-ray spectra in the tungsten assembly measured by the BC-537 spectrometer in the unit of [photons / cm^2 / lethargy / source]. (1/2)

Photon Energy [MeV]	Flux at z=76mm	Abs. Error	Window [%]	Flux at z=228mm	Abs. Error	Window [%]	Flux at z=380mm	Abs. Error	Window [%]
3.020e-1	2.14e-5	1.07e-6	29.6	1.99e-6	1.30e-7	29.8	2.18e-7	1.73e-8	29.8
3.162e-1	1.90e-5	1.16e-6	29.3	1.81e-6	1.42e-7	29.5	2.13e-7	1.90e-8	29.5
3.311e-1	1.74e-5	1.09e-6	29.1	1.73e-6	1.37e-7	29.2	2.15e-7	1.85e-8	29.2
3.467e-1	1.67e-5	1.05e-6	28.9	1.74e-6	1.35e-7	28.9	2.24e-7	1.86e-8	28.9
3.631e-1	1.64e-5	1.04e-6	28.6	1.80e-6	1.40e-7	28.6	2.38e-7	1.95e-8	28.6
3.802e-1	1.66e-5	1.07e-6	28.3	1.91e-6	1.46e-7	28.3	2.55e-7	2.06e-8	28.3
3.981e-1	1.70e-5	1.06e-6	28.1	2.07e-6	1.48e-7	28.1	2.80e-7	2.09e-8	28.1
4.169e-1	1.79e-5	1.05e-6	27.9	2.30e-6	1.47e-7	27.8	3.17e-7	2.08e-8	27.8
4.365e-1	1.93e-5	1.07e-6	27.5	2.65e-6	1.53e-7	27.3	3.72e-7	2.19e-8	27.2
4.571e-1	2.14e-5	1.12e-6	26.9	3.11e-6	1.65e-7	26.5	4.46e-7	2.40e-8	26.3
4.786e-1	2.39e-5	1.16e-6	26.3	3.66e-6	1.75e-7	25.8	5.34e-7	2.56e-8	25.4
5.012e-1	2.65e-5	1.20e-6	25.8	4.17e-6	1.81e-7	25.1	6.15e-7	2.64e-8	24.7
5.248e-1	2.80e-5	1.27e-6	25.5	4.44e-6	1.94e-7	24.7	6.58e-7	2.88e-8	24.3
5.495e-1	2.78e-5	1.33e-6	25.5	4.33e-6	2.03e-7	24.9	6.38e-7	3.02e-8	24.6
5.754e-1	2.58e-5	1.29e-6	25.8	3.87e-6	1.92e-7	25.4	5.61e-7	2.78e-8	25.2
6.026e-1	2.32e-5	1.24e-6	26.1	3.30e-6	1.83e-7	25.8	4.69e-7	2.66e-8	25.8
6.310e-1	2.13e-5	1.19e-6	26.3	2.91e-6	1.72e-7	26.2	4.05e-7	2.47e-8	26.2
6.607e-1	2.09e-5	1.13e-6	26.2	2.80e-6	1.59e-7	26.4	3.83e-7	2.24e-8	26.5
6.918e-1	2.16e-5	1.13e-6	25.9	2.89e-6	1.56e-7	26.2	3.92e-7	2.18e-8	26.3
7.244e-1	2.28e-5	1.14e-6	25.4	3.06e-6	1.56e-7	25.7	4.15e-7	2.17e-8	25.9
7.586e-1	2.40e-5	1.16e-6	24.8	3.23e-6	1.59e-7	25.3	4.41e-7	2.19e-8	25.5
7.943e-1	2.52e-5	1.18e-6	24.3	3.38e-6	1.61e-7	24.8	4.64e-7	2.21e-8	25.0
8.318e-1	2.60e-5	1.21e-6	23.9	3.49e-6	1.63e-7	24.4	4.82e-7	2.26e-8	24.6
8.710e-1	2.65e-5	1.24e-6	23.6	3.55e-6	1.68e-7	24.1	4.91e-7	2.33e-8	24.3
9.120e-1	2.64e-5	1.25e-6	23.4	3.53e-6	1.69e-7	24.0	4.87e-7	2.34e-8	24.3
9.550e-1	2.59e-5	1.21e-6	23.3	3.42e-6	1.63e-7	24.1	4.70e-7	2.25e-8	24.4
1.000e+0	2.52e-5	1.21e-6	23.0	3.26e-6	1.59e-7	24.3	4.47e-7	2.19e-8	24.7
1.047e+0	2.48e-5	1.23e-6	22.5	3.12e-6	1.57e-7	24.5	4.27e-7	2.17e-8	24.9
1.097e+0	2.52e-5	1.26e-6	21.9	3.07e-6	1.57e-7	24.5	4.17e-7	2.17e-8	25.0
1.148e+0	2.62e-5	1.30e-6	21.2	3.11e-6	1.57e-7	24.2	4.19e-7	2.15e-8	24.9
1.202e+0	2.74e-5	1.34e-6	20.4	3.20e-6	1.61e-7	23.6	4.32e-7	2.18e-8	24.5
1.259e+0	2.82e-5	1.38e-6	19.8	3.33e-6	1.66e-7	22.8	4.52e-7	2.25e-8	23.7
1.318e+0	2.85e-5	1.42e-6	19.3	3.51e-6	1.75e-7	21.9	4.80e-7	2.37e-8	22.8
1.380e+0	2.81e-5	1.42e-6	19.0	3.73e-6	1.84e-7	20.9	5.10e-7	2.50e-8	21.7
1.445e+0	2.74e-5	1.40e-6	18.9	3.90e-6	1.90e-7	20.1	5.35e-7	2.61e-8	20.8

Table 3.5.5 Continued. (2/2)

Photon Energy [MeV]	Flux at z=76mm	Abs. Error	Window [%]	Flux at z=228mm	Abs. Error	Window [%]	Flux at z=380mm	Abs. Error	Window [%]
1.514e+0	2.67e-5	1.35e-6	18.7	3.97e-6	1.95e-7	19.6	5.52e-7	2.70e-8	20.0
1.585e+0	2.63e-5	1.33e-6	18.5	3.95e-6	1.96e-7	19.2	5.62e-7	2.77e-8	19.5
1.660e+0	2.61e-5	1.33e-6	18.3	3.91e-6	2.00e-7	19.0	5.68e-7	2.86e-8	19.1
1.738e+0	2.61e-5	1.31e-6	18.0	3.93e-6	2.00e-7	18.8	5.73e-7	2.89e-8	18.8
1.820e+0	2.63e-5	1.31e-6	17.7	3.98e-6	2.03e-7	18.5	5.77e-7	2.94e-8	18.6
1.906e+0	2.63e-5	1.33e-6	17.4	4.01e-6	2.05e-7	18.2	5.79e-7	2.98e-8	18.3
1.995e+0	2.57e-5	1.28e-6	17.0	4.01e-6	2.00e-7	17.8	5.80e-7	2.91e-8	17.9
2.089e+0	2.52e-5	1.26e-6	16.6	3.98e-6	2.00e-7	17.4	5.81e-7	2.92e-8	17.5
2.188e+0	2.53e-5	1.27e-6	16.2	4.00e-6	2.05e-7	16.9	5.90e-7	2.99e-8	16.9
2.291e+0	2.55e-5	1.24e-6	15.8	4.10e-6	2.03e-7	16.4	6.05e-7	2.98e-8	16.4
2.399e+0	2.49e-5	1.20e-6	15.5	4.22e-6	2.01e-7	15.9	6.14e-7	2.93e-8	16.0
2.512e+0	2.41e-5	1.17e-6	15.1	4.22e-6	2.01e-7	15.5	6.10e-7	2.93e-8	15.6
2.630e+0	2.36e-5	1.15e-6	14.9	4.07e-6	1.97e-7	15.2	5.93e-7	2.89e-8	15.2
2.754e+0	2.28e-5	1.09e-6	14.7	3.86e-6	1.88e-7	15.0	5.67e-7	2.78e-8	15.0
2.884e+0	2.13e-5	1.05e-6	14.6	3.68e-6	1.83e-7	14.8	5.46e-7	2.73e-8	14.8
3.020e+0	1.98e-5	9.66e-7	14.6	3.53e-6	1.73e-7	14.6	5.29e-7	2.59e-8	14.5
3.162e+0	1.84e-5	9.07e-7	14.6	3.37e-6	1.65e-7	14.5	5.06e-7	2.48e-8	14.3
3.311e+0	1.72e-5	8.28e-7	14.6	3.19e-6	1.53e-7	14.4	4.83e-7	2.30e-8	14.1
3.467e+0	1.66e-5	7.90e-7	14.7	2.97e-6	1.46e-7	14.3	4.67e-7	2.19e-8	14.0
3.631e+0	1.62e-5	7.63e-7	15.4	2.85e-6	1.40e-7	14.5	4.41e-7	2.12e-8	14.1
3.802e+0	1.50e-5	6.17e-7	16.8	2.80e-6	1.22e-7	15.1	4.02e-7	1.81e-8	14.6
3.981e+0	1.34e-5	6.39e-7	18.4	2.65e-6	1.19e-7	16.1	3.72e-7	1.64e-8	15.7
4.169e+0	1.19e-5	6.78e-7	19.7	2.39e-6	1.28e-7	17.0	3.41e-7	1.74e-8	16.7
4.365e+0	1.06e-5	5.99e-7	21.4	2.13e-6	1.16e-7	18.4	2.98e-7	1.66e-8	18.0
4.571e+0	9.58e-6	4.35e-7	22.9	1.87e-6	8.61e-8	19.9	2.55e-7	1.21e-8	19.5
4.786e+0	8.68e-6	4.03e-7	23.8	1.58e-6	8.52e-8	21.1	2.26e-7	1.13e-8	20.5
5.012e+0	7.51e-6	3.66e-7	24.5	1.30e-6	7.65e-8	22.4	2.03e-7	1.05e-8	21.8
5.248e+0	6.07e-6	2.92e-7	25.4	1.04e-6	6.05e-8	23.8	1.74e-7	8.24e-9	23.2
5.495e+0	4.70e-6	2.83e-7	25.7	8.22e-7	5.91e-8	24.8	1.36e-7	7.85e-9	24.2
5.754e+0	3.74e-6	2.39e-7	25.7	6.79e-7	4.90e-8	25.3	1.01e-7	6.75e-9	24.9
6.026e+0	3.25e-6	2.18e-7	25.7	5.95e-7	3.69e-8	25.7	7.89e-8	4.90e-9	25.5
6.310e+0	2.92e-6	1.98e-7	25.7	5.25e-7	3.13e-8	25.7	6.86e-8	4.03e-9	25.5
6.607e+0	2.46e-6	1.69e-7	25.7	4.33e-7	2.34e-8	25.7	5.93e-8	3.07e-9	25.5
6.918e+0	1.90e-6	1.84e-7	25.7	3.27e-7	2.14e-8	25.7	4.63e-8	2.61e-9	25.5
7.244e+0	1.47e-6	1.49e-7	25.7	2.38e-7	1.72e-8	25.7	3.38e-8	2.06e-9	25.5
7.586e+0	1.26e-6	1.17e-7	25.7	1.77e-7	1.34e-8	25.7	2.67e-8	1.53e-9	25.7
7.943e+0	1.10e-6	1.16e-7	25.7	1.34e-7	1.36e-8	25.7	2.30e-8	1.55e-9	25.7
8.318e+0	8.93e-7	1.05e-7	25.7	9.92e-8	1.32e-8	25.7	1.87e-8	1.43e-9	25.7
8.710e+0	6.82e-7	9.35e-8	25.7	7.24e-8	1.43e-8	25.7	1.31e-8	1.41e-9	25.7
9.120e+0	5.46e-7	8.58e-8	25.7	5.62e-8	1.63e-8	25.7	8.22e-9	1.53e-9	25.7
9.550e+0	4.79e-7	8.63e-8	25.7	4.69e-8	1.65e-8	25.7	5.13e-9	1.65e-9	25.7
1.000e+1	4.27e-7	9.21e-8	25.7	3.94e-8	1.28e-8	25.7	3.37e-9	1.60e-9	25.7
1.047e+1	3.57e-7	9.17e-8	25.7	3.12e-8	7.98e-9	25.7	2.37e-9	1.23e-9	25.7
1.097e+1	2.71e-7	7.56e-8	25.7	2.28e-8	1.20e-8	25.7	1.86e-9	1.01e-9	25.7
1.148e+1	1.77e-7	5.24e-8	25.7	1.60e-8	1.63e-8	25.7	1.58e-9	1.33e-9	25.7
1.202e+1	8.82e-8	5.43e-8	25.7	1.15e-8	1.49e-8	25.7	1.26e-9	1.61e-9	25.7
1.259e+1	2.37e-8	6.51e-8	25.7	8.35e-9	9.78e-9	25.7	8.35-10	1.46e-9	25.7
1.318e+1	-7.30e-9	-5.69e-8	25.7	5.39e-9	4.84e-9	25.7	4.32-10	9.66-10	25.7
1.380e+1	-1.22e-8	-3.48e-8	25.7	2.71e-9	1.96e-9	25.7	1.70-10	4.67-10	25.7
1.445e+1	-6.95e-9	-1.48e-8	25.7	9.73-10	6.86-10	25.7	5.06-11	1.65-10	25.7
1.514e+1	-2.33e-9	-4.31e-9	25.7	2.40-10	1.91-10	25.7	1.11-11	4.18-11	25.7

Table 3.5.6 Measured gamma-ray heating rates of tungsten in the unit of [Gy / source neutron].

Detector Position [mm]	Gamma Heating	Error [%]
0	5.41e-16	58
76	5.95e-16	19
228	9.38e-17	17
380	1.26e-17	18

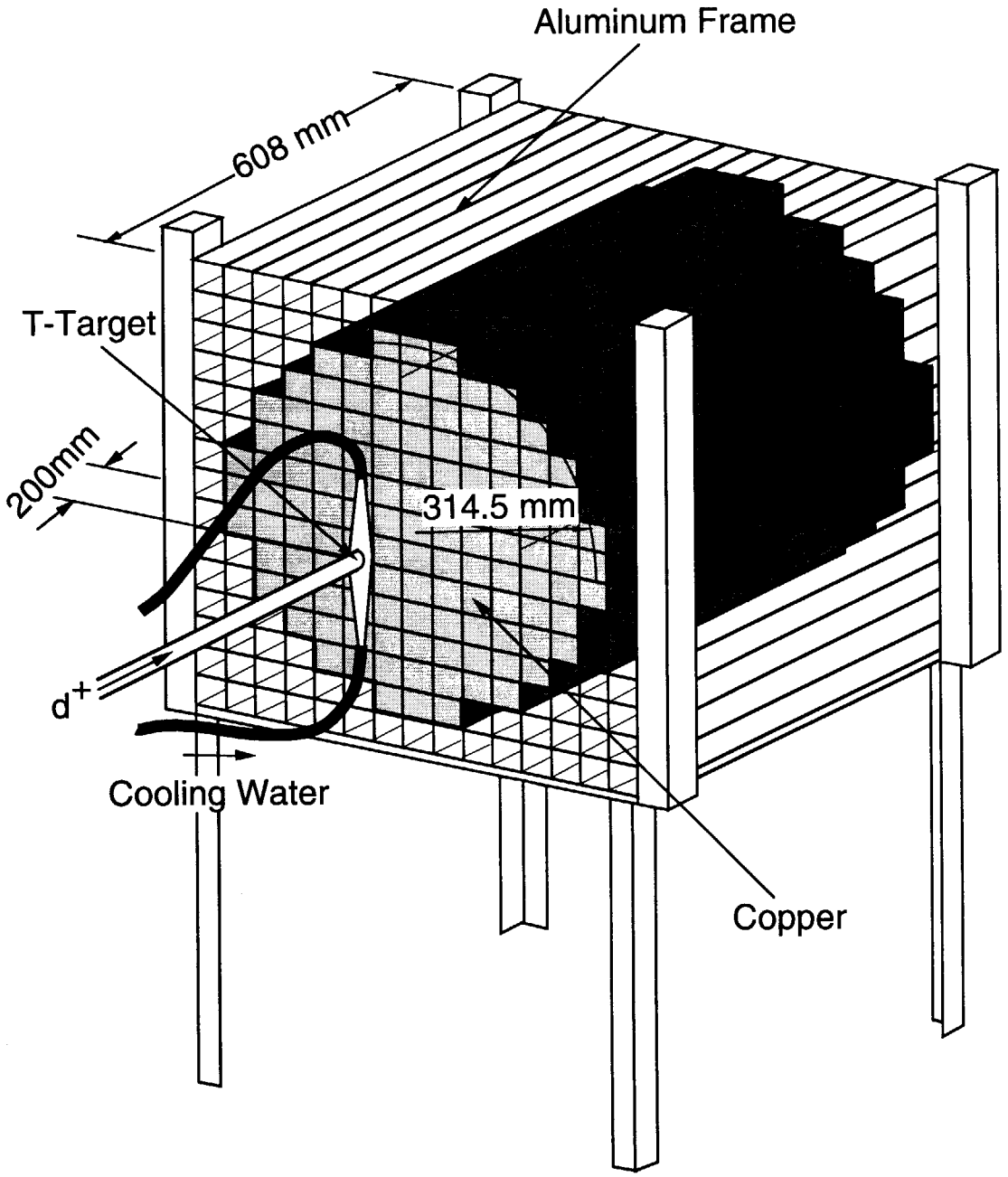

Fig. 2.1.1 Experimental assembly of copper.

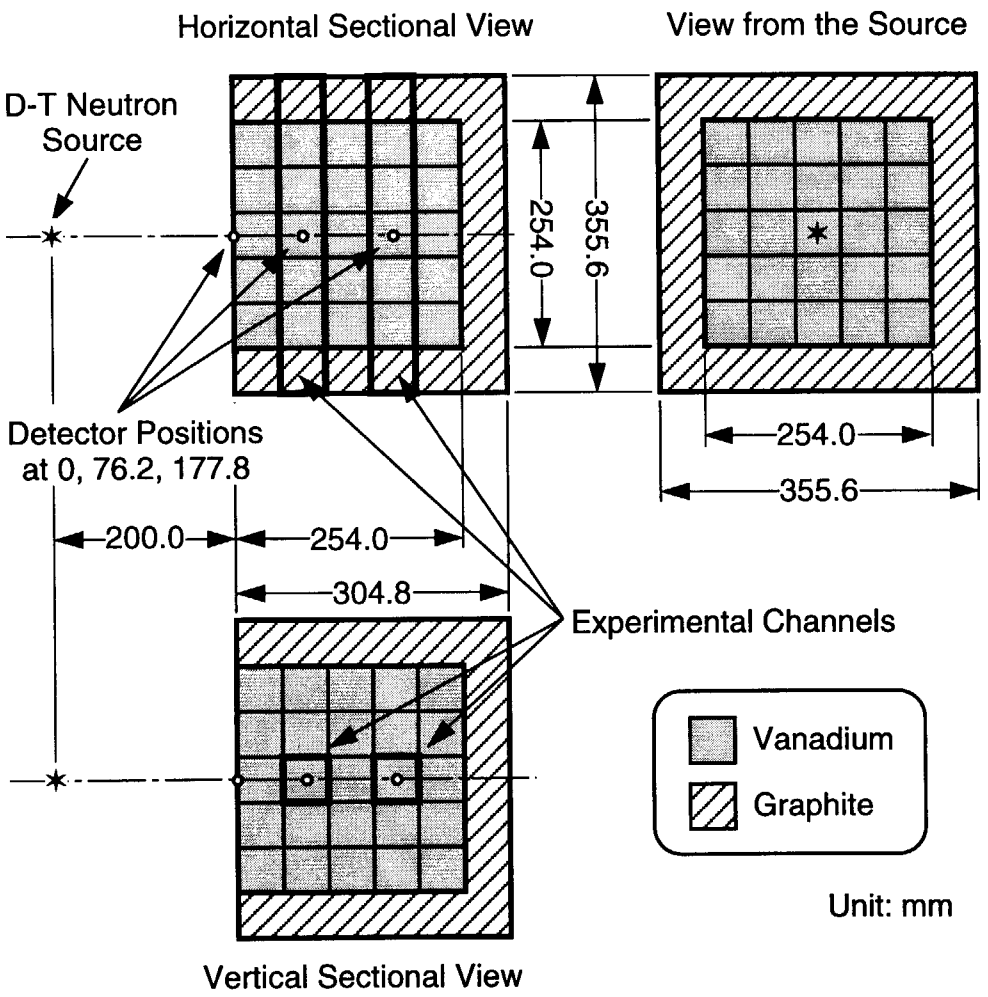

Fig. 2.1.2 Experimental assembly of vanadium.

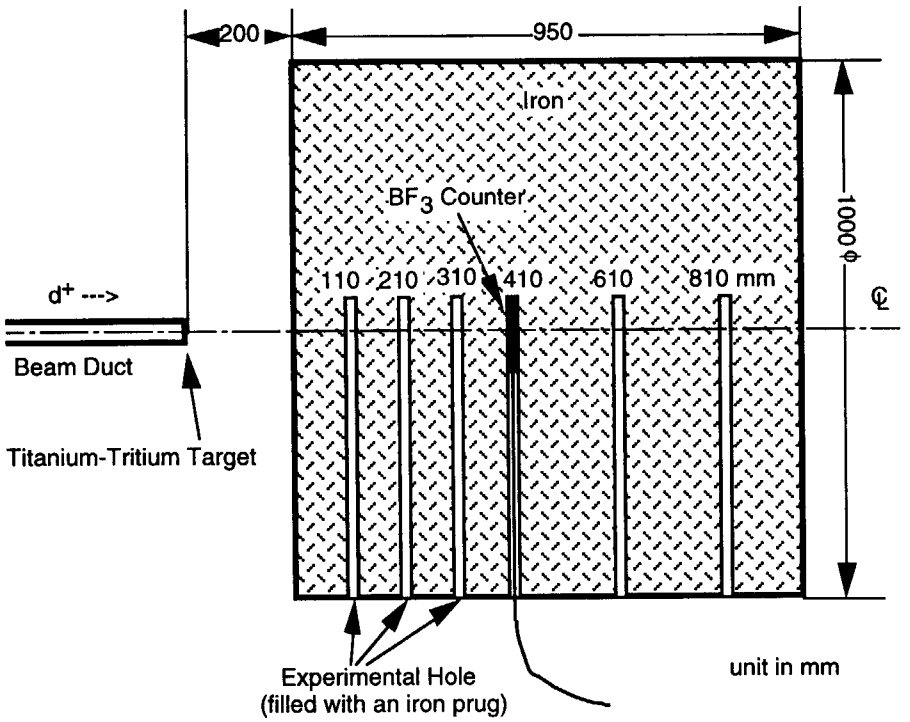

Fig. 2.1.3 Experimental assembly of iron when a BF_3 counter is inserted.

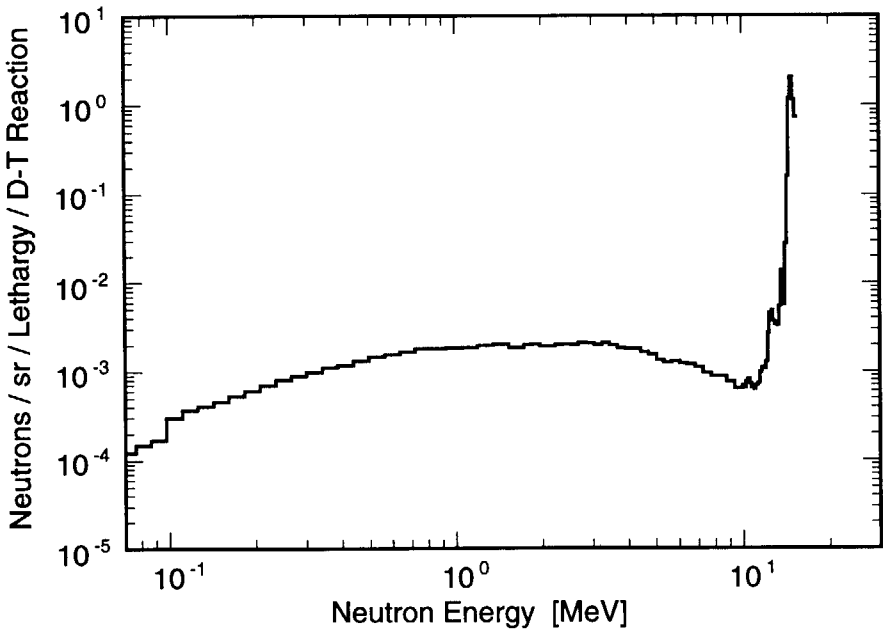

Fig. 2.2.1 Source neutron spectrum emitted toward the 0 degree from the target.

```
sc1   Source Neutron Spectrum for FNS 1TR NWCT at 0 Degree
sdef  erg=d1  dir=d2  vec=0 0 1  pos=0 0 -20  wgt=1.1261
sb2   -31  4.0
si1   1.0010-11  3.2241-07
      5.3156-07  8.7640-07  1.4449-06  2.3823-06  3.9278-06
      6.4758-06  1.0677-05  1.7603-05  2.9023-05  4.7850-05
      7.8891-05  1.3007-04  2.1445-04  3.5357-04  5.8293-04
      9.6110-04  1.2341-03  1.5846-03  2.0346-03  2.6125-03
      3.3546-03  4.3073-03  5.5307-03  7.1016-03  9.1186-03
      1.1709-02  1.5034-02  1.9304-02  2.1874-02  2.4787-02
      2.8087-02  3.1827-02  3.6065-02  4.0867-02  4.6308-02
      5.2474-02  5.9461-02  6.7378-02  7.6349-02  8.6515-02
      9.8035-02  1.1109-01  1.2588-01  1.4264-01  1.6163-01
      1.8315-01  2.0754-01  2.3517-01  2.6649-01  3.0197-01
      3.4217-01  3.8774-01  4.3936-01  4.9786-01  5.6415-01
      6.3927-01  7.2438-01  8.2084-01  9.3013-01  1.0540+00
      1.1943+00  1.3533+00  1.5335+00  1.7377+00  1.8498+00
      1.9691+00  2.0961+00  2.2313+00  2.3752+00  2.5284+00
      2.6914+00  2.8650+00  3.0498+00  3.2465+00  3.4559+00
      3.6787+00  3.9160+00  4.1686+00  4.4374+00  4.7236+00
      5.0282+00  5.3525+00  5.6978+00  6.0652+00  6.4564+00
      6.8728+00  7.3161+00  7.7879+00  8.2902+00  8.8249+00
      9.3940+00  9.9999+00  1.0157+01  1.0317+01  1.0480+01
      1.0645+01  1.0812+01  1.0983+01  1.1156+01  1.1331+01
      1.1510+01  1.1691+01  1.1875+01  1.2062+01  1.2252+01
      1.2445+01  1.2641+01  1.2840+01  1.3042+01  1.3248+01
      1.3456+01  1.3668+01  1.3883+01  1.4102+01  1.4324+01
      1.4550+01  1.4779+01  1.5012+01  1.5248+01  1.5488+01
sp1   0.0        1.5142-07
      2.2732-09  4.2225-09  7.4848-09  1.4264-08  8.3975-08
      1.8398-07  2.2450-07  1.3922-07  1.6817-07  2.9754-07
      3.8068-06  3.0541-06  2.2612-06  6.9372-06  7.2049-06
      8.7622-06  7.8013-06  1.4320-05  1.1820-05  1.6544-05
      1.4791-05  1.7624-05  2.8404-05  2.4899-05  3.7633-05
      4.4237-05  4.6320-05  6.1572-05  3.7185-05  5.3362-05
      4.8831-05  5.0292-05  5.7202-05  6.9230-05  8.0602-05
      8.3190-05  9.7450-05  1.0531-04  1.2632-04  1.4874-04
      1.7906-04  3.7225-04  4.9933-04  5.3824-04  6.0762-04
      7.0593-04  8.0965-04  9.5392-04  1.0785-03  1.2232-03
      1.3867-03  1.5803-03  1.6473-03  1.8238-03  2.0605-03
      2.2042-03  2.3040-03  2.5211-03  2.5709-03  2.5872-03
      2.5765-03  2.7699-03  2.8528-03  2.5945-03  1.3898-03
      1.4298-03  1.3270-03  1.3489-03  1.3820-03  1.4312-03
      1.3760-03  1.4329-03  1.4558-03  1.3518-03  1.4053-03
      1.2861-03  1.2741-03  1.1711-03  1.1937-03  1.0563-03
      1.0018-03  8.8451-04  7.9827-04  7.9293-04  7.5872-04
      6.9228-04  6.2956-04  5.1710-04  5.0750-04  5.1007-04
      4.1280-04  3.5649-04  9.0768-05  8.2287-05  9.2862-05
      9.1407-05  9.3708-05  7.9567-05  8.8737-05  8.7841-05
      1.1227-04  1.6798-04  1.5985-04  1.6563-04  2.1025-04
      4.1363-04  7.4899-04  7.8183-04  5.1771-04  4.5938-04
      4.6458-04  9.1020-04  2.6083-03  9.5007-04  5.1474-03
      3.0897-02  2.3565-01  4.0901-01  2.2296-01  1.4419-01
```

Fig. 2.2.2 Input cards of the MCNP-4 code to describe the source spectrum of neutrons emitted toward 0 degree from the target.

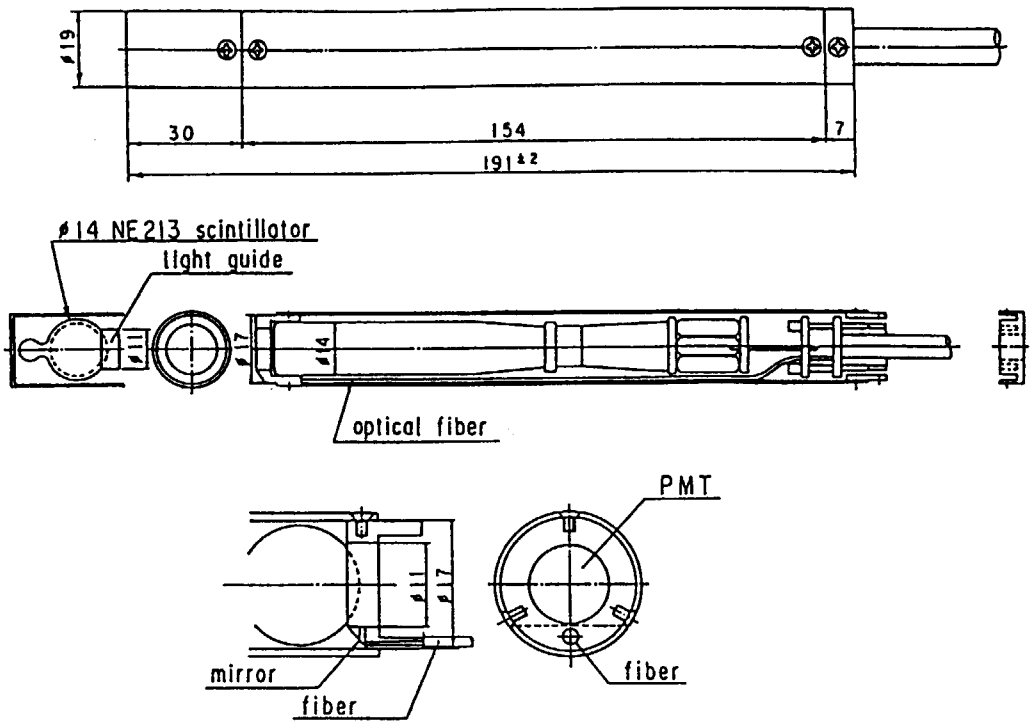

Fig. 2.3.1 Sectional view of the 14 mm ϕ small sphere NE213 neutron spectrometer.

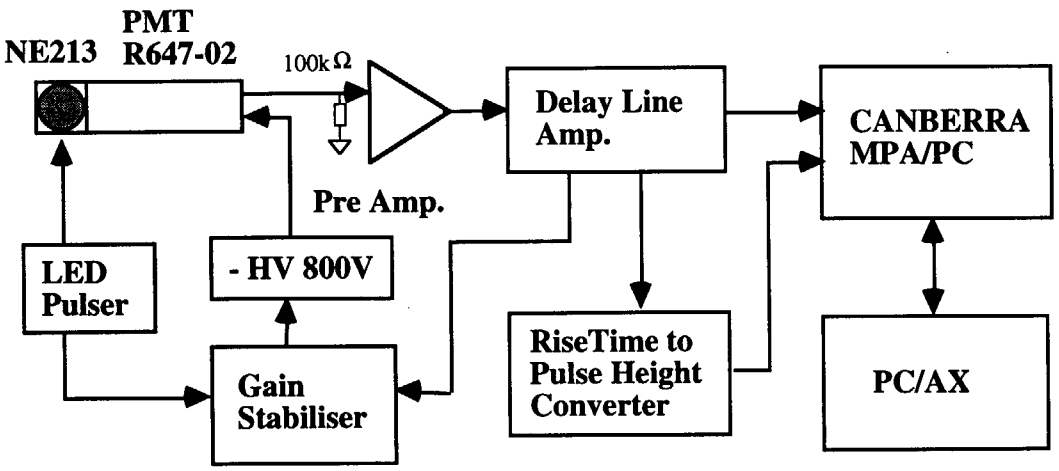

Fig. 2.3.2 Schematic diagram of electronic circuit for the NE213 spectrometer.

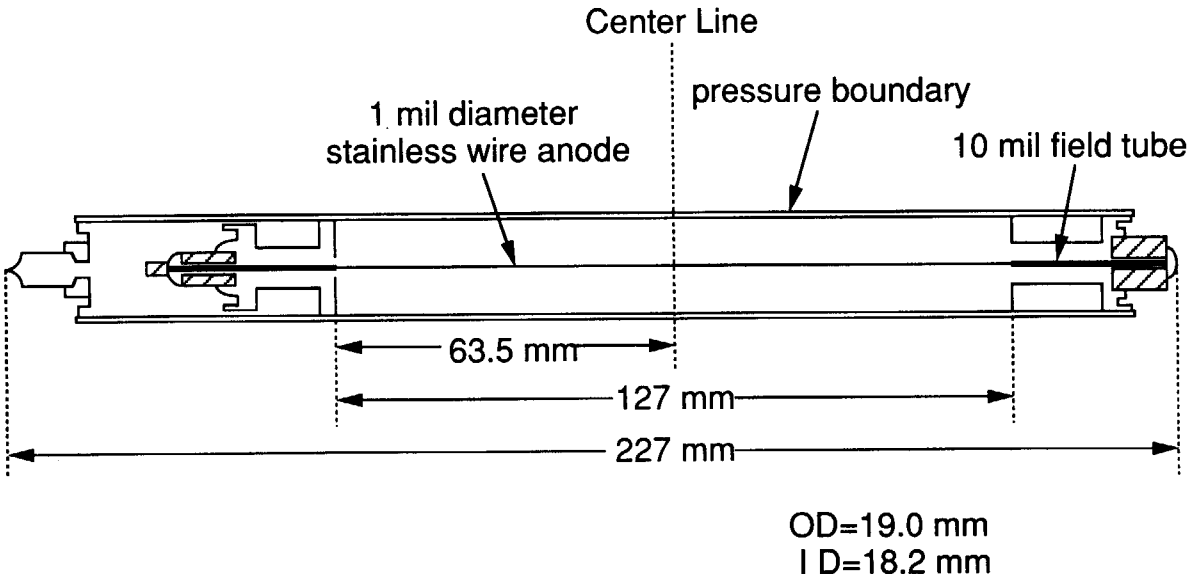

Fig. 2.3.3 Sectional view of the proton recoil gas proportional counter (PRC).

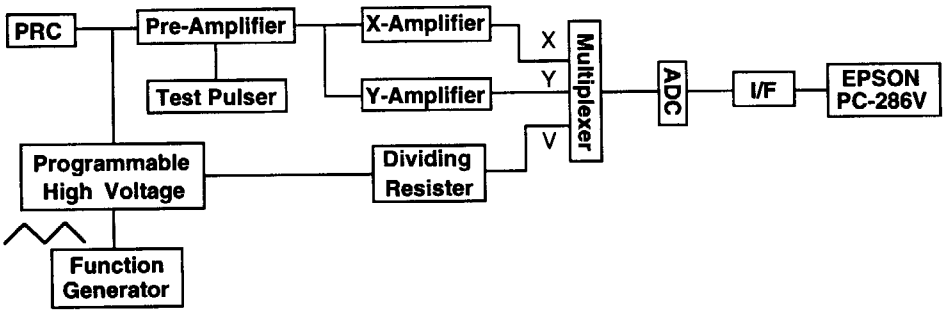

Fig. 2.3.4 Block diagram of the data acquisition system for PRC.

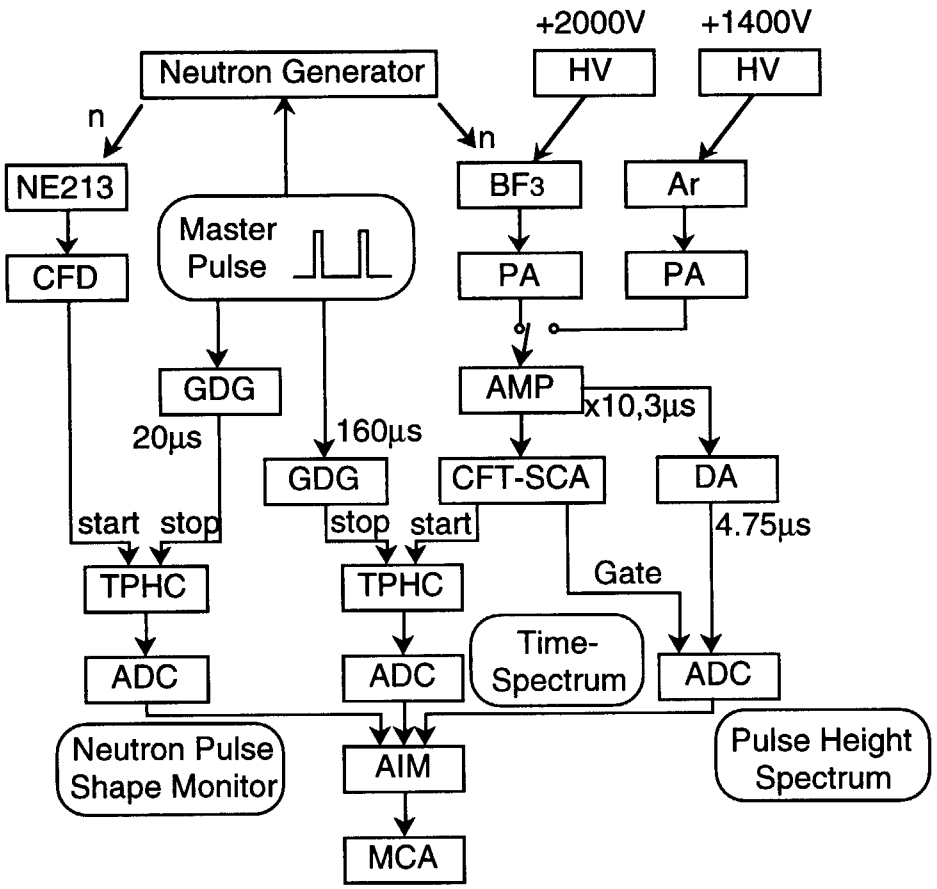

HV:	High Voltage Power Supply	NAIG D-112A
PA:	Pre-Amplifier	JAERI 124
AMP:	Amplifier	ORTEC 571
CFT-SCA:	Constant Fraction Timing Single Channel Analyzer	CANBERRA 2035A
TPHC:	Time-to-Pulse Height Convertor	ORTEC 567
DA:	Delay Amplifier	CANBERRA 1457
CFD:	Constant Fraction Discriminator	CANBERRA 1428A
GDG:	Gate and Delay Generator	ORTEC 416A
ADC:	Analog-Digital Convertor	CANBERRA 6075
AIM:	Acquisition Interface Module	CANBERRA ND556
MCA:	Multi-Channel Analyzer	CANBERRA Genie

Fig. 2.3.5 Block diagram of the electronic circuit employed for the slowing down time method.

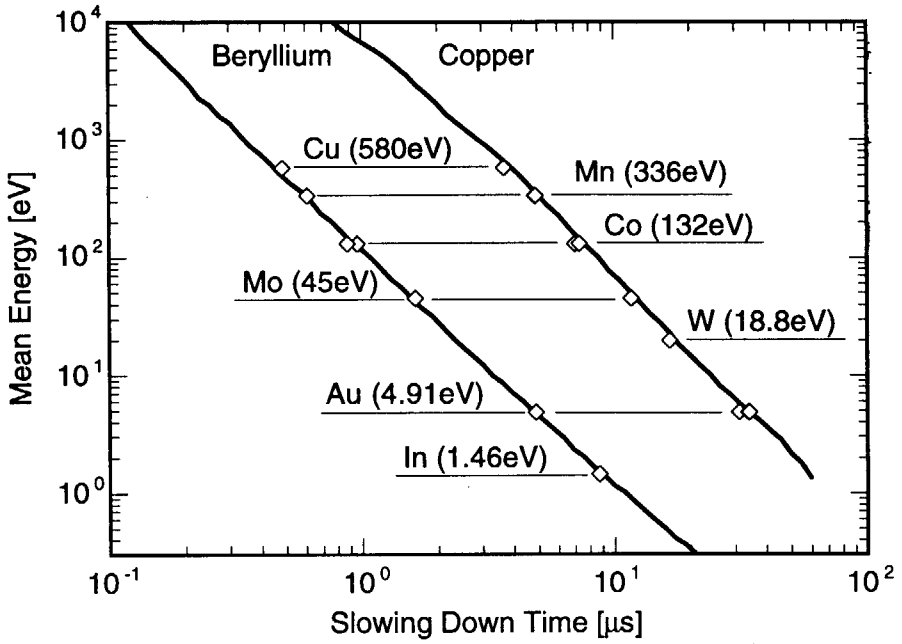

Fig. 2.3.6 Examples of the calibration curves for the beryllium and copper assemblies: experimental data (open diamonds) and calculated curves (solid lines).

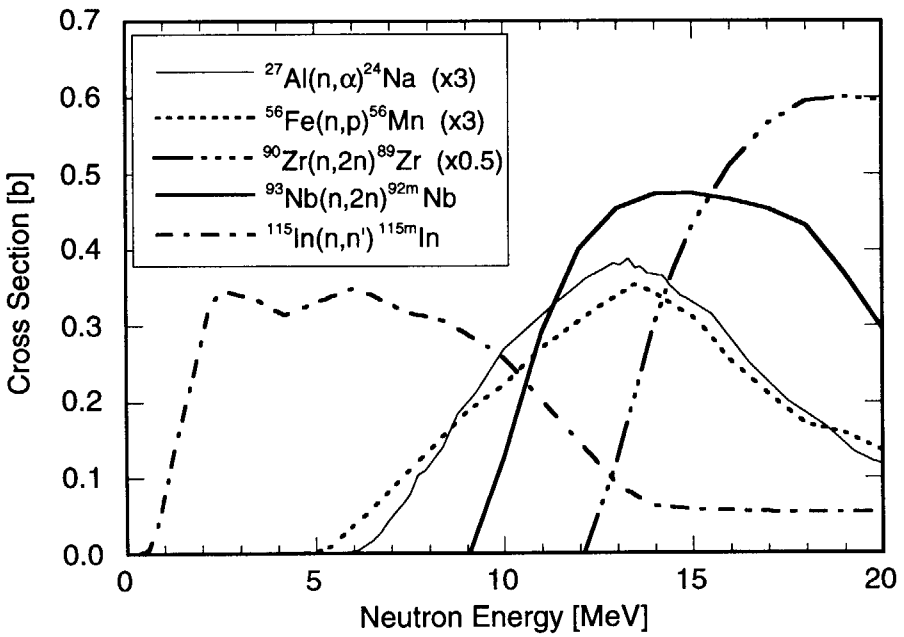

Fig. 2.3.7 Threshold dosimetry cross sections used for the foil activation experiments taken from JENDL Dosimetry File.

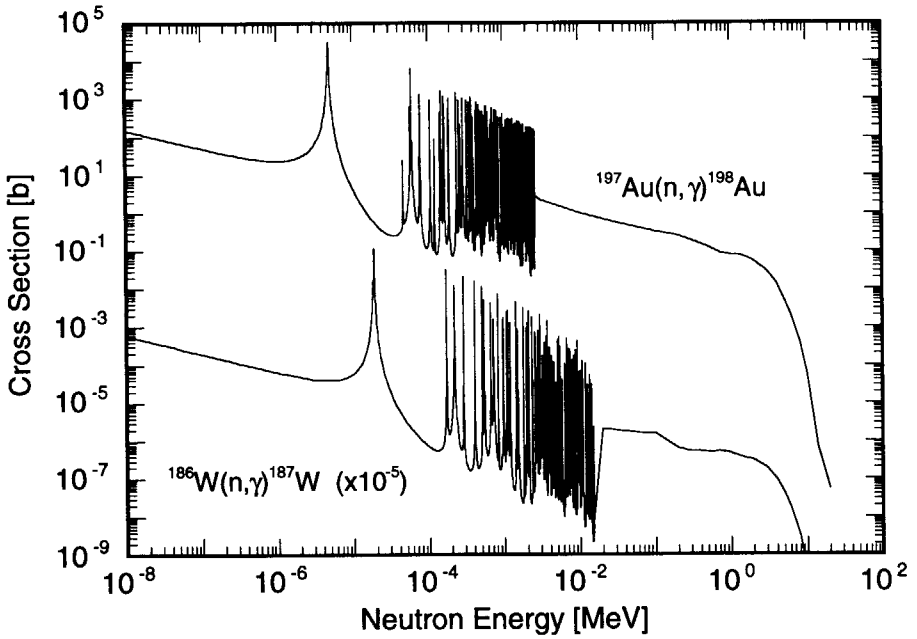

Fig. 2.3.8 Non-threshold dosimetry cross sections used for the foil activation experiments taken from JENDL Dosimetry File.

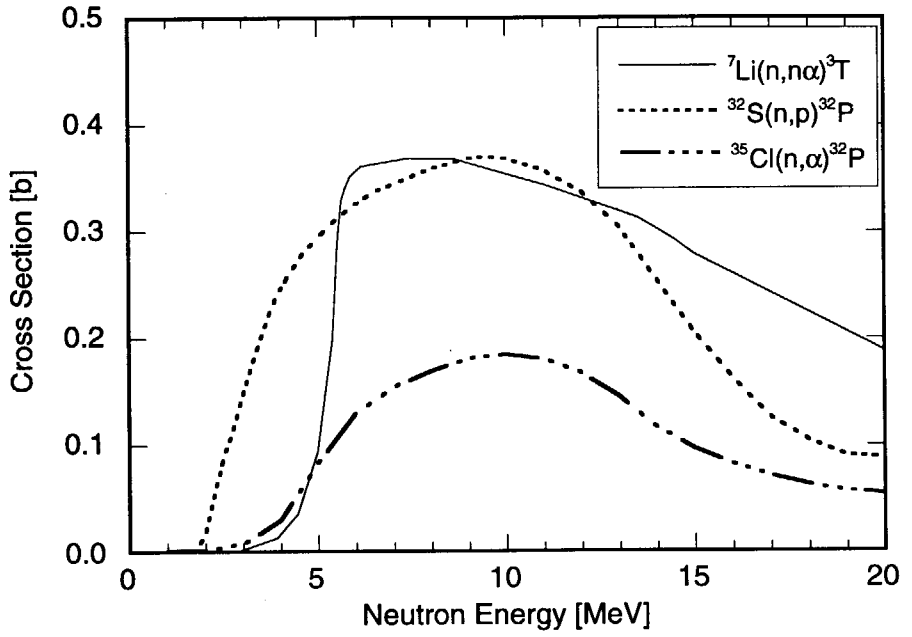

Fig. 2.3.9 The ^{7}Li(n,n'α)^{3}T and ^{32}S(n,p)^{32}P cross sections taken from JENDL Dosimetry File and the ^{35}Cl(n,α)^{32}P cross section from FENDL/A-2.0.

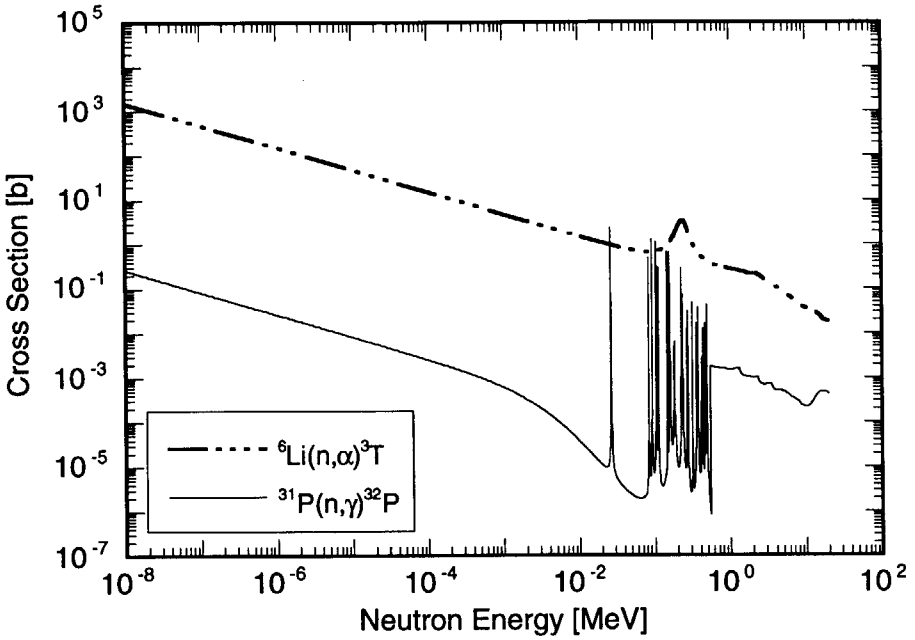

Fig. 2.3.10 The $^{6}Li(n,\alpha)^{3}T$ cross section taken from JENDL Dosimetry File and the $^{31}P(n,\gamma)^{32}P$ cross section from FENDL/A-2.0.

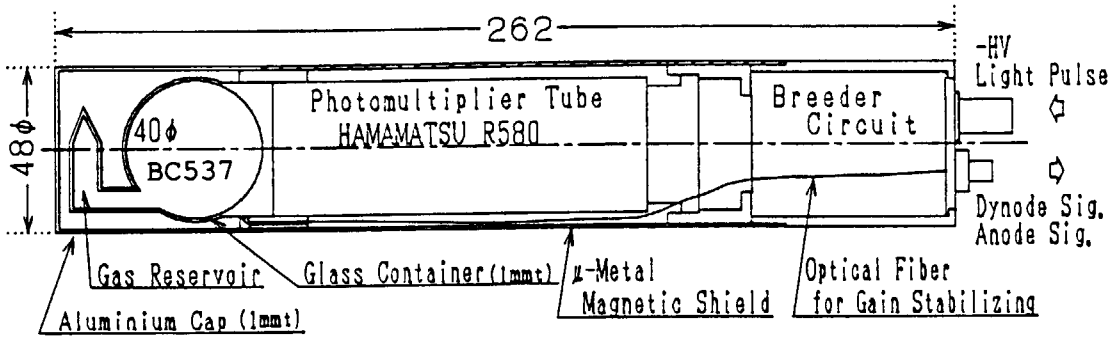

Fig. 2.3.11 The 40 mm φ spherical gamma-ray spectrometer.

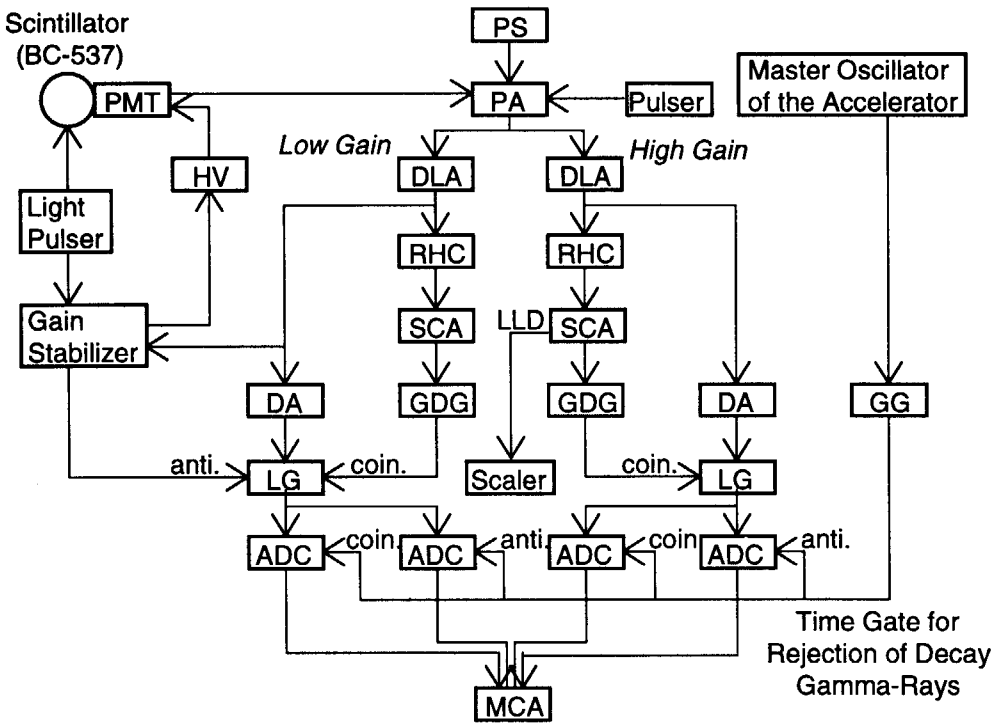

PMT : Photomultiplier Tube
HV : High Voltage Power Supply
PS : Power Supply
PA : Preamplifier
Pulser : Research Pulser
DLA : Delay Line Amplifier
RHC : Risetime to Height Convertor
SCA : Single Channel Analyzer
GDG : Gate & Delay Generator
Scaler : Timer & Scaler
DA : Delay Amplifier
LG : Linear Gate & Slow Coincidence
GG : Dual Gate Generator
ADC : Analog to Digital Convertor
MCA : Multichannel Analyzer

Fig. 2.3.12 Schematic diagram of the electronic circuit employed for the gamma-ray spectrum measurement.

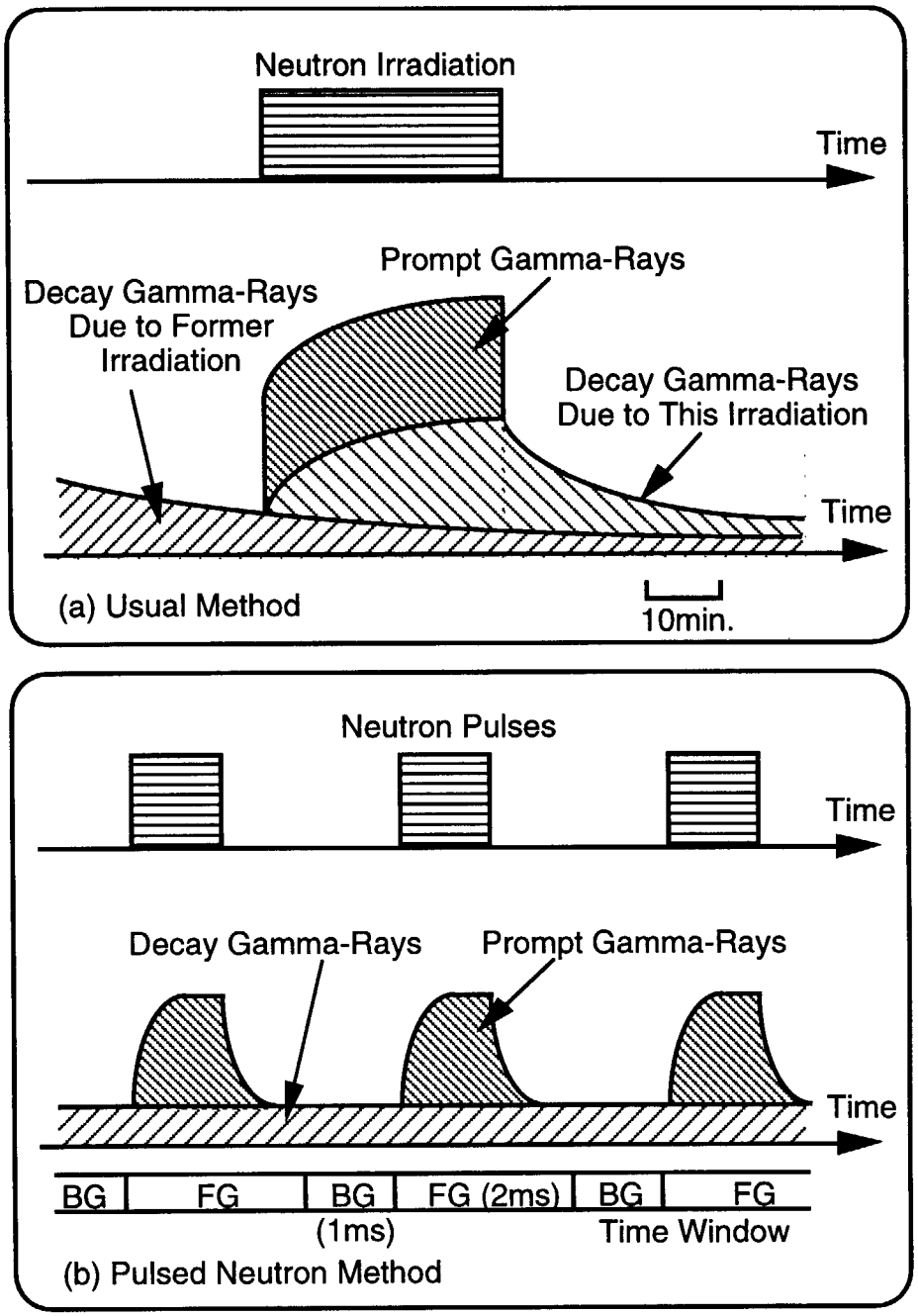

Fig. 2.3.13 Explanation of prompt gamma-ray measurement with (a) an usual method and (b) the pulsed neutron method for rejection of decay gamma-rays.

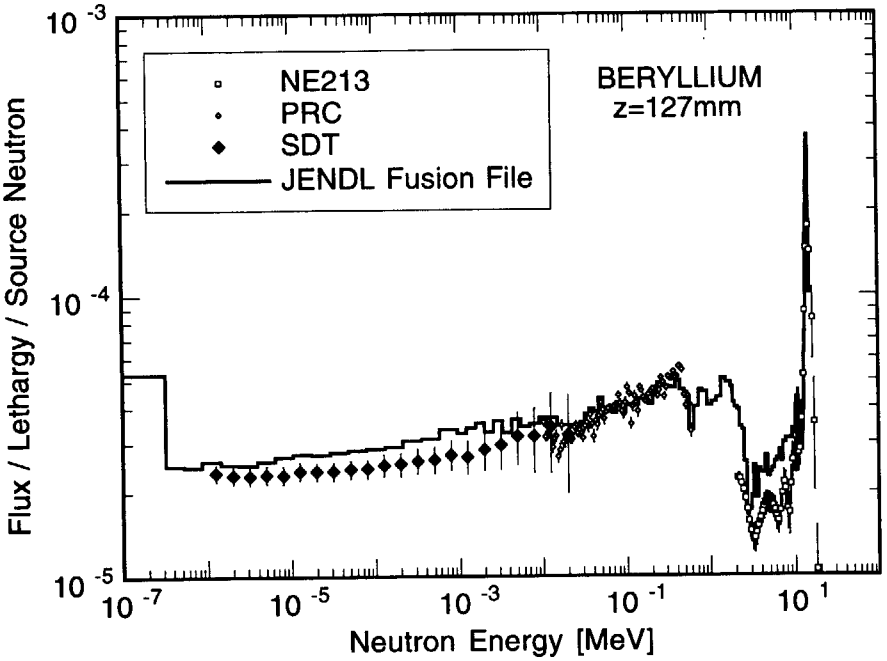

Fig. 3.1.1 Neutron spectrum at z= 127 mm in the beryllium assembly.

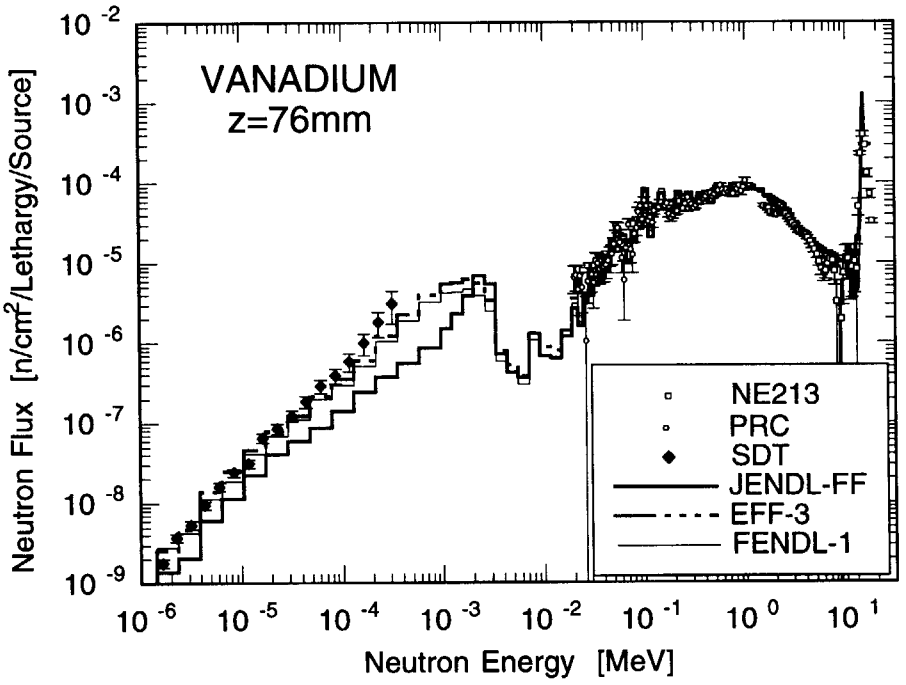

Fig. 3.2.1 Neutron spectrum at z= 76 mm in the vanadium assembly.

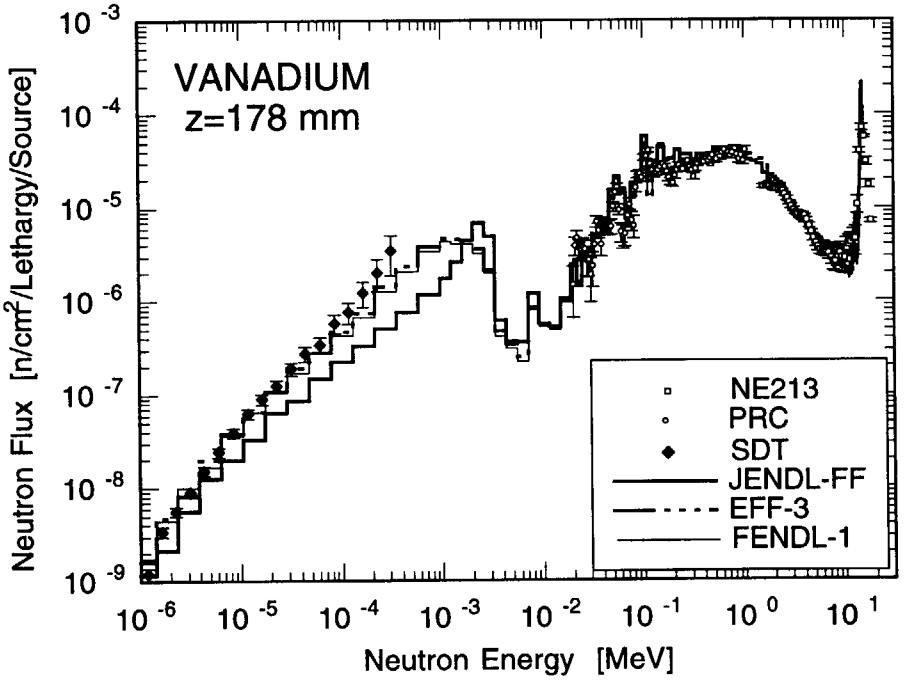

Fig. 3.2.2 Neutron spectrum at z= 178 mm in the vanadium assembly.

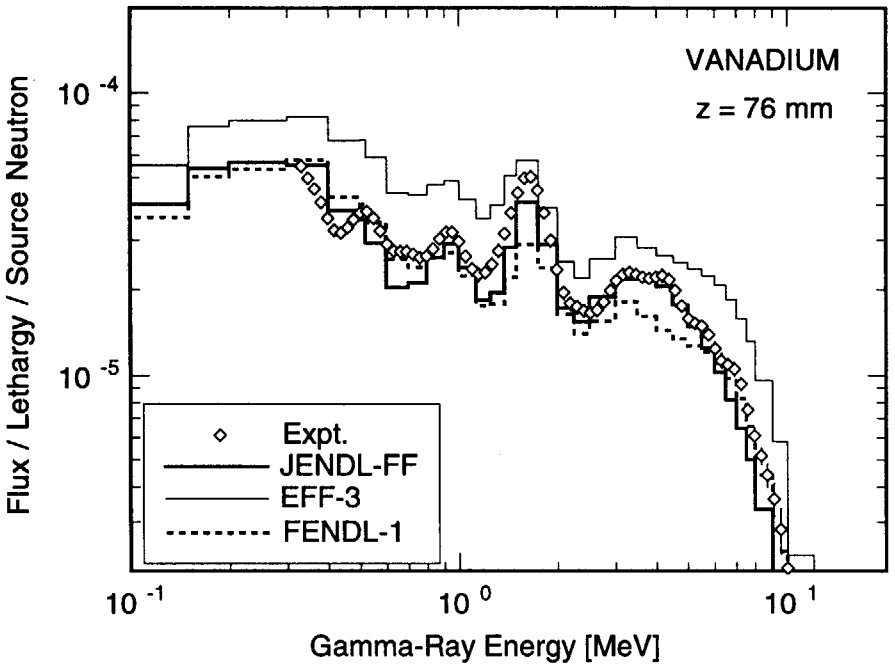

Fig. 3.2.3 Gamma-ray spectrum at z= 76 mm in the vanadium assembly.

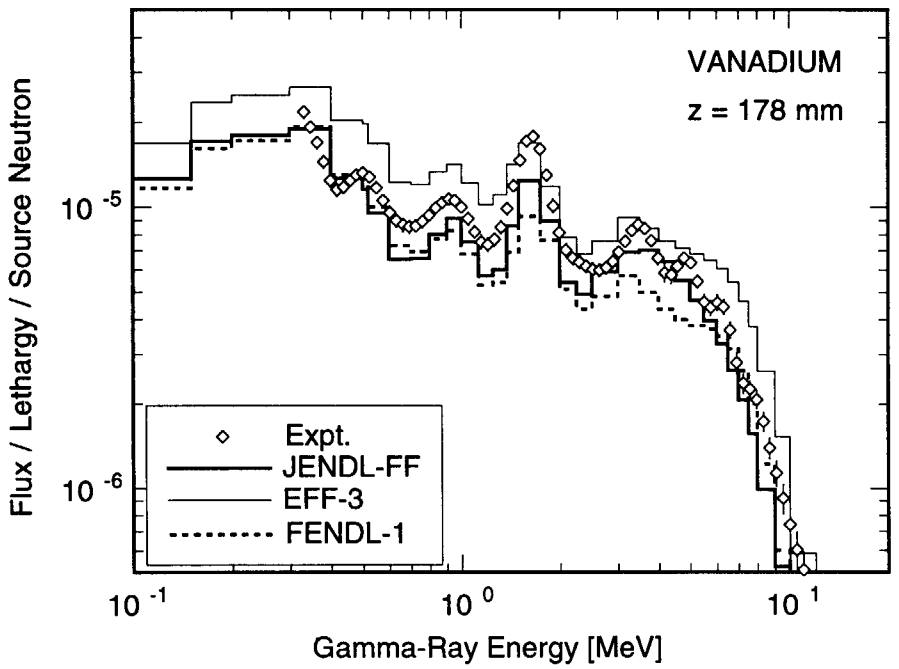

Fig. 3.2.4 Gamma-ray spectrum at z= 178 mm in the vanadium assembly.

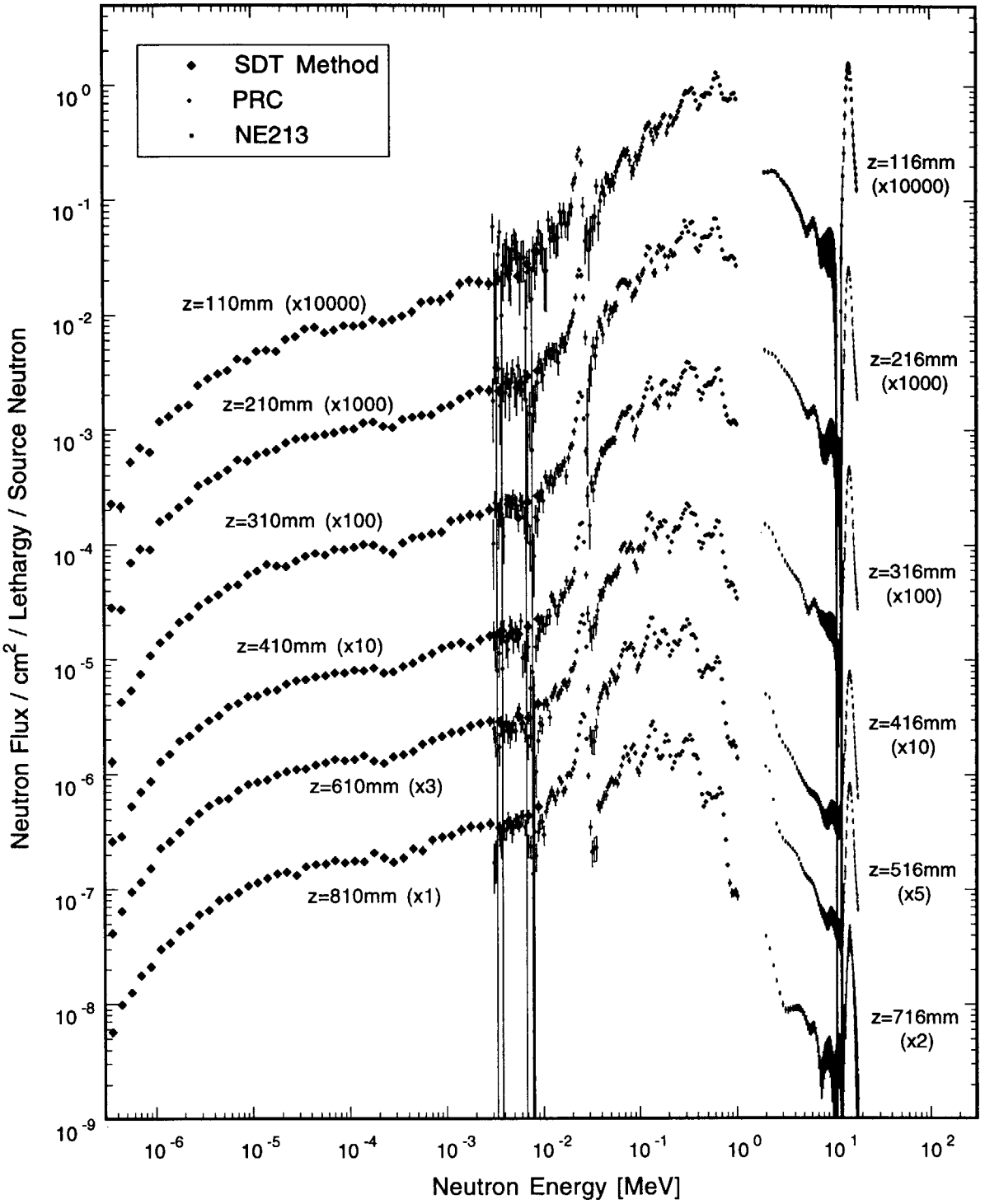

Fig. 3.3.1 Neutron spectra in the iron assembly.

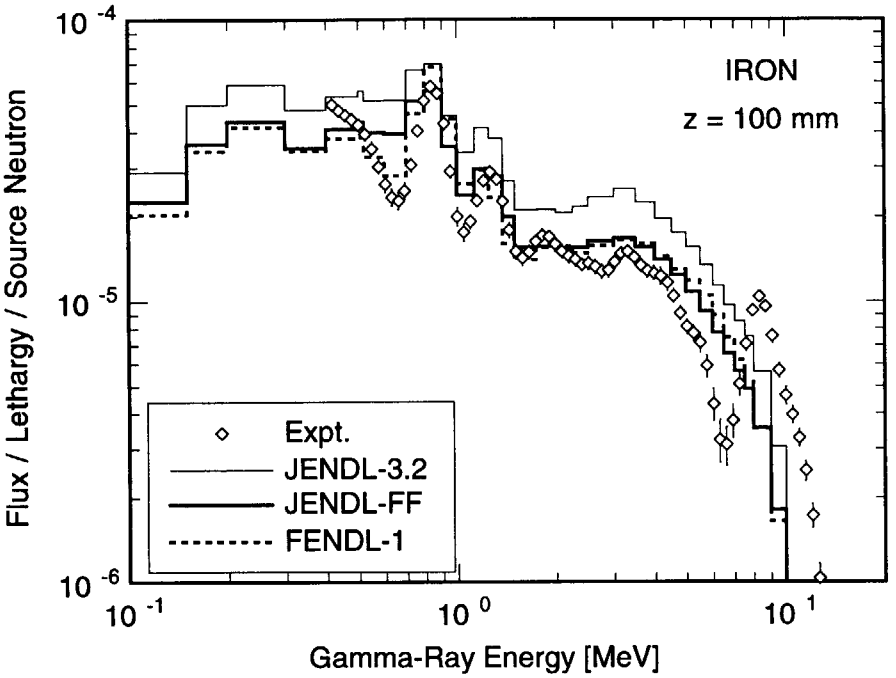

Fig. 3.3.2 Gamma-ray spectrum at z= 100 mm in the iron assembly.

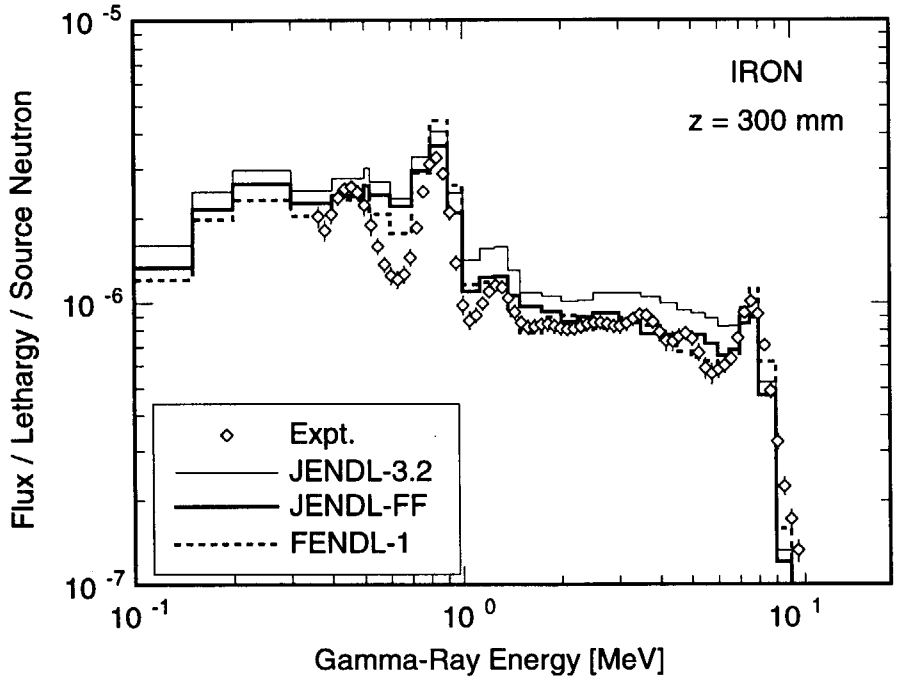

Fig. 3.3.3 Gamma-ray spectrum at z= 300 mm in the iron assembly.

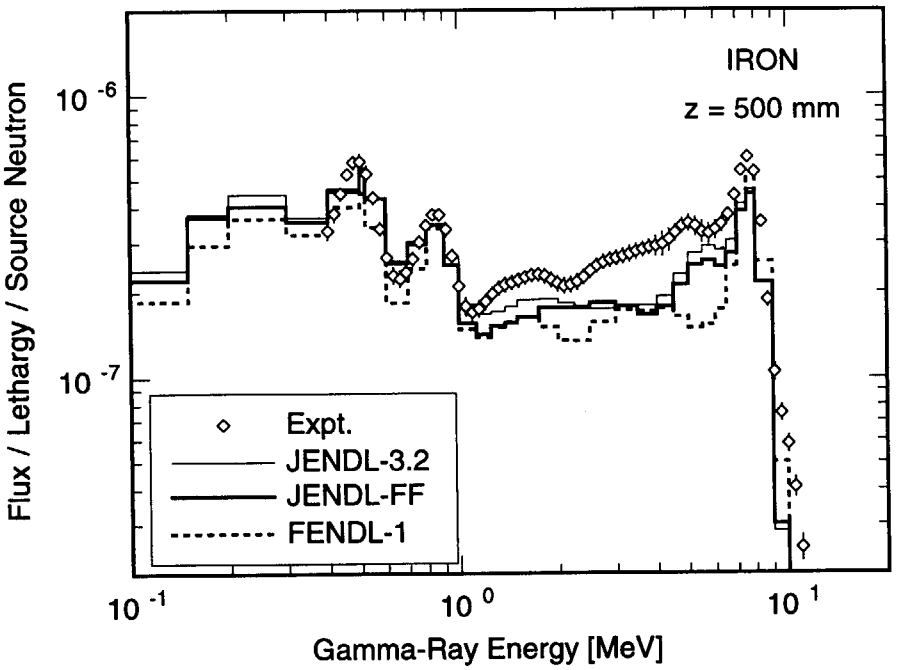

Fig. 3.3.4 Gamma-ray spectrum at z= 500 mm in the iron assembly.

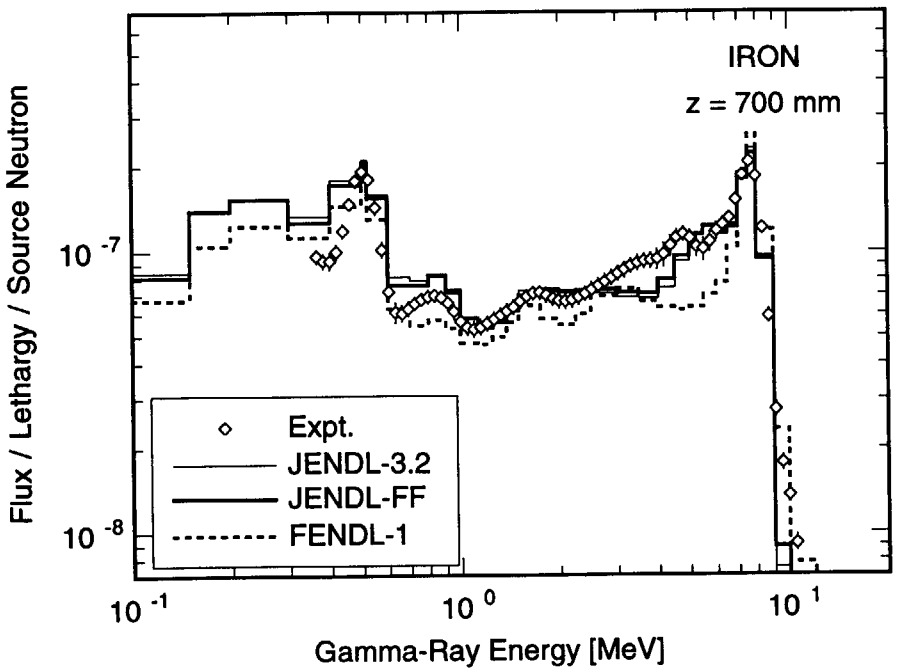

Fig. 3.3.5 Gamma-ray spectrum at z= 700 mm in the iron assembly.

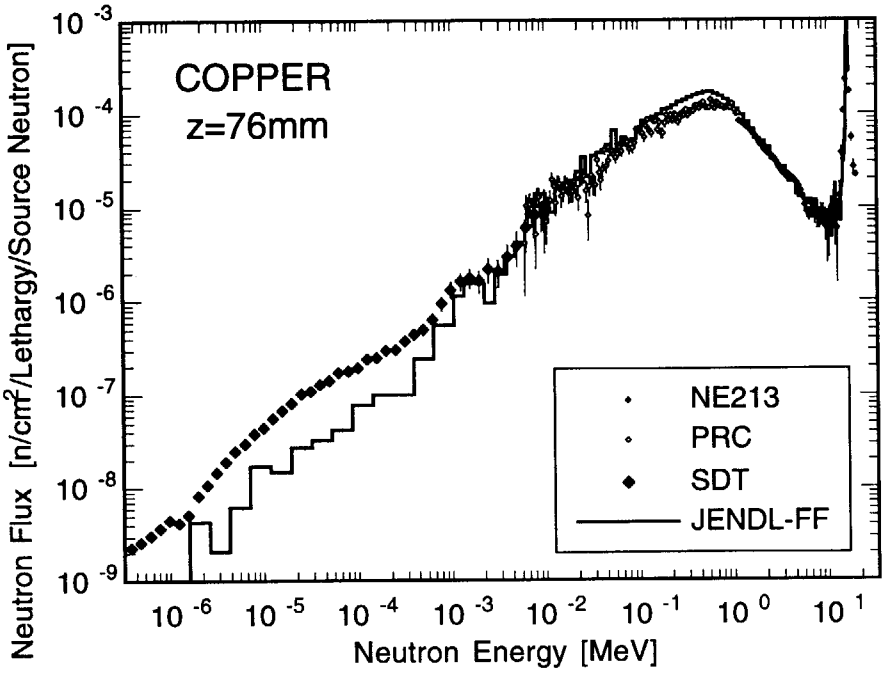

Fig. 3.4.1 Neutron spectrum at z= 76 mm in the copper assembly.

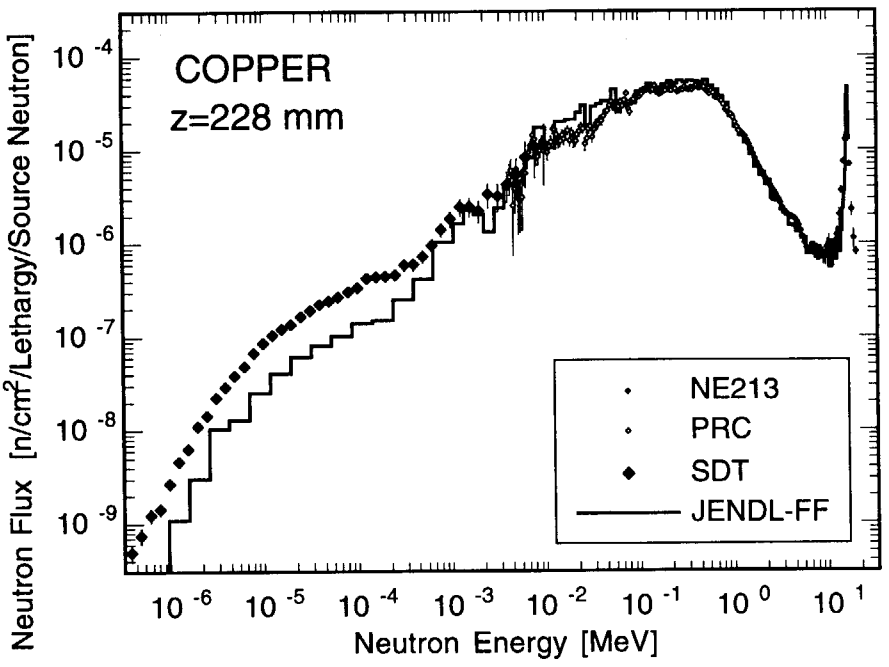

Fig. 3.4.2 Neutron spectrum at z= 228 mm in the copper assembly.

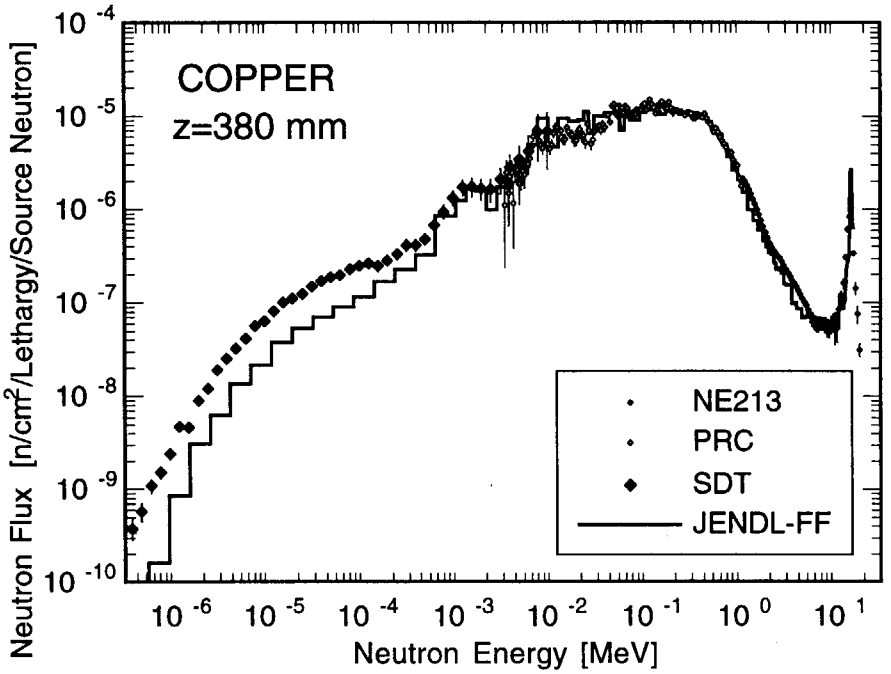

Fig. 3.4.3 Neutron spectrum at z= 380 mm in the copper assembly.

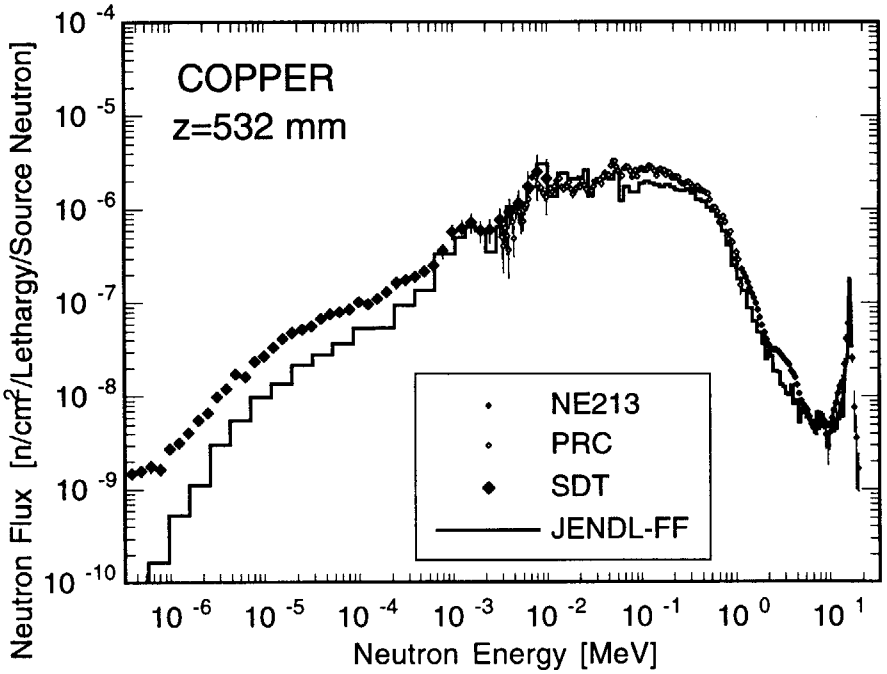

Fig. 3.4.4 Neutron spectrum at z= 532 mm in the copper assembly.

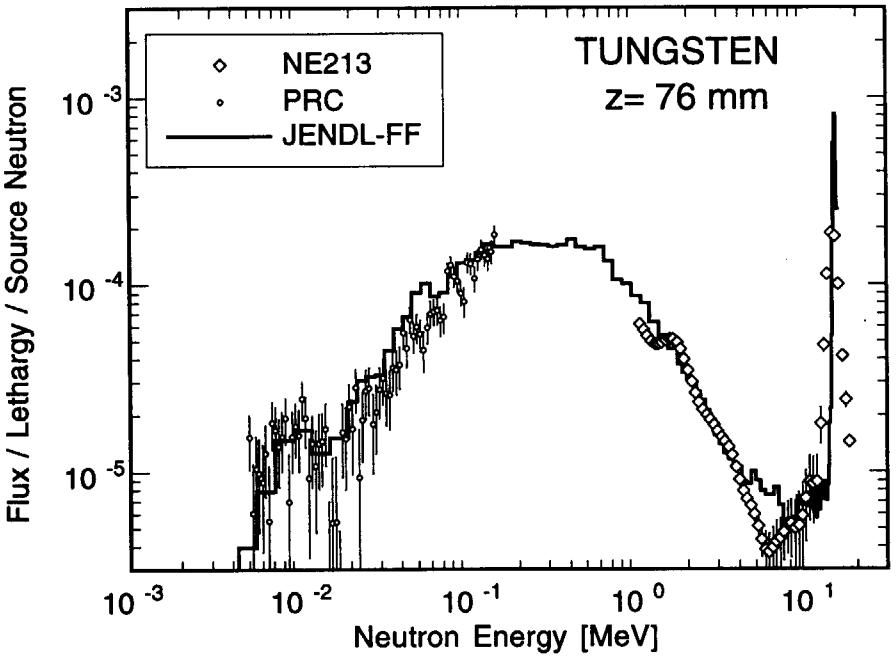

Fig. 3.5.1 Neutron spectrum at z= 76 mm in the tungsten assembly.

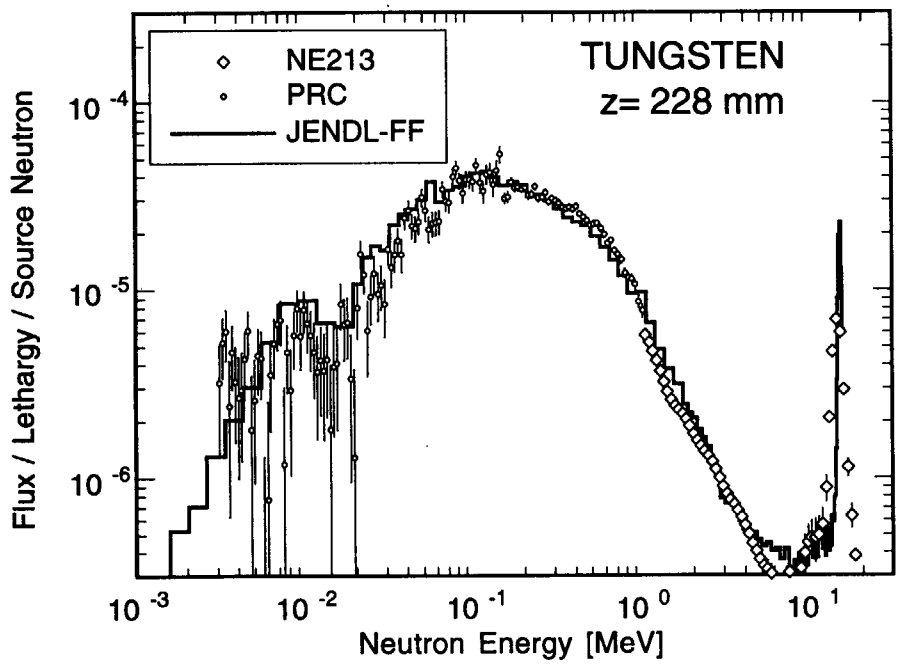

Fig. 3.5.2 Neutron spectrum at z= 228 mm in the tungsten assembly.

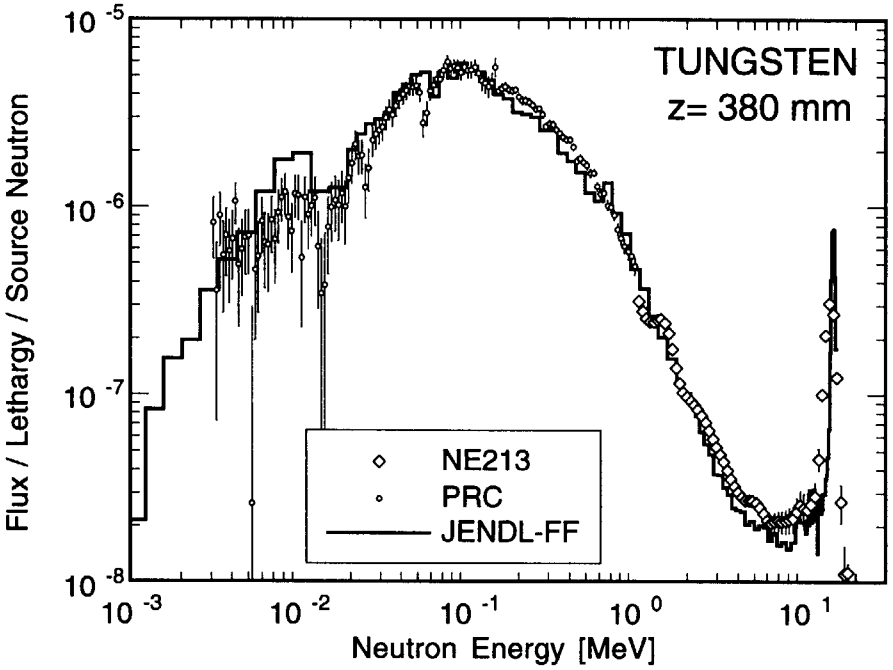

Fig. 3.5.3 Neutron spectrum at z= 380 mm in the tungsten assembly.

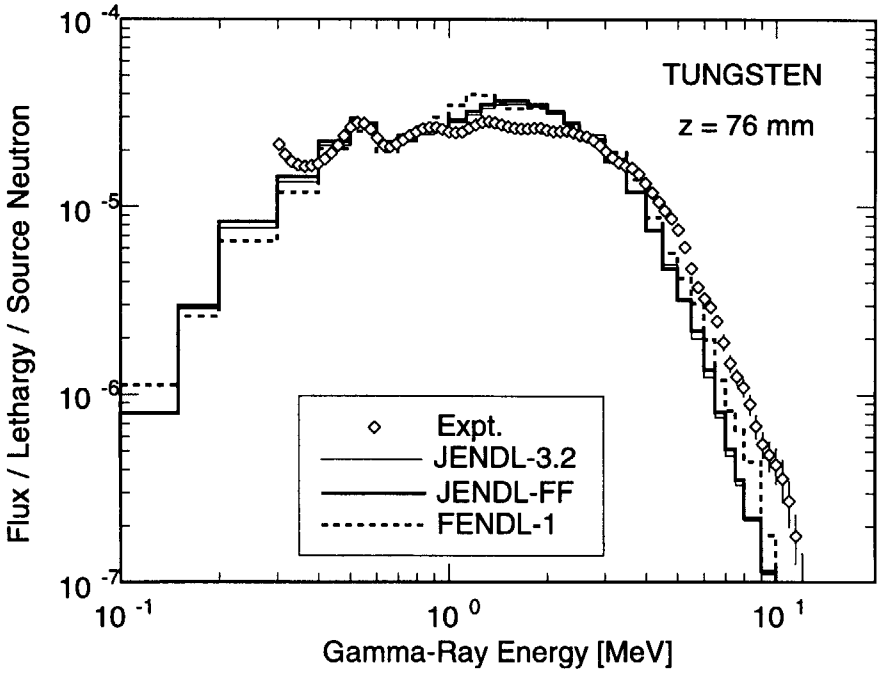

Fig. 3.5.4 Gamma-ray spectrum at z= 76 mm in the tungsten assembly.

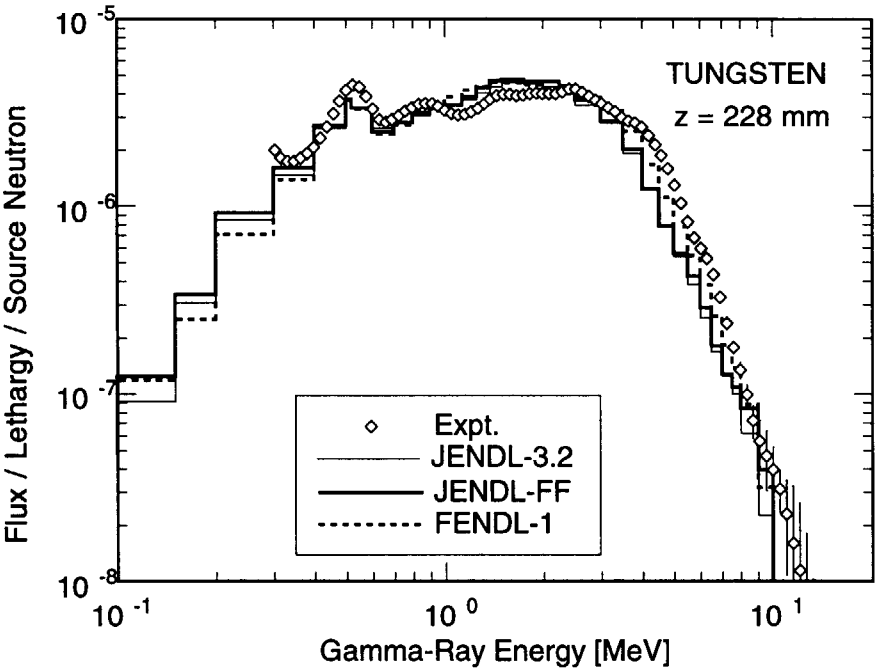

Fig. 3.5.5 Gamma-ray spectrum at z= 228 mm in the tungsten assembly.

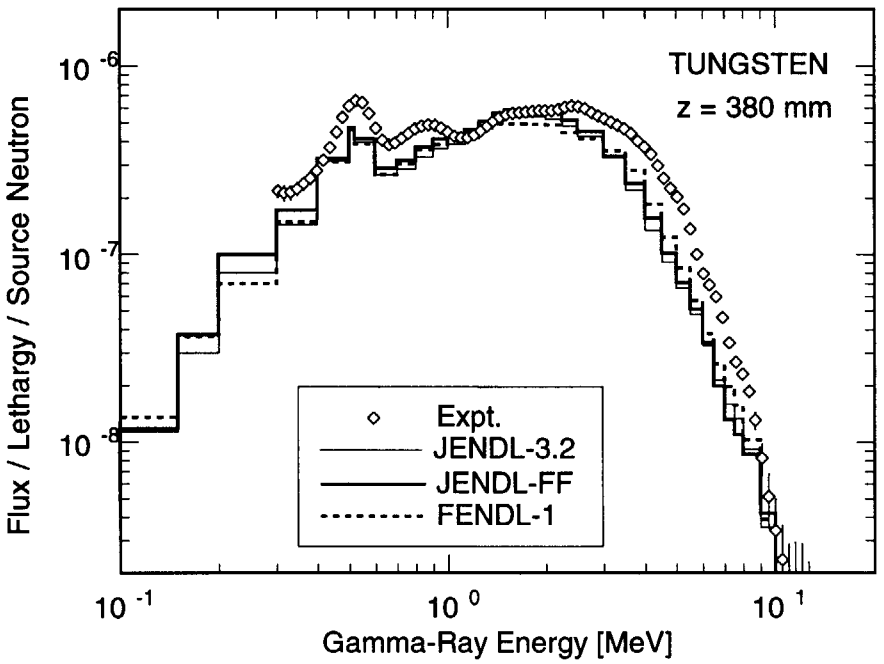

Fig. 3.5.6 Gamma-ray spectrum at z= 380 mm in the tungsten assembly.

Appendix Input Data of MCNP

Examples of input data for MCNP calculations are given. Figures A-1 ~ A-5 show the input data for beryllium, vanadium, iron, copper and tungsten, respectively.

```
Analysis of Beryllium Experiment
c    *****  front air region  *****
 1    2 4.921-5   +1  -2  -27        $
c    *****  Beryllium region  *****
 2    1 1.2215-1  +2  -3  -27        $
 3    1 1.2215-1  +3  -4  -27        $
 4    1 1.2215-1  +4  -5  -27        $
 5    1 1.2215-1  +5  -6  -27        $
 6    1 1.2215-1  +6  -7  -27        $
 7    1 1.2215-1  +7  -8  -27        $
 8    1 1.2215-1  +8  -9  -27        $
 9    1 1.2215-1  +9  -10 -27        $
10    1 1.2215-1  +10 -11 -27        $
11    1 1.2215-1  +11 -12 -27        $
12    1 1.2215-1  +12 -13 -27        $
c    *****  external void  *****
20    0         -1 : +13 : +27       $

 1             pz           -1.00  $ Source
 2             pz           20.00  $ reac
 3             pz           25.22  $ reac
 4             pz           30.00  $
 5             pz           32.68  $ n-spec
 6             pz           35.67  $ reac
 7             pz           40.00  $
 8             pz           46.13  $ reac
 9             pz           47.89  $ n-spec
10             pz           50.00  $
11             pz           56.56  $ reac
12             pz           60.00  $
13             pz           67.03  $ reac
c
27             cz           31.50
31             cz            2.00
32             cz            4.00

imp:n 1  1  1  2  2  2  4  4  4  8  8  8  0
c    ********************************************
c    *  source specification cards                *
c    ********************************************
sdef  erg=d1  pos=0 0 0  vec=0 0 1  dir=d2  wgt=1.1261
sb2   -31  4.0
si1   1.0010-11  3.2241-07
      5.3156-07  8.7640-07  1.4449-06  2.3826-06  3.9278-06
      6.4758-06  1.0677-05  1.7603-05  2.9023-05  4.7850-05
      7.8891-05  1.3007-04  2.1455-04  3.5357-04  5.8293-04
      9.6110-04  1.2341-03  1.5846-03  2.0346-03  2.6125-03
      3.3546-03  4.3073-03  5.5307-03  7.1016-03  9.1186-03
      1.1709-02  1.5034-02  1.9304-02  2.1874-02  2.4787-02
      2.8087-02  3.1827-02  3.6065-02  4.0867-02  4.6308-02
      5.2474-02  5.9461-02  6.7378-02  7.6349-02  8.6515-02
      9.8035-02  1.1109-01  1.2588-01  1.4264-01  1.6163-01
      1.8315-01  2.0754-01  2.3517-01  2.6649-01  3.0197-01
      3.4217-01  3.8774-01  4.3936-01  4.9786-01  5.6415-01
      6.3927-01  7.2438-01  8.2084-01  9.3013-01  1.0540+00
      1.1943+00  1.3533+00  1.5335+00  1.7377+00  1.8498+00
      1.9691+00  2.0961+00  2.2313+00  2.3752+00  2.5284+00
      2.6914+00  2.8650+00  3.0498+00  3.2465+00  3.4559+00
      3.6787+00  3.9160+00  4.1686+00  4.4374+00  4.7236+00
      5.0282+00  5.3525+00  5.6978+00  6.0652+00  6.4564+00
      6.8728+00  7.3161+00  7.7879+00  8.2902+00  8.8249+00
      9.3940+00  9.9999+00  1.0157+01  1.0317+01  1.0480+01
      1.0645+01  1.0812+01  1.0983+01  1.1156+01  1.1331+01
      1.1510+01  1.1691+01  1.1875+01  1.2062+01  1.2252+01
      1.2445+01  1.2641+01  1.2840+01  1.3042+01  1.3248+01
```

Fig. A-1 Input data of MCNP for the analysis of the beryllium experiment. (1/3)

```
      1.3456+01  1.3668+01  1.3883+01  1.4102+01  1.4324+01
      1.4550+01  1.4779+01  1.5012+01  1.5248+01  1.5488+01
sp1   0.0        1.5142-07
      2.2732-09  4.2225-09  7.4848-09  1.4264-08  8.3975-08
      1.8398-07  2.2450-07  1.3922-07  1.6817-07  2.9754-07
      3.8068-06  3.0541-06  2.2612-06  6.9372-06  7.2049-06
      8.7622-06  7.8013-06  1.4320-05  1.1820-05  1.6544-05
      1.4791-05  1.7624-05  2.8404-05  2.4899-05  3.7633-05
      4.4237-05  4.6320-05  6.1572-05  3.7185-05  5.3362-05
      4.4831-05  5.0292-05  5.7202-05  6.9230-05  8.0602-05
      8.3190-05  9.7450-05  1.0531-04  1.2632-04  1.4874-04
      1.7906-04  3.7225-04  4.9933-04  5.3824-04  6.0762-04
      7.0593-04  8.0965-04  9.5392-04  1.0785-03  1.2232-03
      1.3867-03  1.5803-03  1.6473-03  1.8238-03  2.0605-03
      2.2042-03  2.3040-03  2.5211-03  2.5709-03  2.5872-03
      2.5765-03  2.7699-03  2.8528-03  2.5945-03  1.3898-03
      1.4298-03  1.3270-03  1.3489-03  1.3820-03  1.4312-03
      1.3760-03  1.4329-03  1.4558-03  1.3518-03  1.4053-03
      1.2861-03  1.2741-03  1.1711-03  1.1937-03  1.0563-03
      1.0018-03  8.8451-04  7.9827-04  7.9293-04  7.5872-04
      6.9228-04  6.2956-04  5.1710-04  5.0750-04  5.1007-04
      4.1280-04  3.5649-04  9.0768-05  8.2287-05  9.2862-05
      9.1407-05  9.3708-05  7.9567-05  8.8737-05  8.7841-05
      1.1227-04  1.6798-04  1.5985-04  1.6563-04  2.1025-04
      4.1363-04  7.4899-04  7.8183-04  5.1771-04  4.5938-04
      4.6458-04  9.1020-04  2.6083-03  9.5007-04  5.1474-03
      3.0897-02  2.3565-01  4.0901-01  2.2296-01  1.4419-01
c     ***********************************************
c     *  material specification cards                *
c     ***********************************************
c      --- Beryllium
m1     4009.41c  1.2152-1    6012.41c  7.7109-5
       8016.37c  4.9813-4   13027.41c  2.9013-4
      26000.41c  2.4678-5
mt1   be.01t
c      --- air
m2     7014.37c  3.8810-5    8016.37c  1.0400-5
c      --- Dosimetry Reactions
m3     3006.03y  1
m4     3007.03y  1
m5     5010.03y  1
m6    16032.03y  1
m7    48000.37c  1
c     ***********************************************
c     *  tally specification cards                   *
c     ***********************************************
fc02 ---- neutron energy spectrum  (125g) surface r=2cm
f02:n  2 3 5 6 8 9 11 13
fq02   s  m  e  f
fs02   -31
fm02   (1)       (1 3 105)  (1 3 207)  (1 4 205)  (1 5 107)
       (1 6 103) ((1 5 107) (1 -1 7 -0.864))
e02    1.0010-11  3.2241-07
       5.3156-07  8.7640-07  1.4449-06  2.3823-06  3.9278-06
       6.4758-06  1.0677-05  1.7603-05  2.9023-05  4.7850-05
       7.8891-05  1.3007-04  2.1445-04  3.5357-04  5.8293-04
       9.6110-04  1.2341-03  1.5846-03  2.0346-03  2.6125-03
       3.3546-03  4.3073-03  5.5307-03  7.1016-03  9.1186-03
       1.1709-02  1.5034-02  1.9304-02  2.1874-02  2.4787-02
       2.8087-02  3.1827-02  3.6065-02  4.0867-02  4.6308-02
       5.2474-02  5.9461-02  6.7378-02  7.6349-02  8.6515-02
       9.8035-02  1.1109-01  1.2588-01  1.4264-01  1.6163-01
       1.8315-01  2.0754-01  2.3517-01  2.6649-01  3.0197-01
       3.4217-01  3.8774-01  4.3936-01  4.9786-01  5.6415-01
       6.3927-01  7.2438-01  8.2084-01  9.3013-01  1.0540+00
       1.1943+00  1.3533+00  1.5335+00  1.7377+00  1.8498+00
       1.9691+00  2.0961+00  2.2313+00  2.3752+00  2.5284+00
       2.6914+00  2.8650+00  3.0498+00  3.2465+00  3.4559+00
       3.6787+00  3.9160+00  4.1686+00  4.4374+00  4.7236+00
       5.0282+00  5.3525+00  5.6978+00  6.0652+00  6.4564+00
       6.8728+00  7.3161+00  7.7879+00  8.2902+00  8.8249+00
       9.3940+00  9.9999+00  1.0157+01  1.0317+01  1.0480+01
       1.0645+01  1.0812+01  1.0983+01  1.1156+01  1.1331+01
       1.1510+01  1.1691+01  1.1875+01  1.2062+01  1.2252+01
       1.2445+01  1.2641+01  1.2840+01  1.3042+01  1.3248+01
       1.3456+01  1.3668+01  1.3883+01  1.4102+01  1.4324+01
       1.4550+01  1.4779+01  1.5012+01  1.5248+01  1.5488+01
fc12 ---- neutron reaction rate surface r=2cm
f12:n  2 3 5 6 8 9 11 13
```

Fig. A-1 Continued. (2/3)

```
fq12  s  e  f  m
fm12  (1)       (1 3 105)  (1 3 207)  (1 4 205)  (1 5 107)
      (1 6 103) ((1 5 107) (1 -1 7 -0.864))
fs12  -31
fc32 ---- neutron decade spectrum  surface r=2cm
f32:n  2 3 5 6 8 9 11 13
fq32  s  m  e  f
fs32  -31
fm32  (1)       (1 3 105)  (1 3 207)  (1 4 205)  (1 5 107)
      (1 6 103) ((1 5 107) (1 -1 7 -0.864))
e32   1e-7 1e-6 1e-5 1e-4 1e-3 1e-2 1e-1 1e+0 1e+1 1e+2
c    *************************
c    * problem cutoff cards  *
c    *************************
phys:n 16.0  0.0
mode   n
cut:n  0  0
nps    1500000
ctme   1000000
c    *************************
c    * peripheral cards      *
c    *************************
prdmp   10000000 100000  1  1
lost    10       10
print
```

Fig. A-1 Continued. (3/3)

```
Analysis of Vanadium Experiment
c    ********************************************
c    * cell carad   for Vanadium Assembly       *
c    ********************************************
 1    3  4.921e-5  +25 -26 +27 -28 +1 -4 #(+2 -4 -29) $ source region
                                    imp:n=1 imp:p=1
 2    3  4.921e-5  +2 -3 -29                         $ cell detector
                                    imp:n=1 imp:p=1
 3    3  4.921e-5  +3 -4 -29                         $ cell detector
                                    imp:n=1 imp:p=1
 4    1  -6.033    +5 -6 -29                         $ cell detector
                                    imp:n=2 imp:p=2
 5    1  -6.033    +8 -9 -29                         $ cell detector
                                    imp:n=4 imp:p=4
 6    1  -6.033    +21 -22 +23 -24 +4 -7 #4          $ vanadium
                                    imp:n=2 imp:p=2
 7    1  -6.033    +21 -22 +23 -24 +7 -10 #5         $ vanadium
                                    imp:n=4 imp:p=4
 8    2  -1.625    +25 -26 +27 -28 +4 -7  #(+21 -22 +23 -24 +4 -7)
                                    imp:n=1 imp:p=1   $ graphite
 9    2  -1.625    +25 -26 +27 -28 +7 -11 #(+21 -22 +23 -24 +7 -10)
                                    imp:n=2 imp:p=2   $ graphite
10    0            -25 : +26 : -27 : +28 : -1 : +11   $ external region
                                    imp:n=0 imp:p=0

c    ********************************************
c    * surface card                             *
c    ********************************************
 1    pz     -21.00 $  source region
 2    pz      -2.00 $  cell detector in front of vanadium
 3    pz      -0.10 $  cell detector in front of vanadium
 4    pz       0.00 $  front surface of vanadium
 5    pz       7.37 $  cell detector in vanadium #1
 6    pz       7.87 $  cell detector in vanadium #1
 7    pz      10.00 $  boundary to change cell importance
 8    pz      17.53 $  cell detector in vanadium #2
 9    pz      18.03 $  cell detector in vanadium #2
10    pz      25.40 $  rear surface of vanadium
11    pz      30.48 $  rear surface of graphite
c
21    px     -12.70 $  side surface of vanadium
```

Fig. A-2 Input data of MCNP for the analysis of the vanadium experiment. (1/3)

```
22    px      +12.70 $  side surface of vanadium
23    py      -12.70 $  side surface of vanadium
24    py      +12.70 $  side surface of vanadium
25    px      -17.78 $  side surface of graphite
26    px      +17.78 $  side surface of graphite
27    py      -17.78 $  side surface of graphite
28    py      +17.78 $  side surface of graphite
29    cz        1.00 $  side surface of detector

c     ********************************************
c     * mode card                                *
c     ********************************************
mode   n p
c     ********************************************
c     * source specification cards               *
c     * a user supplied source subroutine is used. *
c     ********************************************
c     * material specification cards             *
c     ********************************************
c      --- vanadium
m1     23051.41c -0.99777
       13027.41c -0.00073
       14000.41c -0.00108
       26000.41c -0.00042
c      --- graphite
m2      6012.37c  1.0
c      --- air
m3      7014.37c -23.1
        8016.37c -75.6
       18040.37c  -1.3
c      --- materials for reaction rate
m11     5010.03y   1      $  B-10(n,alpha)
m12    13027.03y   1      $  Al-27(n,alpha)
m13    41093.03y   1      $  Nb-93(n,2n)Nb-92m
m14    49115.03y   1      $  In-115(n,n')In-115m
m15    79197.03y   1      $  Au-197(n,gamma)
m16    92235.03y   1      $  U-235(n,fission)
c     ********************************************
c     *  tally specification cards               *
c     ********************************************
fq0    s  m  e  f
c
fc04 ---- reaction rate ---
f04:n  (2 3) 3 4 5
fm04   (1)          (1 11 107)  (1 12 107)  (1 13  16)
       (1 14  51)   (1 15 102)  (1 16  18)
fq04     s  e  f  m
c
fc14 ---- neutron spectrum in 125 groups ---
f14:n  (2 3) 3 4 5
e14    1.0010-11  3.2241-07
       5.3156-07  8.7640-07  1.4449-06  2.3823-06  3.9278-06
       6.4758-06  1.0677-05  1.7603-05  2.9023-05  4.7850-05
       7.8891-05  1.3007-04  2.1445-04  3.5357-04  5.8293-04
       9.6110-04  1.2341-03  1.5846-03  2.0346-03  2.6125-03
       3.3546-03  4.3073-03  5.5307-03  7.1016-03  9.1186-03
       1.1709-02  1.5034-02  1.9304-02  2.1874-02  2.4787-02
       2.8087-02  3.1827-02  3.6065-02  4.0867-02  4.6308-02
       5.2474-02  5.9461-02  6.7378-02  7.6349-02  8.6515-02
       9.8035-02  1.1109-01  1.2588-01  1.4264-01  1.6163-01
       1.8315-01  2.0754-01  2.3517-01  2.6649-01  3.0197-01
       3.4217-01  3.8774-01  4.3936-01  4.9786-01  5.6415-01
       6.3927-01  7.2438-01  8.2084-01  9.3013-01  1.0540+00
       1.1943+00  1.3533+00  1.5335+00  1.7377+00  1.8498+00
       1.9691+00  2.0961+00  2.2313+00  2.3752+00  2.5284+00
       2.6914+00  2.8650+00  3.0498+00  3.2465+00  3.4559+00
       3.6787+00  3.9160+00  4.1686+00  4.4374+00  4.7236+00
       5.0282+00  5.3525+00  5.6978+00  6.0652+00  6.4564+00
       6.8728+00  7.3161+00  7.7879+00  8.2902+00  8.8249+00
       9.3940+00  9.9999+00  1.0157+01  1.0317+01  1.0480+01
       1.0645+01  1.0812+01  1.0983+01  1.1156+01  1.1331+01
       1.1510+01  1.1691+01  1.1875+01  1.2062+01  1.2252+01
       1.2445+01  1.2641+01  1.2840+01  1.3042+01  1.3248+01
       1.3456+01  1.3668+01  1.3883+01  1.4102+01  1.4324+01
       1.4550+01  1.4779+01  1.5012+01  1.5248+01  1.5488+01
c
fc24 ---- neutron spectrum in 175 groups ---
f24:n  (2 3) 3 4 5
e24    1.00001-11 1.00001e-7 4.13994e-7 5.31578e-7 6.82560e-7 8.76425e-7
```

Fig. A-2 Continued. (2/3)

```
      1.12535e-6 1.44498e-6 1.85539e-6 2.38237e-6 3.05902e-6 3.92786e-6
      5.04348e-6 6.47595e-6 8.31529e-6 1.06770e-5 1.37096e-5 1.76035e-5
      2.26033e-5 2.90232e-5 3.72665e-5 4.78512e-5 6.14421e-5 7.88932e-5
      1.01301e-4 1.30073e-4 1.67017e-4 2.14454e-4 2.75364e-4 3.53575e-4
      4.53999e-4 5.82947e-4 7.48518e-4 9.61116e-4 1.23410e-3 1.58461e-3
      2.03468e-3 2.24867e-3 2.48517e-3 2.61259e-3 2.74654e-3 3.03539e-3
      3.35463e-3 3.70744e-3 4.30742e-3 5.53084e-3 7.10174e-3 9.11882e-3
      1.05946e-2 1.17088e-2 1.50344e-2 1.93045e-2 2.18749e-2 2.35786e-2
      2.41755e-2 2.47875e-2 2.60584e-2 2.70001e-2 2.85011e-2 3.18278e-2
      3.43067e-2 4.08677e-2 4.63092e-2 5.24752e-2 5.65622e-2 6.73794e-2
      7.19981e-2 7.94987e-2 8.25034e-2 8.65169e-2 9.80366e-2 1.11090e-1
      1.16786e-1 1.22773e-1 1.29068e-1 1.35686e-1 1.42642e-1 1.49956e-1
      1.57644e-1 1.65727e-1 1.74224e-1 1.83156e-1 1.92547e-1 2.02419e-1
      2.12797e-1 2.23708e-1 2.35177e-1 2.47235e-1 2.73237e-1 2.87247e-1
      2.94518e-1 2.97211e-1 2.98491e-1 3.01974e-1 3.33733e-1 3.68832e-1
      3.87742e-1 4.07622e-1 4.50492e-1 4.97871e-1 5.23397e-1 5.50232e-1
      5.78444e-1 6.08101e-1 6.39279e-1 6.72055e-1 7.06512e-1 7.42736e-1
      7.80817e-1 8.20850e-1 8.62936e-1 9.07180e-1 9.61640e-1 1.00259e+0
      1.10803e+0 1.16484e+0 1.22456e+0 1.28735e+0 1.35335e+0 1.42274e+0
      1.49569e+0 1.57237e+0 1.65299e+0 1.73774e+0 1.82684e+0 1.92050e+0
      2.01897e+0 2.12248e+0 2.23130e+0 2.30686e+0 2.34570e+0 2.36525e+0
      2.38521e+0 2.46597e+0 2.59240e+0 2.72532e+0 2.86505e+0 3.01194e+0
      3.16637e+0 3.32871e+0 3.67879e+0 4.06570e+0 4.49329e+0 4.72367e+0
      4.96585e+0 5.22046e+0 5.48812e+0 5.76950e+0 6.06531e+0 6.37628e+0
      6.59238e+0 6.70320e+0 7.04688e+0 7.40818e+0 7.78801e+0 8.18731e+0
      8.60708e+0 9.04837e+0 9.51229e+0 1.00000e+1 1.05127e+1 1.10517e+1
      1.16183E+1 1.22140E+1 1.25232E+1 1.28400E+1 1.34986E+1 1.38403E+1
      1.41907E+1 1.45499E+1 1.49183E+1 1.56831E+1 1.64872E+1 1.69046E+1
      1.73325E+1 1.96403E+1
c
fc34 ---- neutron spectrum in each decade ---
f34:n  (2 3) 3 4 5
e34   1e-7 1e-6 1e-5 1e-4 1e-3 1e-2 1e-1 1 2 5 10 20
fm34  (1)          (1 11 107)  (1 12 107)  (1 13  16)
      (1 14  51)   (1 15 102)  (1 16  18)
c
fc114 ---- gamma-ray spectrum in 40 groups ---
f114:p  (2 3) 3 4 5
e114  1.0000-02  2.0000-02  3.0000-02  4.5000-02  6.0000-02
      8.0000-02  1.0000-01  1.5000-01  2.0000-01  3.0000-01
      4.0000-01  5.0000-01  5.2000-01  6.0000-01  7.0000-01
      8.0000-01  9.0000-01  1.0000+00  1.1300+00  1.2500+00
      1.3800+00  1.5000+00  1.7500+00  2.0000+00  2.2500+00
      2.5000+00  3.0000+00  3.5000+00  4.0000+00  4.5000+00
      5.0000+00  5.5000+00  6.0000+00  6.5000+00  7.0000+00
      7.5000+00  8.0000+00  9.0000+00  1.0000+01  1.2000+01
      1.4000+01
c
fc124 ---- gamma-ray spectrum in 42 groups ---
f124:p  (2 3) 3 4 5
e124  1.000e-03  1.000e-02  2.000e-02  3.000e-02  4.500e-02
      6.000e-02  7.000e-02  7.500e-02  1.000e-01  1.500e-01
      2.000e-01  3.000e-01  4.000e-01  4.500e-01  5.100e-01
      5.120e-01  6.000e-01  7.000e-01  8.000e-01  1.000e+00
      1.330e+00  1.340e+00  1.500e+00  1.660e+00  2.000e+00
      2.500e+00  3.000e+00  3.500e+00  4.000e+00  4.500e+00
      5.000e+00  5.500e+00  6.000e+00  6.500e+00  7.000e+00
      7.500e+00  8.000e+00  1.000e+01  1.200e+01  1.400e+01
      2.000e+01  3.000e+01  5.000e+01
c
c    ***********************************************
c    * energy crads                                *
c    ***********************************************
phys:n   16.0    0
phys:p   30.0    1   0
phys:e   30.0    1   1   1   1   0   0   0   0
c    ***********************************************
c    * peripheral crads                            *
c    ***********************************************
idum    1
rdum    0 0 -20
prdmp   1000000000  100000000   0  1
lost    10          10
print
c    ***********************************************
c    * problem cutoff cards                        *
c    ***********************************************
nps     1000000000
ctme    1000000
```

Fig. A-2 Continued. (3/3)

```
Analysis of Iron Experiment
c    ****************************************
c    * cell carad   for Iron Assembly        *
c    ****************************************
c    *****  air region  *****
 1    2 4.9210-5 (+1  -2  -42) : (+2  -3  +41  -42)       $   source void
 3    2 4.9210-5  +2  -3  -41       $   cell detecter
c    *****  test region  *****
 4    1 8.5182-2  +3  -4  -42       $    0.0 -  1.5 cm
 5    1 8.5182-2  +4  -5  -42       $    1.5 -  2.5 cm
 6    1 8.5182-2  +5  -6  -42       $    2.5 -  4.0 cm
 7    1 8.5182-2  +6  -7  -42       $    4.0 -  5.0 cm
 8    1 8.5182-2  +7  -8  -42       $    5.0 -  6.5 cm
 9    1 8.5182-2  +8  -9  -42       $    6.5 - 10.0 cm
10    1 8.5182-2  +9  -10 -42       $   10.0 - 11.0 cm
11    1 8.5182-2  +10 -11 -42       $   11.0 - 11.5 cm
12    1 8.5182-2  +11 -12 -42       $   11.5 - 20.0 cm
13    1 8.5182-2  +12 -13 -42       $   20.0 - 21.0 cm
14    1 8.5182-2  +13 -14 -42       $   21.0 - 21.5 cm
15    1 8.5182-2  +14 -15 -42       $   21.5 - 30.0 cm
16    1 8.5182-2  +15 -16 -42       $   30.0 - 31.0 cm
17    1 8.5182-2  +16 -17 -42       $   31.0 - 31.5 cm
18    1 8.5182-2  +17 -18 -42       $   31.5 - 40.0 cm
19    1 8.5182-2  +18 -19 -42       $   40.0 - 41.0 cm
20    1 8.5182-2  +19 -20 -42       $   41.0 - 41.5 cm
21    1 8.5182-2  +20 -21 -42       $   41.5 - 50.0 cm
22    1 8.5182-2  +21 -22 -42       $   50.0 - 51.5 cm
23    1 8.5182-2  +22 -23 -42       $   51.5 - 60.0 cm
24    1 8.5182-2  +23 -24 -42       $   60.0 - 61.0 cm
25    1 8.5182-2  +24 -25 -42       $   61.0 - 70.0 cm
26    1 8.5182-2  +25 -26 -42       $   70.0 - 71.5 cm
27    1 8.5182-2  +26 -27 -42       $   71.5 - 80.0 cm
28    1 8.5182-2  +27 -28 -42       $   80.0 - 81.0 cm
29    1 8.5182-2  +28 -29 -42       $   81.0 - 90.0 cm
30    1 8.5182-2  +29 -30 -42       $   90.0 - 91.5 cm
31    1 8.5182-2  +30 -31 -42       $   91.5 - 95.0 cm
c    *****  rear air region  *****
32    2 4.9210-5  +31 -32 -41       $  cell detecter
33    2 4.9210-5  +31 -32 +41 -42   $
c    *****  external void  *****
34    0          -1 : +32 : +42     $
c    ------ blank delimeter

c    ************************************
c    * surface card  *
c    ************************************
 1            pz          -21.0   $  Source
 2            pz           -2.0   $  keV
 3            pz            0.0   $  foil, TLD
 4            pz            1.5   $  MeV,  NE-g
 5            pz            2.5   $  foil, TLD
 6            pz            4.0   $  MeV
 7            pz            5.0   $  foil
 8            pz            6.5   $  MeV,  NE-g
 9            pz           10.0   $  foil, TLD, g-spec
10            pz           11.0   $  keV, eV
11            pz           11.5   $  MeV,  NE-g
12            pz           20.0   $  foil, TLD
13            pz           21.0   $  keV, eV
14            pz           21.5   $  MeV,  NE-g
15            pz           30.0   $  foil, TLD, g-spec
16            pz           31.0   $  keV, eV
17            pz           31.5   $  MeV,  NE-g
18            pz           40.0   $  foil, TLD
19            pz           41.0   $  keV, eV
20            pz           41.5   $  MeV,  NE-g
21            pz           50.0   $  foil, TLD, g-spec
22            pz           51.5   $  MeV
23            pz           60.0   $  TLD
24            pz           61.0   $  keV, eV
25            pz           70.0   $  foil, TLD, g-spec
26            pz           71.5   $  MeV,  NE-g
27            pz           80.0   $  TLD
28            pz           81.0   $  keV, eV
29            pz           90.0   $  TLD
30            pz           91.5   $  NE-g
31            pz           95.0   $  TLD
32            pz           97.0   $  keV
c
```

Fig. A-3 Input data of MCNP for the analysis of the iron experiment. (1/4)

```
41              cz              4.0
42              cz             50.0
43              cz             10.0
c      ------- blank delimeter

c     ************************************
c     *  mode card                       *
c     ************************************
mode   n p
c     ************************************
c     *  weight window cards             *
c     ************************************
ext:n   0      0      0.1z  0.1z  0.1z  0.1z  0.1z  0.1z  0.1z  0.1z
        0.1z   0.1z   0.1z  0.1z  0.1z  0.1z  0.1z  0.1z  0.1z  0.1z
        0.1z   0.1z   0.1z  0.1z  0.1z  0.1z  0.1z  0.1z  0.1z  0.1z
        0      0      0
wwe:n   1.0e-3  1.0  5.0  10.0  16.0
wwp:n   5  3  5  0  0
wwn1:n  $  for eV neutrons
        1.0e-1  1.0e-1  1.0e-1  1.0e-1
        5.0e-2  2.0e-2  1.0e-2  0.7e-2  0.5e-2
        0.3e-2  0.2e-2  1.0e-3  1.0e-3  1.0e-3
        1.0e-3  1.0e-3  1.0e-3  1.0e-3  1.0e-3
        1.0e-3  1.0e-3  1.0e-3  7.0e-4  5.0e-4
        3.0e-4  2.0e-4  1.0e-4  1.0e-4  1.0e-4
        1.0e-4  1.0e-4  1.0e-4 -1
wwn2:n  $  for keV neutrons
        1.0e-1  1.0e-1  1.0e-1  1.0e-1
        5.0e-2  3.0e-2  2.0e-2  1.4e-2  1.0e-2
        1.0e-2  1.0e-2  1.0e-2  1.0e-2  1.0e-2
        1.0e-2  1.0e-2  1.0e-2  1.0e-2  1.0e-2
        1.0e-2  1.0e-2  1.0e-2  7.0e-3  5.0e-3
        3.0e-3  2.0e-3  1.0e-3  1.0e-3  1.0e-3
        1.0e-3  1.0e-3  1.0e-3 -1
wwn3:n  $  for 1-5MeV neutrons
        1.0e-1  1.0e-1  1.0e-1  1.0e-1
        5.0e-2  5.0e-2  5.0e-2  2.0e-2  2.0e-2
        2.0e-2  1.0e-2  5.0e-3  5.0e-3  3.0e-3
        2.0e-3  2.0e-3  1.0e-3  5.0e-4  5.0e-4
        2.0e-4  1.0e-4  5.0e-5  2.0e-5  1.0e-5
        5.0e-6  2.0e-6  1.0e-6  1.0e-6  1.0e-6
        1.0e-6  1.0e-6  1.0e-6 -1
wwn4:n  $  for 5-13 MeV Neutrons
        1.0e-1  1.0e-1  1.0e-1  1.0e-1
        5.0e-2  5.0e-2  5.0e-2  1.5e-2  1.5e-2
        1.5e-2  5.0e-3  1.5e-3  1.5e-3  6.4e-4
        3.2e-4  3.2e-4  1.6e-4  8.0e-5  8.0e-5
        4.0e-5  2.0e-5  1.0e-5  5.0e-6  2.5e-6
        1.2e-6  6.0e-7  3.0e-7  3.0e-7  3.0e-7
        3.0e-7  3.0e-7  3.0e-7 -1
wwn5:n  $  for 14 MeV Neutrons
        1.0e-1  1.0e-1  1.0e-1  8.5e-2
        7.0e-2  5.0e-2  4.0e-2  3.0e-2  2.0e-2
        1.0e-2  5.0e-3  1.5e-3  1.5e-3  5.0e-4
        1.5e-4  1.5e-4  5.0e-5  1.5e-5  1.5e-5
        6.4e-6  3.2e-6  1.6e-6  8.0e-7  4.0e-7
        2.0e-7  1.0e-7  5.0e-8  5.0e-8  5.0e-8
        5.0e-8  5.0e-8  5.0e-8 -1
wwe:p   100.0
wwp:p   5  3  5  0  0
wwn1:p  $  for gamma-rays
        1.0e-1  1.0e-1  1.0e-1  1.0e-1
        5.0e-2  5.0e-2  5.0e-2  2.0e-2  2.0e-2
        2.0e-2  1.0e-2  7.0e-3  7.0e-3  5.0e-3
        3.0e-3  3.0e-3  2.0e-3  1.4e-3  1.4e-3
        1.0e-3  7.0e-4  5.0e-4  3.0e-4  2.0e-4
        1.0e-4  7.0e-5  5.0e-5  5.0e-5  5.0e-5
        5.0e-5  5.0e-5  5.0e-5 -1
c     ***********************************************
c     *  source specification cards                 *
c     *  a user supplied source subroutine is used. *
c     ***********************************************
c     *  material specification cards               *
c     ***********************************************
c      --- Iron
m1     26000.41c 0.083490        12000.34c  0.000727
       14000.41c 0.000249        25055.41c  0.000716
c      --- air
m2     7014.34c 3.8810-5         8016.34c  1.0400-5
```

Fig. A-3 Continued. (2/4)

```
c     --- materials for reaction rate
m3     5010.03y   1.0  $  B-10(n,alpha)
m4    13027.03y   1.0  $  Al-27(n,alpha)
m5    22000.03y   1.0  $  Ti-nat((n,x)Sc-48
m6    25055.34c   1.0  $  Mn-55(n,gamma)
m7    26056.03y   1.0  $  Fe-56(n,p)
m8    28058.03y   1.0  $  Ni-58(n,2n)       &  Ni-58(n,p)
m9    30064.03y   1.0  $  Zn-64(n,p)
m10   40090.03y   1.0  $  Zr-90(n,2n)
m11   41093.03y   1.0  $  Nb-93(n,2n)Nb-92m
m12   49115.03y   1.0  $  In-115(n,n')In-115m
m13   79197.03y   1.0  $  Au-197(n,gamma)
m14   92235.03y   1.0  $  U-235(n,fission)
c    ********************************************
c    *  tally specification cards                *
c    ********************************************
fc02 ---- neutron reaction rate       surface r=4cm
f02:n  3  4  5  6  7  8  9 10 11 12
      13 14 15 16 17 18 19 20 21 22
      23 24 25 26 27 28 29 30 31
fs02  -41
fq02  s  e  f  m
e02   16.0
fm02  (1)          (1  1   1)  (1  1   2)  (1  1 102)
      (1  3 107)   (1  3 207)  (1  4 107)  (1  5 212)  (1  6 102)
      (1  7 103)   (1  8  16)  (1  8 103)  (1  9 103)  (1 10  16)
      (1 11  16)   (1 12  51)  (1 13 102)  (1 14  18)
fc12 ---- neutron energy spectrum (decade)    surface r=4cm
f12:n  3  4  5  6  7  8  9 10 11 12
      13 14 15 16 17 18 19 20 21 22
      23 24 25 26 27 28 29 30 31
fq12  s  f  e
fs12  -41
e12   1e-7 1e-6 1e-5 1e-4 1e-3 1e-2 1e-1 1e+0 1e+1 2e+1
fc24 ---- neutron energy spectrum (decade)    cell
f24:n  3 32
e24   1e-7 1e-6 1e-5 1e-4 1e-3 1e-2 1e-1 1e+0 1e+1 2e+1
fc32 ---- neutron energy spectrum     surface r=4cm
f32:n  3  4  5  6  7  8  9 10 11 12
      13 14 15 16 17 18 19 20 21 22
      23 24 25 26 27 28 29 30 31
fs32  -41
fc44 ---- neutron energy spectrum     cell
f44:n 3 32
fc62 ---- neutron energy reaction rate       surface r=10cm
f62:n 10 13 16 19 24 28
fs62  -43
fm62  (1)  (1 1   1)  (1 1   2)  (1 1 102)
fc102 ---- gamma-ray energy spectrum     surface r=4cm
f102:p 3  4  5  6  7  8  9 10 11 12
      13 14 15 16 17 18 19 20 21 22
      23 24 25 26 27 28 29 30 31
fs102 -41
fu102 1  2  3  4  5 6 7
fq102 s  u  m  e  f
e102  1.0000-02  2.0000-02  3.0000-02  4.5000-02  6.0000-02
      8.0000-02  1.0000-01  1.5000-01  2.0000-01  3.0000-01
      4.0000-01  5.0000-01  5.2000-01  6.0000-01  7.0000-01
      8.0000-01  9.0000-01  1.0000+00  1.1300+00  1.2500+00
      1.3800+00  1.5000+00  1.7500+00  2.0000+00  2.2500+00
      2.5000+00  3.0000+00  3.5000+00  4.0000+00  4.5000+00
      5.0000+00  5.5000+00  6.0000+00  6.5000+00  7.0000+00
      7.5000+00  8.0000+00  9.0000+00  1.0000+01  1.2000+01
      1.4000+01
c     ------------------------------------------------------------
fq0   s  m  e  f
e0    1.0010-11  3.2241-07
      5.3156-07  8.7640-07  1.4449-06  2.3823-06  3.9278-06
      6.4758-06  1.0677-05  1.7603-05  2.9023-05  4.7850-05
      7.8891-05  1.3007-04  2.1445-04  3.5357-04  5.8293-04
      9.6110-04  1.2341-03  1.5846-03  2.0346-03  2.6125-03
      3.3546-03  4.3073-03  5.5307-03  7.1016-03  9.1186-03
      1.1709-02  1.5034-02  1.9304-02  2.1874-02  2.4787-02
      2.8087-02  3.1827-02  3.6065-02  4.0867-02  4.6308-02
      5.2474-02  5.9461-02  6.7378-02  7.6349-02  8.6515-02
      9.8035-02  1.1109-01  1.2588-01  1.4264-01  1.6163-01
      1.8315-01  2.0754-01  2.3517-01  2.6649-01  3.0197-01
      3.4217-01  3.8774-01  4.3936-01  4.9786-01  5.6415-01
      6.3927-01  7.2438-01  8.2084-01  9.3013-01  1.0540+00
```

Fig. A-3 Continued. (3/4)

```
      1.1943+00  1.3533+00  1.5335+00  1.7377+00  1.8498+00
      1.9691+00  2.0961+00  2.2313+00  2.3752+00  2.5284+00
      2.6914+00  2.8650+00  3.0498+00  3.2465+00  3.4559+00
      3.6787+00  3.9160+00  4.1686+00  4.4374+00  4.7236+00
      5.0282+00  5.3525+00  5.6978+00  6.0652+00  6.4564+00
      6.8728+00  7.3161+00  7.7879+00  8.2902+00  8.8249+00
      9.3940+00  9.9999+00  1.0157+01  1.0317+01  1.0480+01
      1.0645+01  1.0812+01  1.0983+01  1.1156+01  1.1331+01
      1.1510+01  1.1691+01  1.1875+01  1.2062+01  1.2252+01
      1.2445+01  1.2641+01  1.2840+01  1.3042+01  1.3248+01
      1.3456+01  1.3668+01  1.3883+01  1.4102+01  1.4324+01
      1.4550+01  1.4779+01  1.5012+01  1.5248+01  1.5488+01
c     *************************
c     * problem cutoff cards  *
c     *************************
phys:n   16.0  0.0
phys:p   30.0    1   0
phys:e   30.0    1   1   1   1   1   1   1   1
cut:n    0  1.0e-11      -0.5   -0.25   0
cut:p    0  0.0099       -0.5   -0.25   0
nps     1000000
ctme    1000000
c     *************************
c     * peripheral crads      *
c     *************************
idum    7 6 5
rdum    1 2 3 4 5 6 7
prdmp   100000   100000    1  1
lost    10         10
print
```

Fig. A-3 Continued. (4/4)

```
Analysis of Copper Experiment
c     ************************************
c     *   cell card                      *
c     ************************************
 1     2 4.9210-5  1  -2 -22
 2     2 4.9210-5  2  -3 -22
 3     1 8.4627-2  3  -4 -22
 4     1 8.4627-2  4  -5 -22
 5     1 8.4627-2  5  -6 -22
 6     1 8.4627-2  6  -7 -22
 7     1 8.4627-2  7  -8 -22
 8     1 8.4627-2  8  -9 -22
 9     1 8.4627-2  9 -10 -22
10     1 8.4627-2 10 -11 -22
11     1 8.4627-2 11 -12 -22
12     1 8.4627-2 12 -13 -22
13     1 8.4627-2 13 -14 -22
14     1 8.4627-2 14 -15 -22
15     1 8.4627-2 15 -16 -22
16     1 8.4627-2 16 -17 -22
17     1 8.4627-2 17 -18 -22
18     1 8.4627-2 18 -19 -22
19     2 4.9210-5 19 -20 -22
20     0          -1 : 20 : 22

c     ************************************
c     * surface card                     *
c     ************************************
c     ------------------------------< surfaces normal to z-axis >--
 1      pz   -21.00
 2      pz    -1.00      $ n & gamma spectrum
 3      pz     0.00      $ foil & tld
 4      pz     5.77      $ tld
 5      pz     7.605     $ n & gamma spectrum
 6      pz    10.11      $ foil
 7      pz    15.00      $ change cell importance
 8      pz    20.37      $ foil
```

Fig. A-4 Input data of MCNP for the analysis of the copper experiment. (1/3)

```
 9     pz    20.98      $ tld
10     pz    22.815     $ n & gamma spectrum
11     pz    30.00      $ change cell importance
12     pz    35.61      $ foil
13     pz    36.19      $ tld
14     pz    38.025     $ n & gamma spectrum
15     pz    45.00      $ change cell importance
16     pz    50.85      $ foil
17     pz    51.40      $ tld
18     pz    53.235     $ n & gamma spectrum
19     pz    60.84      $ foil & tld
20     pz    61.84      $ n & gamma spectrum
c    ----------------------------< cylinders centered on z-axis >--
21     cz     3.00
22     cz    31.50
c    ******* blank delimiter *******

c    ************************************
c    *  mode card      - neutron & photon *
c    ************************************
mode  n p
wwe:n  1e-4 1e-2 1 5 13 16
wwp:n  5 3 5 0 0
wwe:p  100
wwp:p  5 3 5 0 0
ext:n    0      0      0.1z   0.1z   0.1z   0.1z   0.1z   0.1z
         0.1z   0.1z   0.1z   0.1z   0.1z   0.1z   0.1z   0.1z
         0.1z   0.1z   0      0
wwn1:n 1.0e-3 1.0e-3 1.0e-3 1.0e-3 3.0e-4 1.0e-4 1.0e-4 1.0e-4
       1.0e-4 1.0e-4 1.0e-4 7.0e-5 7.0e-5 5.0e-5 2.0e-5 2.0e-5
       1.0e-5 1.0e-5 1.0e-5     -1
wwn2:n 1.0e-2 1.0e-2 1.0e-2 1.0e-2 3.0e-3 1.0e-3 1.0e-3 1.0e-3
       1.0e-3 1.0e-3 1.0e-3 7.0e-4 7.0e-4 5.0e-4 2.0e-4 2.0e-4
       1.0e-4 1.0e-4 1.0e-4     -1
wwn3:n 1.0e-1 1.0e-1 3.0e-2 2.0e-2 1.0e-2 1.0e-2 1.0e-2 1.0e-2
       1.0e-2 1.0e-2 1.0e-2 7.0e-3 5.0e-3 2.0e-3 1.0e-3 1.0e-3
       5.0e-4 5.0e-4 5.0e-4     -1
wwn4:n 1.0e-1 1.0e-1 4.0e-2 2.0e-2 2.0e-2 1.0e-2 5.0e-3 5.0e-3
       4.0e-3 2.0e-3 1.0e-3 7.0e-4 5.0e-4 2.0e-4 1.0e-4 1.0e-4
       5.0e-5 5.0e-5 5.0e-5     -1
wwn5:n 1.0e-1 1.0e-1 4.0e-2 2.0e-2 2.0e-2 1.0e-2 5.0e-3 5.0e-3
       2.0e-3 5.0e-4 2.0e-4 2.0e-4 1.0e-4 5.0e-5 2.0e-5 2.0e-5
       1.0e-5 1.0e-5 1.0e-5     -1
wwn6:n 1.0e-1 1.0e-1 4.0e-2 2.0e-2 1.0e-2 3.0e-3 1.0e-3 1.0e-3
       7.0e-4 2.0e-4 5.0e-5 4.0e-5 2.0e-5 5.0e-6 2.0e-6 2.0e-6
       1.0e-6 1.0e-6 1.0e-6     -1
wwn1:p 1.0e-1 1.0e-1 4.0e-2 2.0e-2 2.0e-2 1.0e-2 5.0e-3 5.0e-3
       4.0e-3 2.0e-3 1.0e-3 1.0e-3 1.0e-3 7.0e-4 5.0e-4 5.0e-4
       3.0e-4  3.0e-4  3.0e-4      -1
c    ************************************************
c    *  source specificatio cards                   *
c    ************************************************
c     ******************************************
c     *  material specification cards           *
c     ******************************************
c     --------------------------------< copper >--
m1    29000.41c  1
c     --------------------------------< air >--
m2     7014.37c  3.8810-5   8016.37c  1.0400-5
c     --------------------------------< materials for reaction rate>--
m3     5010.03y  1.0    $ B-10      (n,a)
m4    13027.03y  1.0    $ Al-27     (n,a)
m5    22000.03y  1.0    $ Ti-0      (n,x)Sc-46  (n,x)Sc-47  (n,x)Sc-48
m6    25055.03y  1.0    $ Mn-55     (n,g)
m7    26054.03y  1.0    $ Fe-54     (n,p)
m8    26056.03y  1.0    $ Fe-56     (n,p)
m9    27059.37c  1.0    $ Co-59     (n,2n)  (n,g)  (n,a)  (n,p)
m10   28058.03y  1.0    $ Ni-58     (n,2n)  (n,p)
m11   29063.41c  1.0    $ Cu-63     (n,2n)  (n,g)   (n,a)
m12   29065.41c  1.0    $ Cu-65     (n,2n)  (n,g)
m13   30064.03y  1.0    $ Zn-64     (n,p)
m14   40090.03y  1.0    $ Zr-90     (n,2n)
m15   41093.03y  1.0    $ Nb-93     (n,2n)Nb-92m
m16   49115.03y  1.0    $ In-115    (n,n')In-115m
m17   79197.03y  1.0    $ Au-197    (n,g)
m18   92235.03y  1.0    $ U-235     (n,f)
c    ******************************************
c    *  tally specification cards               *
c    ******************************************
```

Fig. A-4 Continued. (2/3)

```
fc2   --  neutron spectrum          surface  ----------------------------
f2:n    2    3    4    5    6    7    8    9   10   11
       12   13   14   15   16   17   18   19   20
fs2   -21
fc12  --  neutron reaction rate    surface  ----------------------------
f12:n   2    3    4    5    6    7    8    9   10   11
       12   13   14   15   16   17   18   19   20
fm12  (1   1 102)   (1   3 107)   (1   4 107)   (1   5 210)   (1   5 211)
      (1   5 212)   (1   6 102)   (1   7 103)   (1   8 103)   (1   9  16)
      (1   9 102)   (1   9 103)   (1   9 107)   (1 10  16)   (1 10 103)
      (1 11  16)   (1 11 102)   (1 11 107)   (1 12  16)   (1 12 102)
      (1 13 103)   (1 14  16)   (1 15  16)   (1 16  51)   (1 17 102)
      (1 18  18)
fs12  -21
e12   20
fq12    s  e  f  m
fc22  --  neutron decade spectrum         surface  ----------------------------
f22:n   2    3    4    5    6    7    8    9   10   11
       12   13   14   15   16   17   18   19   20
fs22  -21
e22   1e-7 1e-6 1e-5 1e-4 1e-3 1e-2 1e-1 1e+0 1e+1 1e+2
fc32  --  gamma-ray spectrum       surface  ----------------------------
f32:p   2    3    4    5    6    7    8    9   10   11
       12   13   14   15   16   17   18   19   20
fs32  -21
e32   1.0000-02  2.0000-02  3.0000-02  4.5000-02  6.0000-02
      8.0000-02  1.0000-01  1.5000-01  2.0000-01  3.0000-01
      4.0000-01  5.0000-01  5.2000-01  6.0000-01  7.0000-01
      8.0000-01  9.0000-01  1.0000+00  1.1300+00  1.2500+00
      1.3800+00  1.5000+00  1.7500+00  2.0000+00  2.2500+00
      2.5000+00  3.0000+00  3.5000+00  4.0000+00  4.5000+00
      5.0000+00  5.5000+00  6.0000+00  6.5000+00  7.0000+00
      7.5000+00  8.0000+00  9.0000+00  1.0000+01  1.2000+01
      1.4000+01
c     ---------------------------------------------------------------------
fq0     s  m  e  f
e0    1.0010-11  3.2241-07
      5.3156-07  8.7640-07  1.4449-06  2.3823-06  3.9278-06
      6.4758-06  1.0677-05  1.7603-05  2.9023-05  4.7850-05
      7.8891-05  1.3007-04  2.1445-04  3.5357-04  5.8293-04
      9.6110-04  1.2341-03  1.5846-03  2.0346-03  2.6125-03
      3.3546-03  4.3073-03  5.5307-03  7.1016-03  9.1186-03
      1.1709-02  1.5034-02  1.9304-02  2.1874-02  2.4787-02
      2.8087-02  3.1827-02  3.6065-02  4.0867-02  4.6308-02
      5.2474-02  5.9461-02  6.7378-02  7.6349-02  8.6515-02
      9.8035-02  1.1109-01  1.2588-01  1.4264-01  1.6163-01
      1.8315-01  2.0754-01  2.3517-01  2.6649-01  3.0197-01
      3.4217-01  3.8774-01  4.3936-01  4.9786-01  5.6415-01
      6.3927-01  7.2438-01  8.2084-01  9.3013-01  1.0540+00
      1.1943+00  1.3533+00  1.5335+00  1.7377+00  1.8498+00
      1.9691+00  2.0961+00  2.2313+00  2.3752+00  2.5284+00
      2.6914+00  2.8650+00  3.0498+00  3.2465+00  3.4559+00
      3.6787+00  3.9160+00  4.1686+00  4.4374+00  4.7236+00
      5.0282+00  5.3525+00  5.6978+00  6.0652+00  6.4564+00
      6.8728+00  7.3161+00  7.7879+00  8.2902+00  8.8249+00
      9.3940+00  9.9999+00  1.0157+01  1.0317+01  1.0480+01
      1.0645+01  1.0812+01  1.0983+01  1.1156+01  1.1331+01
      1.1510+01  1.1691+01  1.1875+01  1.2062+01  1.2252+01
      1.2445+01  1.2641+01  1.2840+01  1.3042+01  1.3248+01
      1.3456+01  1.3668+01  1.3883+01  1.4102+01  1.4324+01
      1.4550+01  1.4779+01  1.5012+01  1.5248+01  1.5488+01
c     ***********************************************
c     * problem cutoff cards                        *
c     ***********************************************
phys:n  20  0
phys:p  20  1  0
phys:e  20  1  1  1  1  1  1  1  1
cut:n   0  0.0       -0.5    -0.25   0
cut:p   0  0.999-02  -0.5    -0.25   0
nps      1000000
ctme     1000000
c     ***********************************************
c     * peripheral cards                            *
c     ***********************************************
idum    1
rdum    0 0 -20
prdmp    1000000   100000   1  1
lost     10        10
print
```

Fig. A-4 Continued. (3/3)

```
>>> Analysis of Tungsten Slab Eperiment  April 1994 <<<
c    *****  front air region  *****
 1    2 4.921-5 (+1  -2  -22) : (+2  -3  +21  -22)       $   source void
 2    2 4.921-5  +2  -3  -21       $  cell detecter
c    *****  test region  *****
 3    1 6.423-2  +3  -4  -21       $  0.00 -  5.07 cm
 4    1 6.544-2  +3  -4  +21  -22  $
 5    1 6.423-2  +4  -5  -21       $  5.07 -  7.605cm
 6    1 6.544-2  +4  -5  +21  -22  $
 7    1 6.423-2  +5  -6  -21       $  7.605- 10.14 cm
 8    1 6.544-2  +5  -6  +21  -22  $
 9    1 6.423-2  +6  -7  -21       $ 10.14 - 20.28 cm
10    1 6.544-2  +6  -7  +21  -22  $
11    1 6.423-2  +7  -8  -21       $ 20.28 - 22.815cm
12    1 6.544-2  +7  -8  +21  -22  $
13    1 6.423-2  +8  -9  -21       $ 22.815- 25.35 cm
14    1 6.544-2  +8  -9  +21  -22  $
15    1 6.423-2  +9  -10 -21       $ 25.35 - 35.49 cm
16    1 6.544-2  +9  -10 +21  -22  $
17    1 6.423-2  +10 -11 -21       $ 35.49 - 38.025cm
18    1 6.544-2  +10 -11 +21  -22  $
19    1 6.423-2  +11 -12 -21       $ 38.025- 40.56 cm
20    1 6.544-2  +11 -12 +21  -22  $
21    1 6.423-2  +12 -13 -21       $ 40.56 - 50.70 cm
22    1 6.544-2  +12 -13 +21  -22  $
c    *****  rear air region  *****
23    2 4.921-5  +13 -14 -21       $  cell detector
24    2 4.921-5  +13 -14 +21 -22   $
c    *****  external void  *****
25    0          -1 : +14 : +22    $

 1             pz          -21.00  $  Source
 2             pz           -2.00  $  n-spec
 3             pz            0.00  $  Front Surface
 4             pz            5.07  $  #1-1
 5             pz            7.605 $  Drawer #1
 6             pz           10.14  $  #1-2
 7             pz           20.28  $  #2-1
 8             pz           22.815 $  Drawer #2
 9             pz           25.35  $  #2-2
10             pz           35.49  $  #3-1
11             pz           38.025 $  Drawer #3
12             pz           40.56  $  #3-2
13             pz           50.70  $  Rear Surface
14             pz           52.70  $  n-spec
c
21             cz            2.86
22             cz           23.76

ext:n   0     0     0.1z  0.1z  0.1z  0.1z  0.1z  0.1z  0.1z  0.1z
        0.1z  0.1z  0.1z  0.1z  0.1z  0.1z  0.1z  0.1z  0.1z  0.1z
        0.1z  0.1z  0     0     0
wwe:n   1.0e-3  1.0e-2  1.0  10.0  16.0
wwp:n   5  3  5  0  0
wwn1:n  $  for eV Neutrons
        0.08    1r    0.02    1r  0.005   1r     0.00128  1r
        0.00032 1r    0.00008 1r  0.00002 1r     0.000005 1r
        0.0000025     7r     -1
wwn2:n  $  for 1-10keV Neutrons
        0.08    1r      0.03    1r      0.008    3r      0.003  1r
        0.0008  3r      0.0003  1r      0.00008  7r      -1
wwn3:n  $  for 0.01-1MeV Neutrons
        0.08    1r      0.08    1r      0.08    3r      0.04    1r
        0.02    3r      0.01    1r      0.005   7r      -1
wwn4:n  $  for 1-13 MeV Neutrons
        0.08    1r    0.02    1r    0.005   3r      0.00128 1r
        0.00032 3r    0.00008 1r    0.00002 7r      -1
wwn5:n  $  for 14 MeV Neutrons
        0.08    1r    0.02    1r    0.005   3r      0.00128 1r
        0.00032 3r    0.00008 1r    0.00002 7r      -1
wwe:p   100.0
wwp:p   5  3  5  0  0
wwn1:p  $  for Gamma-Rays
        0.4     1r      0.15    1r      0.04    3r      0.015   1r
        0.004   3r      0.0015  1r      0.0004  7r      -1
wwe:e   100.0
wwp:e   5  3  5  0  0
wwn1:e  $  for Electrons
        0.4     1r      0.15    1r      0.04    3r      0.015   1r
```

Fig. A-5 Input data of MCNP for the analysis of the tungsten experiment. (1/4)

```
        0.004  3r     0.0015 1r     0.0004 7r     -1
c    ***********************************************
c    *  source specification cards                 *
c    *  a user supplied source subroutine is used. *
c    ***********************************************
sc1   Source Spectrum for FNS 1TR NWCT (125-g)
sdef  erg=d1  dir=d2  vec=0 0 1  pos=0 0 -20  wgt=1.1261
sb2   -31  4.0
si1   1.0010-11  3.2241-07
      5.3156-07  8.7640-07  1.4449-06  2.3823-06  3.9278-06
      6.4758-06  1.0677-05  1.7603-05  2.9023-05  4.7850-05
      7.8891-05  1.3007-04  2.1445-04  3.5357-04  5.8293-04
      9.6110-04  1.2341-03  1.5846-03  2.0346-03  2.6125-03
      3.3546-03  4.3073-03  5.5307-03  7.1016-03  9.1186-03
      1.1709-02  1.5034-02  1.9304-02  2.1874-02  2.4787-02
      2.8087-02  3.1827-02  3.6065-02  4.0867-02  4.6308-02
      5.2474-02  5.9461-02  6.7378-02  7.6349-02  8.6515-02
      9.8035-02  1.1109-01  1.2588-01  1.4264-01  1.6163-01
      1.8315-01  2.0754-01  2.3517-01  2.6649-01  3.0197-01
      3.4217-01  3.8774-01  4.3936-01  4.9786-01  5.6415-01
      6.3927-01  7.2438-01  8.2084-01  9.3013-01  1.0540+00
      1.1943+00  1.3533+00  1.5335+00  1.7377+00  1.8498+00
      1.9691+00  2.0961+00  2.2313+00  2.3752+00  2.5284+00
      2.6914+00  2.8650+00  3.0498+00  3.2465+00  3.4559+00
      3.6787+00  3.9160+00  4.1686+00  4.4374+00  4.7236+00
      5.0282+00  5.3525+00  5.6978+00  6.0652+00  6.4564+00
      6.8728+00  7.3161+00  7.7879+00  8.2902+00  8.8249+00
      9.3940+00  9.9999+00  1.0157+01  1.0317+01  1.0480+01
      1.0645+01  1.0812+01  1.0983+01  1.1156+01  1.1331+01
      1.1510+01  1.1691+01  1.1875+01  1.2062+01  1.2252+01
      1.2445+01  1.2641+01  1.2840+01  1.3042+01  1.3248+01
      1.3456+01  1.3668+01  1.3883+01  1.4102+01  1.4324+01
      1.4550+01  1.4779+01  1.5012+01  1.5248+01  1.5488+01
sp1   0.0        1.5142-07
      2.2732-09  4.2225-09  7.4848-09  1.4264-08  8.3975-08
      1.8398-07  2.2450-07  1.3922-07  1.6817-07  2.9754-07
      3.8068-06  3.0541-06  2.2612-06  6.9372-06  7.2049-06
      8.7622-06  7.8013-06  1.4320-05  1.1820-05  1.6544-05
      1.4791-05  1.7624-05  2.8404-05  2.4899-05  3.7633-05
      4.4237-05  4.6320-05  6.1572-05  3.7185-05  5.3362-05
      4.8831-05  5.0292-05  5.7202-05  6.9230-05  8.0602-05
      8.3190-05  9.7450-05  1.0531-04  1.2632-04  1.4874-04
      1.7906-04  3.7225-04  4.9933-04  5.3824-04  6.0762-04
      7.0593-04  8.0965-04  9.5392-04  1.0785-03  1.2232-03
      1.3867-03  1.5803-03  1.6473-03  1.8238-03  2.0605-03
      2.2042-03  2.3040-03  2.5211-03  2.5709-03  2.5872-03
      2.5765-03  2.7699-03  2.8528-03  2.5945-03  1.3898-03
      1.4298-03  1.3270-03  1.3489-03  1.3820-03  1.4312-03
      1.3760-03  1.4329-03  1.4558-03  1.3518-03  1.4053-03
      1.2861-03  1.2741-03  1.1711-03  1.1937-03  1.0563-03
      1.0018-03  8.8451-04  7.9827-04  7.9293-04  7.5872-04
      6.9228-04  6.2956-04  5.1710-04  5.0750-04  5.1007-04
      4.1280-04  3.5649-04  9.0768-05  8.2287-05  9.2862-05
      9.1407-05  9.3708-05  7.9567-05  8.8737-05  8.7841-05
      1.1227-04  1.6798-04  1.5985-04  1.6563-04  2.1025-04
      4.1363-04  7.4899-04  7.8183-04  5.1771-04  4.5938-04
      4.6458-04  9.1020-04  2.6083-03  9.5007-04  5.1474-03
      3.0897-02  2.3565-01  4.0901-01  2.2296-01  1.4419-01
c    ***********************************************
c    *  material specification cards               *
c    ***********************************************
c     --- Tungsten
m1    74000.42c  0.05600   28000.37c  0.00580
      29000.37c  0.00364
c     --- air
m2    7014.37c  3.8810-5    8016.37c  1.0400-5
c     --- materials for reaction rate
m3     5010.03y   1.0  $  B-10(n,alpha)
m4    13027.03y   1.0  $  Al-27(n,alpha)
m5    22000.03y   1.0  $  Ti-nat((n,x)Sc-48
m6    25055.03y   1.0  $  Mn-55(n,gamma)
m7    26056.03y   1.0  $  Fe-56(n,p)
m8    28058.03y   1.0  $  Ni-58(n,2n) &  Ni-58(n,p)
m9    28060.03y   1.0  $  Ni-60(n,p)
m10   29063.03y   1.0  $  Cu-63(n,2n) & Cu-63(n,g) & Cu-63(n,a)
m11   29065.03y   1.0  $  Cu-65(n,2n)
m12   30064.03y   1.0  $  Zn-64(n,p)
m13   40090.03y   1.0  $  Zr-90(n,2n)
m14   41093.03y   1.0  $  Nb-93(n,2n)Nb-92m
```

Fig. A-5 Continued. (2/4)

```
m15   49115.03y   1.0  $  In-115(n,n')In-115m
m16   74186.03y   1.0  $  W-186(n,gamma)
m17   79197.03y   1.0  $  Au-197(n,gamma)
m18   92235.03y   1.0  $  U-235(n,fission)
c
m21   28000.37c   1.0  $  Ni(n,gamma)
m22   29000.37c   1.0  $  Cu(n,gamma)
m23   74000.42c   1.0  $  W(n,gamma)
c    ********************************************
c    *  tally specification cards                *
c    ********************************************
fc22 ---- neutron reaction rate       surface
f22:n  3  4  5  6  7  8  9  10  11  12  13
fs22  -21
fq22  s  e  f  m
e22   16.0
fm22  (1)          (1  3 107)  (1  3 207)  (1  4 107)  (1  5 212)
      (1  6 102)   (1  7 103)  (1  8  16)  (1  8 103)  (1  9 103)
      (1 10  16)   (1 10 102)  (1 10 107)  (1 11  16)  (1 12 103)
      (1 13  16)   (1 14  16)  (1 15  51)  (1 16 102)  (1 17 102)
      (1 18  18)   (1 21 102)  (1 22 102)  (1 23 102)
fc34 ---- neutron reaction rate       cell
f34:n  2  5  7  11  13  17  19  23
fq34  s  e  f  m
e34   16.0
fm34  (1)          (1  3 107)  (1  3 207)  (1  4 107)  (1  5 212)
      (1  6 102)   (1  7 103)  (1  8  16)  (1  8 103)  (1  9 103)
      (1 10  16)   (1 10 102)  (1 10 107)  (1 11  16)  (1 12 103)
      (1 13  16)   (1 14  16)  (1 15  51)  (1 16 102)  (1 17 102)
      (1 18  18)   (1 21 102)  (1 22 102)  (1 23 102)
fc42 ---- neutron energy spectrum     surface
f42:n  3  4  5  6  7  8  9  10  11  12  13
fs42  -21
fc54 ---- neutron energy spectrum     cell
f54:n  2  5  7  11  13  17  19  23
fc102 ---- gamma-ray energy spectrum     surface r=4cm
f102:p 3  4  5  6  7  8  9  10  11  12  13
fs102 -21
fu102 1  2  3  4  5  6
fq102 s  u  m  e  f
e102  1.0000-02  2.0000-02  3.0000-02  4.5000-02  6.0000-02
      8.0000-02  1.0000-01  1.5000-01  2.0000-01  3.0000-01
      4.0000-01  5.0000-01  5.2000-01  6.0000-01  7.0000-01
      8.0000-01  9.0000-01  1.0000+00  1.1300+00  1.2500+00
      1.3800+00  1.5000+00  1.7500+00  2.0000+00  2.2500+00
      2.5000+00  3.0000+00  3.5000+00  4.0000+00  4.5000+00
      5.0000+00  5.5000+00  6.0000+00  6.5000+00  7.0000+00
      7.5000+00  8.0000+00  9.0000+00  1.0000+01  1.2000+01
      1.4000+01
c    -----------------------------------------------------------
fq0   s  m  e  f
e0    1.0010-11  3.2241-07
      5.3156-07  8.7640-07  1.4449-06  2.3823-06  3.9278-06
      6.4758-06  1.0677-05  1.7603-05  2.9023-05  4.7850-05
      7.8891-05  1.3007-04  2.1445-04  3.5357-04  5.8293-04
      9.6110-04  1.2341-03  1.5846-03  2.0346-03  2.6125-03
      3.3546-03  4.3073-03  5.5307-03  7.1016-03  9.1186-03
      1.1709-02  1.5034-02  1.9304-02  2.1874-02  2.4787-02
      2.8087-02  3.1827-02  3.6065-02  4.0867-02  4.6308-02
      5.2474-02  5.9461-02  6.7378-02  7.6349-02  8.6515-02
      9.8035-02  1.1109-01  1.2588-01  1.4264-01  1.6163-01
      1.8315-01  2.0754-01  2.3517-01  2.6649-01  3.0197-01
      3.4217-01  3.8774-01  4.3936-01  4.9786-01  5.6415-01
      6.3927-01  7.2438-01  8.2084-01  9.3013-01  1.0540+00
      1.1943+00  1.3533+00  1.5335+00  1.7377+00  1.8498+00
      1.9691+00  2.0961+00  2.2313+00  2.3752+00  2.5284+00
      2.6914+00  2.8650+00  3.0498+00  3.2465+00  3.4559+00
      3.6787+00  3.9160+00  4.1686+00  4.4374+00  4.7236+00
      5.0282+00  5.3525+00  5.6978+00  6.0652+00  6.4564+00
      6.8728+00  7.3161+00  7.7879+00  8.2902+00  8.8249+00
      9.3940+00  9.9999+00  1.0157+01  1.0317+01  1.0480+01
      1.0645+01  1.0812+01  1.0983+01  1.1156+01  1.1331+01
      1.1510+01  1.1691+01  1.1875+01  1.2062+01  1.2252+01
      1.2445+01  1.2641+01  1.2840+01  1.3042+01  1.3248+01
      1.3456+01  1.3668+01  1.3883+01  1.4102+01  1.4324+01
      1.4550+01  1.4779+01  1.5012+01  1.5248+01  1.5488+01
c    *************************
c    * problem cutoff cards  *
c    *************************
```

Fig. A-5 Continued. (3/4)

```
phys:n 16.0  0.0
phys:p 30.0    1   0
phys:e 30.0    1   1   1   1   1   1   1   1
mode   n p
cut:n  0  1.0e-10      -0.5   -0.25   0
cut:p  0  0.0099       -0.5   -0.25   0
cut:e  0  0.3          -0.5   -0.25   0
nps    2000000
ctme   72000
c    *************************
c    * peripheral crads      *
c    *************************
idum    6 3 4 5
rdum    1 2 3 4 5 6
prdmp   200000   200000  1  1
lost    10       10
print
```

Fig. A-5 Continued. (4/4)

This is a blank page.

国際単位系（SI）と換算表

表1　SI基本単位および補助単位

量	名称	記号
長さ	メートル	m
質量	キログラム	kg
時間	秒	s
電流	アンペア	A
熱力学温度	ケルビン	K
物質量	モル	mol
光度	カンデラ	cd
平面角	ラジアン	rad
立体角	ステラジアン	sr

表2　SIと併用される単位

名称	記号
分，時，日	min，h，d
度，分，秒	°，′，″
リットル	l，L
トン	t
電子ボルト	eV
原子質量単位	u

1 eV=1.60218×10^{-19}J

1 u=1.66054×10^{-27}kg

表3　固有の名称をもつSI組立単位

量	名称	記号	他のSI単位による表現
周波数	ヘルツ	Hz	s^{-1}
力	ニュートン	N	m·kg/s^2
圧力，応力	パスカル	Pa	N/m^2
エネルギー,仕事,熱量	ジュール	J	N·m
工率，放射束	ワット	W	J/s
電気量，電荷	クーロン	C	A·s
電位，電圧，起電力	ボルト	V	W/A
静電容量	ファラド	F	C/V
電気抵抗	オーム	Ω	V/A
コンダクタンス	ジーメンス	S	A/V
磁束	ウェーバ	Wb	V·s
磁束密度	テスラ	T	Wb/m^2
インダクタンス	ヘンリー	H	Wb/A
セルシウス温度	セルシウス度	℃	
光束	ルーメン	lm	cd·sr
照度	ルクス	lx	lm/m^2
放射能	ベクレル	Bq	s^{-1}
吸収線量	グレイ	Gy	J/kg
線量等量	シーベルト	Sv	J/kg

表4　SIと共に暫定的に維持される単位

名称	記号
オングストローム	Å
バーン	b
バール	bar
ガル	Gal
キュリー	Ci
レントゲン	R
ラド	rad
レム	rem

1 Å=0.1nm=10^{-10}m

1 b=100fm^2=10^{-28}m^2

1 bar=0.1MPa=10^{5}Pa

1 Gal=1cm/s^2=10^{-2}m/s^2

1 Ci=3.7×10^{10}Bq

1 R=2.58×10^{-4}C/kg

1 rad=1cGy=10^{-2}Gy

1 rem=1cSv=10^{-2}Sv

表5　SI接頭語

倍数	接頭語	記号
10^{18}	エクサ	E
10^{15}	ペタ	P
10^{12}	テラ	T
10^9	ギガ	G
10^6	メガ	M
10^3	キロ	k
10^2	ヘクト	h
10^1	デカ	da
10^{-1}	デシ	d
10^{-2}	センチ	c
10^{-3}	ミリ	m
10^{-6}	マイクロ	μ
10^{-9}	ナノ	n
10^{-12}	ピコ	p
10^{-15}	フェムト	f
10^{-18}	アト	a

(注)

1．表1－5は「国際単位系」第5版，国際度量衡局1985年刊行による。ただし，1 eVおよび1 uの値はCODATAの1986年推奨値によった。

2．表4には海里，ノット，アール，ヘクタールも含まれているが日常の単位なのでここでは省略した。

3．barは，JISでは流体の圧力を表わす場合に限り表2のカテゴリーに分類されている。

4．EC閣僚理事会指令ではbar，barnおよび「血圧の単位」mmHgを表2のカテゴリーに入れている。

換算表

力	N(=10^{5}dyn)	kgf	lbf
	1	0.101972	0.224809
	9.80665	1	2.20462
	4.44822	0.453592	1

粘度　1 Pa·s(N·s/m^2)=10 P(ポアズ)(g/(cm·s))

動粘度　1m^2/s=10^{4}St(ストークス)(cm^2/s)

圧力	MPa(=10bar)	kgf/cm^2	atm	mmHg(Torr)	lbf/in^2(psi)
	1	10.1972	9.86923	7.50062×10^3	145.038
	0.0980665	1	0.967841	735.559	14.2233
	0.101325	1.03323	1	760	14.6959
	1.33322×10^{-4}	1.35951×10^{-3}	1.31579×10^{-3}	1	1.93368×10^{-2}
	6.89476×10^{-3}	7.03070×10^{-2}	6.80460×10^{-2}	51.7149	1

エネルギー・仕事・熱量	J(=10^7 erg)	kgf·m	kW·h	cal(計量法)	Btu	ft·lbf	eV
	1	0.101972	2.77778×10^{-7}	0.238889	9.47813×10^{-4}	0.737562	6.24150×10^{18}
	9.80665	1	2.72407×10^{-6}	2.34270	9.29487×10^{-3}	7.23301	6.12082×10^{19}
	3.6×10^6	3.67098×10^5	1	8.59999×10^5	3412.13	2.65522×10^6	2.24694×10^{25}
	4.18605	0.426858	1.16279×10^{-6}	1	3.96759×10^{-3}	3.08747	2.61272×10^{19}
	1055.06	107.586	2.93072×10^{-4}	252.042	1	778.172	6.58515×10^{21}
	1.35582	0.138255	3.76616×10^{-7}	0.323890	1.28506×10^{-3}	1	8.46233×10^{18}
	1.60218×10^{-19}	1.63377×10^{-20}	4.45050×10^{-26}	3.82743×10^{-20}	1.51857×10^{-22}	1.18171×10^{-19}	1

1 cal=4.18605J（計量法）

=4.184J（熱化学）

=4.1855J（15℃）

=4.1868J（国際蒸気表）

仕事率　1 PS(仏馬力)

=75 kgf·m/s

=735.499W

放射能	Bq	Ci
	1	2.70270×10^{-11}
	3.7×10^{10}	1

吸収線量	Gy	rad
	1	100
	0.01	1

照射線量	C/kg	R
	1	3876
	2.58×10^{-4}	1

線量当量	Sv	rem
	1	100
	0.01	1

(86年12月26日現在)

DATA COLLECTION OF FUSION NEUTRONICS BENCHMARK EXPERIMENT CONDUCTED AT FNS/JAERI